Institut für Geodäsie und Geoinformation

der Rheinischen Friedrich-Wilhelms-Universität Bonn

Bereich Geodäsie

Quality aspects of short duration VLBI observations for UT1 determinations

I n a u g u r a l - D i s s e r t a t i o n

zur
Erlangung des Grades
Doktor-Ingenieur
(Dr.-Ing.)

der
Hohen Landwirtschaftlichen Fakultät
der
Rheinischen Friedrich-Wilhelms-Universität
zu Bonn

vorgelegt am 17. August 2006 von

Dipl.-Ing. Dorothee Schnell

aus Bonn

D 98

Angefertigt mit Genehmigung der Landwirtschaftlichen Fakultät der Rheinischen Friedrich-Wilhelms-Universität Bonn

Referent: Priv.-Doz. Dr.-Ing. Axel Nothnagel

Korreferenten: Univ.-Prof. Dipl.-Ing. Dr. techn. Harald Schuh

Univ.-Prof. Dr.-Ing. Heiner Kuhlmann

Tag der mündlichen Prüfung: 3. November 2006

Diese Dissertation ist auf dem Hochschulschriftenserver der ULB Bonn
http://hss.ulb.uni-bonn.de/diss_online elektronisch publiziert.

Contents

Abstract

Today geodetic Very Long Baseline Interferometry (VLBI) is the most important technique for the determination of all components of earth rotation. Among all parameters describing the current earth rotation relative to a quasi inertial system the daily earth rotation phase UT1 is the most variable quantity including significant unpredictable variations. Short duration single baseline VLBI sessions, so called *Intensive* sessions, are carried out regularly since 1985 in order to monitor this phase angle of daily earth rotation with minimized operating expense and contemporary analysis.
Due to the importance of a regular and dense UT1 monitoring the International VLBI Service for Geodesy and Astrometry (IVS) established a second baseline for such *Intensive* observations in 2003. In terms of consistency these two independent *Intensive* baselines form two unequal UT1 sensors affected by various sources of error. In order to generate a common and consistent UT1 series from both baselines and towards a combination of *Intensive* UT1 results with those of regular VLBI 24 hours global network sessions, the knowledge of baseline dependent impacts is essential.
In this thesis, the question of consistency and homogeneity of the two independent series of short term single baseline VLBI sessions is approached taking into account the specifics of the VLBI observing technique itself. On the basis of theoretical considerations and empirical studies the error propagation of different impact factors to the final UT1 estimates is verified. Within the framework of these investigations, two special test sessions of parallel observations were designed and carried out in order to allow conclusive empirical studies on the precision of and the systematic effects on the UT1 results from short term VLBI sessions.
Although the formal errors of both *Intensive* series are of equal order of magnitude, significant baseline dependent elements of uncertainty have been identified. These geometry and time dependent impacts affect the relative as well as the absolute accuracy of each *Intensive* series and have to be kept in mind when merging the results of the two series.
At the end, a realistic estimation of the relative and absolute UT1 accuracy of the two different single baseline VLBI series is given. A concise summary of the *Intensive* specific sources of error helps to detect weak points within the analysis process.

Zusammenfassung

Die Radiointerferometrie auf langen Basen (Very Long Baseline Interferometry, VLBI) ist das wichtigste geodätische Beobachtungsverfahren der Gegenwart zur Bestimmung der Erdrotation und das einzige Verfahren mit direktem Bezug zum quasi-inertialen Bezugsrahmen. Unter den Parametern zur Beschreibung der momentanen Drehstellung der Erde im Raum ist die Rotationsphase der täglichen Erddrehung UT1 die bei weitem variabelste Größe mit erheblichen nicht prädizierbaren Anteilen.
Kurzzeit-VLBI-Messungen unter Verwendung von nur einer einzelnen langen Basislinie werden seit 1985 zur regelmäßigen Beobachtung von UT1 durchgeführt. Diese sogenannten *Intensive*-Sessionen ermöglichen ein UT1-Monitoring mit minimalem Aufwand und daher zeitnaher Auswertung.
Aufgrund der Wichtigkeit einer regelmäßigen und engmaschigen UT1-Beobachtung wurde im Jahre 2003 durch den *International VLBI Service for Geodesy and Astrometry* (IVS) eine zweite Basislinie für regelmäßige *Intensive*-Beobachtungen eingerichtet. Somit werden derzeit zwei unabhängige Basislinien abwechselnd für *Intensive*-Sessionen genutzt und dadurch ein beinahe tägliches UT1-Monitoring realisiert.
Im Hinblick auf die Konsistenz der Ergebnisse stellen diese beiden unabhängigen Basislinien zwei ungleiche Sensoren da, die von verschiedenen Fehlereinflüssen in unterschiedlicher Art und Weise beeinflusst werden. Sollen beide Basislinien also zu einer gemeinsamen UT1 Serie beitragen und obendrein deren Ergebnisse mit denen von regulären 24-stündigen VLBI-Netzmessungen kombiniert werden, müssen basislinienabhängige Fehlereinflüsse bekannt sein und so weit wie möglich reduziert werden.
In dieser Arbeit wird die Frage nach Konsistenz und Homogenität der Ergebnisse der beiden unterschiedlichen *Intensive*-Serien untersucht unter Berücksichtigung der Besonderheiten des VLBI-Beobacht-

ungsverfahrens. Auf Grundlage von theoretischen Überlegungen und empirischen Untersuchungen werden die Einflüsse unterschiedlicher Fehlerquellen auf die UT1-Ergebnisse beleuchtet und deren Größenordnungen ermittelt. Zu diesem Zweck wurden u.a. zwei spezielle Beobachtungsserien geplant und durchgeführt als Grundlage für aussagekräftige emprirische Untersuchungen zur Genauigkeit und zu den systematischen Effekten der *Intensive*-UT1-Ergebnisse.
Obgleich die formalen Fehler beider *Intensive*-Serien von ähnlicher Größenordnung sind, wurden erhebliche basislinienabhängige Unsicherheitsfaktoren identifiziert. Diese geometrie- und zeitabhängigen Einflussgrößen betreffen sowohl die relative als auch die absolute Genauigkeit beider Serien.
Am Ende der Arbeit steht eine realistische Abschätzung sowohl der relativen also auch der absoluten Genauigkeit beider *Intensive*-Serien und eine übersichtliche Zusammenstellung ermöglicht es, Schwachstellen im Auswerteprozess zu identifizieren und Verbesserungspotential zu erkennen.

Chapter 1

Motivation

The rotation of the earth has always been used as a natural time scale and at all times clocks have been set according to the length of a solar day. Nowadays, atomic clocks are used for global time keeping and the atomic time is the functional timescale of today. For an alignment of the stable atomic time with the variable solar time, regular precise observations of the earth's rotation angle are necessary.

Today, geodetic Very Long Baseline Interferometry (VLBI) is the most important technique for the determination of earth rotation. VLBI sessions employing a number of globally distributed observing stations are regularly carried out for the determination of all components of earth orientation parameterized as the rotation angle UT1 together with the components of polar motion, precession and nutation. These network sessions generally last 24 hours and require at least two weeks of data shipment, correlation and post-processing until the results are available.

Among the earth orientation parameters the daily earth rotation angle UT1 is the most variable quantity with significant unpredictable variations. In order to monitor its behavior and provide a timely base set for predictions, a very dense series of observations with contemporary analysis is required. For this purpose it is not necessary to schedule a full network of several stations. A single baseline with the correct orientation is sufficient. Thus, VLBI short term single baseline observations have been carried out for the determination of UT1 since 1985. The only objective of these so-called *Intensive* observations is the daily measurement of UT1 with affordable logistics and contemporary analysis. This type of VLBI sessions has generally been carried out four to five times a week using the baseline Wettzell (Germany) - Westford (USA) and later Wettzell - Kokee Park (Hawaii) instead.
Because of the importance of a regular and dense monitoring of the rotation angle UT1, the International VLBI Service for Geodesy and Astrometry (IVS) established a second baseline for *Intensive* VLBI observations in 2002. This second observation series using the baseline Wettzell - Tsukuba (Japan) is a temporal complement of the Wettzell - Kokee Park observations densifying the sequence of UT1 measurements.

From a consistency point of view the 24 hour network sessions and the one hour *Intensive* observations using two independent baselines form three different instruments affected by a number of non-identical peculiarities. Consequently, the three individual, unevenly sampled series of UT1 results cannot be consolidated into one consistent series by simply merging the results.
In order to generate a UT1 series which fulfills all requirements in terms of consistency and homogeneity, a more sophisticated process is needed taking into account the characteristics of each instrument.
Concerning the two *Intensive* series the scientific challenge can be subsumed under the following generalized headings:

- Generation of optimized observing schedules for *Intensive* observations,
- Verification of consistent terrestrial reference frames for both *Intensive* series and also consistent with the frame of the global VLBI network sessions,
- Realization of consistent intermediate reference frames through accurate modeling of polar motion and nutation and
- Avoidance of arbitrary UT1 variations caused by varying performances of the observing geometries.

At present the International Earth Rotation and Reference Systems Service (IERS) is the international institution responsible for the computation and dissemination of official earth orientation parameters. With respect to the earth rotation phase angle UT1, the results of VLBI observations are the crucial input to the IERS product. The reason is that satellite techniques like GPS and Satellite Laser Ranging (SLR) are not sensitive to the phase angle itself but only to its time derivative which is called Length of Day (LOD). Therefore, VLBI UT1 results realizing the direct link to the Celestial Reference Frame are necessary to prevent them from drifting. The IERS combines UT1 results from several analysis centers, which use similar or even identical observations, e.g. [Gambis et. al. 2002]. In its endeavor to generate a homogeneous time series of UT1 values consistent with its historical evolution, the IERS mainly considered statistical aspects of individual UT1 series, e.g. [Gambis et. al. 2003], [Johnson et. al. 2003], neglecting technique specific properties.

In addition to the IERS, investigations in connection with the combination of VLBI UT1 with GPS LOD of the International GNSS Service (IGS), e.g. [Vondrak et. al. 2005], or other investigations isolated from operational requirements, e.g. [Babcock 1988], [Vondrak et. al. 2000], [Fernandez 2001], all start their research at the level of the input series. In this thesis the questions of consistency and homogeneity of the two independent series of short term single baseline VLBI sessions are approached taking into account the specifics of the VLBI technique itself as a necessary step before consolidating results.

On the basis of theoretical considerations and empirical studies a firm basis for a consistent analysis of both short term VLBI series is provided which is a precondition for a proper integration into the series of Earth Orientation Parameters from 24 hours VLBI network sessions. In this context investigations are carried out to study the following areas of concern:

- The precision and accuracy of *Intensive* UT1 results (section 4),
- The requirements for the observing schedules and their impact on the UT1 estimates (section 3.1.2),
- The baseline dependent impact of polar motion information on the UT1 estimates (section 5.1),
- The baseline and session dependent impact of nutation modeling on UT1 estimates (section 5.2),
- The impact of small inconsistencies of the terrestrial reference frame (including local displacements) on the UT1 results (section 5.3) and
- The influence of different models of high frequency EOP variations on *Intensive* UT1 estimates.

Within the framework of these investigations, two special test sessions of parallel observations were designed and carried out in order to allow conclusive empirical studies on the precision of and the systematic effects on the UT1 results from short term VLBI sessions (section 3.3).

At the end, a realistic estimation of the relative and absolute UT1 accuracy of the two different single baseline VLBI series is given. A concise summary of the *Intensive* specific sources of error will help to detect weak points within the analysis process and to identify requirements in terms of merging UT1 *Intensive* session results into the series of 24 hour global network sessions.

Chapter 2

Theoretical Background

Very Long Baseline Interferometry (VLBI) is the only geodetic observing technique providing a direct link to a non-rotation quasi-inertial system. Therefore it is particularly suitable for the determination of the variable earth orientation in space.
After a short depiction of the currently used reference systems, the three most established definitions for the description of earth orientation are briefly introduced with main focus on the diurnal rotation angle (section 2.2). Furthermore the difference $UT1 - UTC$ as the target parameter is characterized (2.3) and its estimation from short term VLBI sessions is shortly outlined (2.4).

2.1 Reference Systems

Celestial Reference

Up to the year 1997 the FK5 axis definitions, realized by the FK5 catalog, served as reference for the description of earth orientation. It is based on positions and proper motions of a group of bright stars and it is oriented so that at a given date the positions are referred to the best estimate of the location of the mean pole and the mean equinox. The complete description of the FK5 celestial reference system is given in [Fricke et. al. 1988]. The accuracy of the positions and proper motions of stars in the FK5 catalog is stated to be $19\,mas$ and $0.7\,mas/century$.
In 1999/2000 a new fundamental catalog, FK6, has been published by the *Astronomisches Recheninstitut* of the University of Heidelberg with a significantly improved accuracy of star positions and proper motions [Whielen et. al. 1999].

The International Astronomical Union (IAU) adopted at its 23rd General Assembly in 1997 the International Celestial Reference Frame (ICRF) as the official realization of the International Celestial Reference System (ICRS), which was specified by an IAU resolution in 1991. The ICRS is defined such that the barycentric directions of quasars show no global rotation with respect to these distant objects. It is currently realized by the directions of 212 defining sources, 294 candidate sources and 102 other radio objects [Ma 1998].
Additionally a geocentric celestial reference system, which is needed for the description of earth rotation, is defined with identical kinematic conditions. The ICRS has been aligned to the FK5 system at epoch J2000.0.

Terrestrial Reference

The International Earth Rotation and Reference System Service (IERS) defined the International Terrestrial Reference System (ITRS) [McCarthy et. al. 2003] as ideal reference system in terms of the

IUGG (International Union of Geodesy and Geophysics) Resolution No. 2 on the Conventional Terrestrial Reference System. Its center of mass is defined for the whole earth, including oceans and atmosphere, and its orientation is initially given by the BIH (Bureau International de l'Heure) orientation at epoch 1984.0. The realization, named International Terrestrial Reference Frame (ITRF), of the ITRS is calculated by the IERS using observations of VLBI, Lunar and Satellite Laser Ranging (LLR and SLR), Global Positioning Service (GPS) and DORIS (Doppler Orbitography and Radio Positioning Integrated by Satellite). ITRF solutions are published in irregular intervals.
For operational VLBI determinations often individual TRF realizations are used, which are calculated from VLBI observations only. A universal and often used, highly accurate terrestrial reference frame for VLBI analyses (VTRF) has been calculated as a combination of five different VLBI TRF realizations [Nothnagel 2005].

2.2 Earth orientation parameters

The earth orientation parameters (EOP) describe the rotatory position of the solid earth relative to a space fixed non-rotating reference system. Essentially there are three different definitions of EOP currently in use, which are going to be introduced in the following.
Unfortunately for historical reasons the ideal consistent unity of ITRF, ICRF and EOP has not been realized so far.

2.2.1 Classical notation of earth orientation parameters (according to IAU1980)

Definition of EOP

The earth orientation is expressed using a number of consecutive rotations transforming the celestial and the terrestrial system into each other. Instead of using the minimum number of three rotations, the transformation is divided into a number of intermediate rotations according to their geophysical interpretations and different temporal variability. The transformation between the terrestrial and the celestial reference frame is then expressed by

$$\vec{x}_{TRS} = W(t) \cdot S(t) \cdot N(t) \cdot P(t) \cdot \vec{x}_{CRS} \tag{2.1}$$

with $W(t)$ = Transformation due to Polar Motion, $S(t)$ = Diurnal earth rotation, $N(t)$ = Nutation and $P(t)$ = Precession. In detail the elemental rotations are e.g. [Mueller 1969]:

$$\begin{aligned} \vec{x}_{TRF} \quad = \quad & \underbrace{R_2(-x_P)R_1(-y_p)}_{Polar Motion} \cdot \underbrace{R_3(GAST)}_{Diurn.Rot.} \cdot \underbrace{R_1(-\varepsilon_0 - \Delta\varepsilon)R_3(-\Delta\psi)R_1(\varepsilon_0)}_{Nutation} \\ & \cdot \underbrace{R_3(-z_A)R_2(\theta_A)R_3(-\zeta_A)}_{Precession} \cdot \vec{x}_{CRF} \end{aligned} \tag{2.2}$$

Here R_1, R_2 and R_3 stand for rotary matrices around the current x, y and z axis respectively. TRS is the conventional terrestrial and CRS the mean celestial reference system at the reference epoch. The individual angels of rotation are:

x_p, y_p	Components of Polar Motion,
$GAST$	Greenwich Apparent Sidereal Time,
ε_0	Mean obliquity of the ecliptic at the observing date,
$\Delta\varepsilon, \Delta\psi$	Nutation in obliquity and in longitude,
z_A, θ_A, ζ_A	Precessional elements.

Rotations describing the precession and the lunisolar nutation transform the mean CRS of the reference epoch into the true CRS of the observing date. The x-axis of this intermediate CRS then points towards the true vernal equinox. In the same manner rotations according to the motion of the terrestrial pole transfer the conventional TRS of reference epoch into the true TRS at the observing date. The x-axis of this intermediate TRS then points towards the current Greenwich meridian.
The remaining rotation between the two intermediate reference frames depends for the most part on the diurnal rotation around the common z-axis but also on precession, nutation and polar motion. Proper corrections as described below have to be applied to derive the solar Universal Time UT1 from GAST (Greenwich Apparent Sidereal Time).

Determination of the solar time UT1

The rotation $R_3(GAST)$ in equation 2.2 denotes the diurnal rotation of the earth. Its argument $GAST$ named Greenwich Apparent Sidereal Time means the current hour angle of the mean Greenwich meridian relative to the direction of the true vernal equinox.
Due to precession and nutation the direction of the vernal equinox varies with time relative to the space-fixed coordinate system. The difference between the true and the mean vernal equinox is referred to as the Equation of Equinoxes (EqE) and the hour angle with respect to the mean equinox is called Greenwich Mean Sidereal Time ($GMST$). The relation between the apparent and the mean sidereal time then is (cp. fig. 2.1)

$$GAST = GMST + EqE\,. \tag{2.3}$$

The Equation of Equinoxes, which is also called the nutation in right ascension, depends on the current nutation in longitude $\Delta\psi$ and on the mean obliquity ε_0:

$$EqE = \Delta\psi \cdot \cos\varepsilon_0\,. \tag{2.4}$$

While $GMST$ is referred to the mean vernal equinox, the epoch of solar time UT1 is given by the hour angle relative to the direction of the mean sun. The solar time therefore depends on the diurnal rotation of the earth and additionally on the revolution of the earth around the sun on a Kepler-orbit (Fig. 2.2). The true sun is thereby replaced by a mean sun because the motion of the earth is not uniform as a result of the 2nd Kepler's Law. The difference between the true and the mean sun is referred to as Equation of Time (EqT).

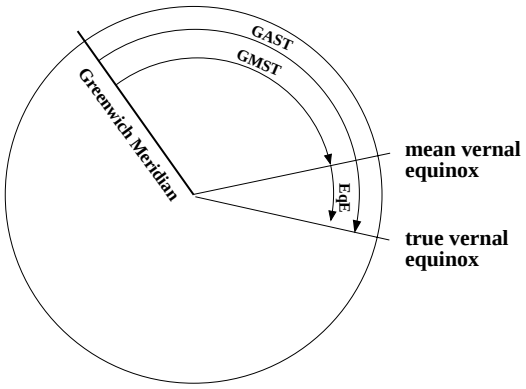

Figure 2.1: Apparent and mean sidereal time (based on [Mueller 1969]).

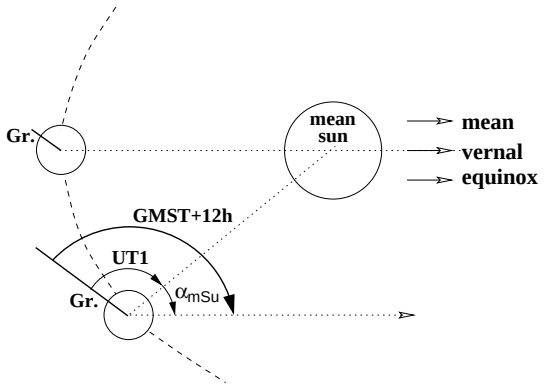

Figure 2.2: UT1 and GMST (based on [Schödlbauer 1999]).

The relationship between solar and sidereal time can easily be recognized from figure 2.2. The epoch of

Greenwich Mean Sidereal Time can be expressed using the solar Universal Time as

$$GMST = \alpha_{mSu} - 12h + UT1 \tag{2.5}$$

where α_{mSu} means the right ascension of the mean sun. 12 hours have to be subtracted because 0 hr UT1 is defined to be midnight as it corresponds to the common way of timekeeping. α_{mSu} following the IAU resolution of 1982 is given by [ASTRON. ALMANAC 1984]

$$\begin{aligned} \alpha_{mSu} = 18^h 41^m 50.54841^s \quad &+ \quad (8640184.812866 \frac{s}{Jc}) \cdot (T_U - T_{U_0}) \\ &+ \quad (0.093104 \frac{s}{Jc^2}) \cdot (T_U - T_{U_0})^2 \\ &- \quad (0.0000062 \frac{s}{Jc^3}) \cdot (T_U - T_{U_0})^3 \end{aligned} \tag{2.6}$$

wherein Jc denotes a Julian century which contains exactly 36525 days. The reference epoch T_{U_0} here is defined to be 2000, January 1st, 12 h UT1, that means Julian Date $T_{U_0} = 2451545.0$.

From $GAST$, which is estimated from VLBI observations, the solar Universal Time $UT1$ can be calculated as [SCHÖDLBAUER 1999]

$$\begin{aligned} UT1 &= GMST - \alpha_{mSu} + 12h & (2.7) \\ &= GAST - \Delta\psi \cdot \cos\varepsilon_0 - \alpha_{mSu} + 12h\,. & (2.8) \end{aligned}$$

Using the ratio C_{Sid} between the length of a sidereal and a solar time interval e.g. [MORITZ ET. AL. 1988]

$$C_{Sid} = \frac{\Delta GMST}{\Delta UT1} = \frac{GMST - GMST(UT1 = 0\,hr)}{UT1} \tag{2.9}$$

$$= 1.002\,737\,909\,350\,795 + 0.59006 \cdot 10^{-10} \cdot (T_U - T_{U_0}) - 0.589 \cdot 10^{-14} \cdot (T_U - T_{U_0})^2 \tag{2.10}$$

the relationship between GMST and UT1 can also be expressed by

$$UT1 = \frac{1}{C_{Sid}} \cdot (GAST - EqE - GMST(0hr\,UT1))\,. \tag{2.11}$$

The most important principle disadvantage of this UT1 definition based on the equinox is that the relation between the solar Universal and the Greenwich Sidereal Time has to be changed as soon as the model of precession and nutation or the definition of the ecliptic is changed [VONDRAK 2002]. Therefore, a change of the nutation or precession model influences the determination of the diurnal earth rotation.
Additionally, the present accuracy and sub-diurnal resolution of space geodetic observations show that nutation as well as polar motion both include diurnal and sub-diurnal frequencies so that the IAU 1980 definition is not sufficient anymore. Nevertheless, this classical notation of Earth Orientation Parameters is still the currently realized definition within the most popular VLBI software packages and, thus, all considerations within this thesis are based on it.

2.2.2 Earth orientation parameters according to IAU2000 resolution

In August 2000 the International Astronomical Union (IAU) at its 24th General Assembly in Manchester adopted a new definition of EOP [IAU 2000]. Its keynotes are (e.g. [CAPITAINE 2000], [VONDRAK 2002]):

- Reduction of the number of consecutive rotations for the transformation between TRS and CRS,
- Parameters for precession, nutation and earth rotation referred to a fixed plane instead of the ecliptic of date,
- A clear separation between precession/nutation and earth rotation,
- Substitution of the vernal equinox as the origin on the moving equator and
- The definition of an earth rotation angle, whose time derivative directly represents the current earth rotation velocity.

Definition of EOP

Similar to the classical notation the new definition again uses intermediate celestial and terrestrial reference frames, in order to divide the total earth orientation into individual rotations according to their geophysical causation and their temporal variability. Now the intermediate CRS and TRS are defined using the concept of non-rotating origins [CAPITAINE ET. AL. 1986]. That means that after the transformations for nutation/precession and for polar motion the intermediate CRS and respectively TRS are not rotated around the z-axis in case of infinitesimal displacements of the pole. Therefore the remaining rotation angle θ between the terrestrial and the celestial intermediate system around their common z-axis directly represents the earth rotation angle and thus its time derivative $\dot{\theta}$ is the current rotational velocity. The transformation between the mean CRS and the conventional TRS is defined to be

$$\vec{x}_{TRF} = \underbrace{R_2(-u)R_1(v)R_3(s')}_{PolarMotion} \cdot \underbrace{R_3(\theta)}_{Diurn.Rot.} \cdot \underbrace{R_3(-s)R_3(-E)R_2(d)R_3(E)}_{Precession,Nutation} \cdot \vec{x}_{CRF} \tag{2.12}$$

with

u, v	Terrestrial coordinates of the current rotation pole,$(u = x_p\,, v = -y_p)$,
θ	Stellar angle of diurnal rotation,
E, d	Celestial coordinates of the current rotation pole,
s, s'	Describe the motion of the NRO on the moving equator due to an infinitesimal displacement of the celestial and the terrestrial pole.

The non-rotating origins (NRO) of the TRF and the CRF are defined that way that small motions of the pole do not cause any rotations around the z-axis. The angle s expresses the motion of the NRO on the moving equator due to motions of the pole and is defined as (compare figure 2.3)

$$s = \sigma N - \Sigma_0 N - (\sigma_0 N_0 - \Sigma_0 N_0) \tag{2.13}$$

with

σ_0, σ	Non-rotating origin on the moving equator at epoch $t_0$and at date t,
N_0, N	Ascending Nodes of the equators before (epoch t_0) and after (date t) the motion of the pole,
Σ_0	Origin of the right ascension.

s' is defined for the TRF in the same manner.

Determination of the Solar Time UT1

The concept of the Non-Rotation Origin has to be applied to both, the celestial and the terrestrial reference system, in order to reach a common intermediate rotation axis of both systems. The stellar hour angle θ is then defined to be the arc on the common equator of date reckoned positively from the celestial NRO (σ) to the terrestrial NRO (ϖ) (see. fig. 2.4). As this definition ensures that $\dot{\theta}$ is strictly equal to the current angular velocity of the earth around the common polar axis, θ rigorously represents the sidereal rotation of the earth.
The IAU2000 resolution defines UT1 to be linearly proportional to the stellar earth rotation angle θ. To ensure the continuity in phase and rate of UT1 with the value obtained by the conventional relationship between GMST and UT1 (Equ. 2.11) the numerical link between θ and UT1 was determined to be

$$\theta = 2\pi(0.779057273264 + 1.00273781191135448 \cdot (UT1 - UT1_0))[rad]\,. \tag{2.14}$$

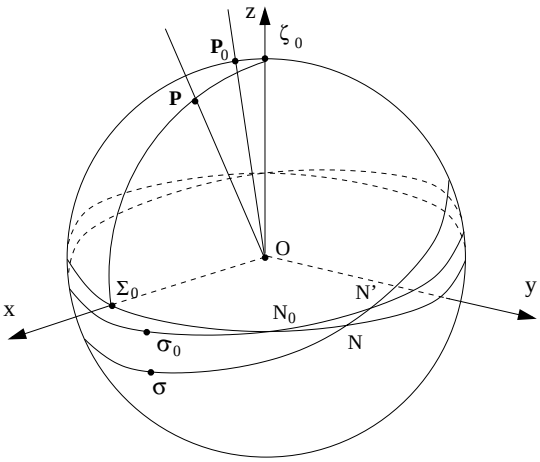

Figure 2.3: Definition of the non-rotating origin (σ) with respect to the ICRF corresponding to a finite displacement of the pole P (ζ_0 = Pole of the ICRF at reference epoch t_0; P_0 and P = Poles of the instantaneous rotation at epoch t_0 and at date t; σ and σ_0 = NROs on the moving equator at epoch t_0 and at date t; Σ_0 = Origin of the right ascension) [Capitaine 2000a].

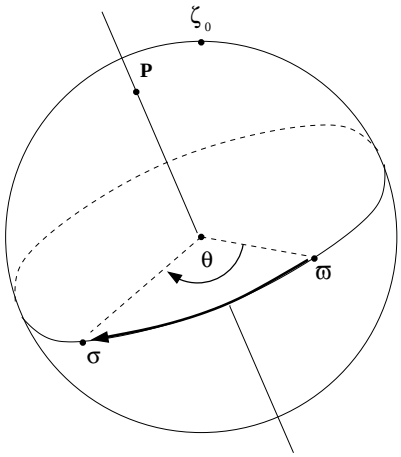

Figure 2.4: The stellar earth rotation angle θ as defined in IAU2000. (ζ_0 = Pole of the ICRF at reference epoch; P = Pole of the instantaneous rotation; ϖ = terrestrial NRO on the moving equator; σ = celestial NRO on the moving equator)

Thus, UT1 can be simply derived from the observed stellar angle according to its definition in the IAU 2000 resolution as

$$UT1[JD] = \frac{(\frac{\theta}{2\pi} - 0.779057273264)}{1.00273781191135448} + UT1_0\,. \tag{2.15}$$

Here again $UT1_0$ is defined to be 2000, January 1st, 12h UT1 (= JD 2451545.0 UT1).

[Capitaine et. al. 1993] showed that UT1 defined by the concept of non-rotating origins (according to IAU2000) is equivalent to its definition using GMST together with the equation of equinoxes (EqE), if the formulation of EqE is not limited to the first order terms, like it is done in the traditional relationship.

If the mean obliquity ε_0 in equation 2.4 is replaced by the true one and all crossterms are used, both definitions of UT1 are compatible. Inaccuracies in UT1 due to its traditional conventional definition (section 2.2.1) compared to its accurate definition using non-rotating origins are stated to be

$$UT1_{IAU1980} - UT1_{IAU2000} = 0.176\,ms \cdot \sin\Omega - 0.006\,ms \cdot \sin 2\Omega \tag{2.16}$$

with Ω = mean longitude of the lunar ascending node [CAPITAINE ET. AL. 1993]. That means that the difference between the two UT1 definitions appears mainly with a period of 18.5996 years with a main amplitude of about 0.176 ms.

2.2.3 Earth orientation parameters expressed in Eulerian Angles

A different and more straightforward way of describing the earth orientation is the simple usage of three consecutive rotations about the coordinate axes. This can be realized using for example *Eulerian* or *Cardanian* angles [RICHTER 1995]. The rotation of the mean terrestrial reference system into the celestial reference system using the *Eulerian angles* Ψ, Θ and ϵ is [MORITZ ET. AL. 1988]

$$\vec{x_{TRS}} = R(\Psi, \Theta, \epsilon) \cdot \vec{x_{CRS}} \tag{2.17}$$

with the Eulerian rotation matrix

$$R(\Psi, \Theta, \epsilon) = R_3(\Theta) R_1(\epsilon) R_3(\Psi)\,. \tag{2.18}$$

The rotations in detail are

1. Rotation about the X_3-axis by angle Ψ, so that the $X1'$-axis is parallel to the instantaneous node line,
2. Rotation about the X_1'-axis by angle ϵ, so that the X_3'-axis is parallel to the true terrestrial x_3-axis,
3. Rotation about the X_3' axis by angle Θ.

This way of describing the rotation is traditionally not used for geodetic earth rotation determination and for EOP studies. It's most important lack is, that the earth's rotation behavior is not longer subdivided into different contributions describing different geophysical phenomena affecting with different frequencies and amplitudes. Therefore the usage of Eulerian Angles does not allow to separate between modeled parts and observed contributions of earth orientation and, thus, it is only applicable for geometrical observing techniques, which are sensitive to all parameters of earth orientation simultaneously and which provide an adequate number of observations.
Because of the continuously increasing precision and accuracy of EOP series obtained from various observations and the growing sophistication of geophysical models, the traditional way of parameterizing earth orientation (sections 2.2.1 and 2.2.2) is unnecessarily complex for users that are only interested in the transformation between CRF and TRF and not in the particularities of the earth's rotation itself. For these applications e.g. [ROTHACHER 2002] proposes a table of Eulerian Angles with a sufficient sampling rate to become a new IERS product, in order to meet the demands of many users.

Determination of the Solar Time UT1

The rotation angle Θ about the X_3'-axis is equivalent to the Greenwich Mean Sidereal Time (GMST) (L. Petrov, personal communication). UT1 is therefore easily to derive from the third Eulerian Angle following equation 2.11:

$$UT1 = \frac{1}{C_{Sid}} \cdot (e_3 - e_{3_0}) \tag{2.19}$$

with

$$e_{3_0} = GMST(0hr\,UT1)\,. \tag{2.20}$$

2.3 The target parameter UT1-UTC

The difference UT1-UTC between the natural time scale UT1 and the atomic time UTC is the only objective of short term single baseline VLBI sessions and will be introduced as such below.

2.3.1 The Universal Coordinated Time UTC

The Coordinated Time UTC is based on the International Atomic Time (TAI), which is generated and officially published at the Bureau International de Poids et Mesures (BIPM). Its time unit is the SI-Second with the definition adopted at the 13th General Conference on Weights and Measures in 1967 [BIPM 1998]:

> *The second is the duration of 9 192 631 770 periods of the radiation corresponding to the transition between the two hyperfine levels of the ground state of the caesium 133 atom.*

In 1997 this definition was affirmed as following:

> *This definition refers to a caesium atom at rest at a temperature of 0 K.*

About 250 globally distributed atomic clocks contribute to the generation of TAI. Due to small technical deficiencies the contributing clocks are not perfectly synchronized, so that each time institute has its own specific atomic time. The TAI is then generated at the (BIPM) by averaging all the contributions using appropriate weighting factors. Before this averaging process all individual contributing time scales have to be reduced onto the level of the geoid, to account for relativity effects depending on the height of the atomic clocks above the geoid [Schödlbauer 1999].
The zero-point of TAI was defined to be identical with UT1 on 1958, January 1st, $0^h00^m00^s$. The BIPM estimates the stability of TAI to be better than 0.1 μsec per year, compared to an imaginary perfect clock. The length of a day in atomic time is defined to be exactly 24 hours = 86400 SI-seconds and it does not account for any irregularities of the earth's rotation.

Due to tidal friction the earth slowly loses rotational energy and, thus, the duration of a day gradually becomes longer. Consequently, the natural solar time UT1 and the uniform atomic time scale TAI diverge over the years. In order to avoid the atomic time scale diverging indefinitely from that of the earth's rotation, a leap second is introduced whenever the difference becomes larger than 0.9 seconds averaged over the year. The resulting atomic time scale UTC runs parallel to TAI but follows UT1 in discrete steps of leap seconds (Fig. 2.5). The choice of the dates and the announcement of the leap seconds is under the responsibility of the International Earth Rotation and Reference Systems Service (IERS) [BIPM 1995].

2.3.2 The parameter UT1-UTC and its monitoring

Due to the fact that UT1 is a natural time scale directly derived from earth rotation and UTC is a constant synthetic time scale, UT1-UTC reflects all variations and irregularities of the earth's rotation about its z-axis. It is an important information for a variety of applications, such as the determination of GNSS satellite orbits, space craft navigation, spaceflight communication, astronomical and geophysical research, space geodetic applications like e.g. satellite gravimetry missions.
A number of components and interactions within the earth system induce variations of the earth's rotation and of the direction of the rotation axis. The main effects are earth and ocean tides, interactions with the atmosphere, core-mantle interactions and loading effects. The time scales of these effects vary between a few hours and tens of thousands of years and their impacts range from one to one thousand microseconds depending on their magnitudes and geophysical dependencies [Schuh et. al. 2003]. A large part of the variability can be described using geophysical models while a smaller but still significant portion is erratic and unpredictable. An impression of the variability of UT1-UTC during one year gives figure 2.6.

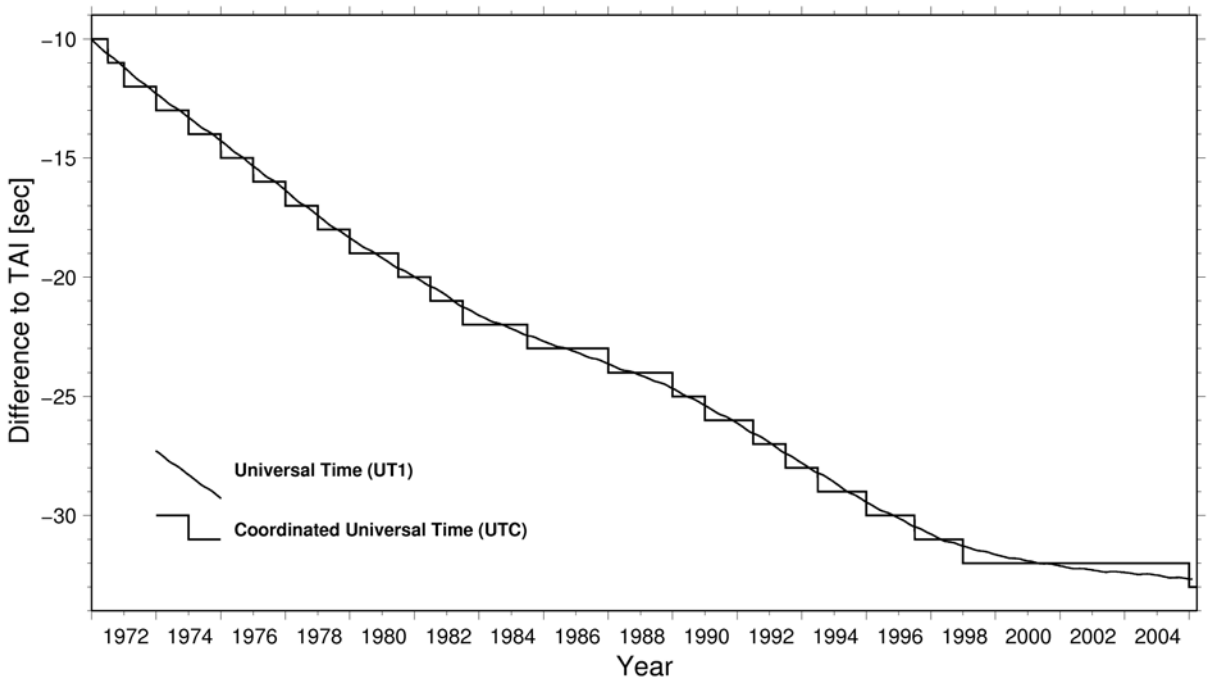

Figure 2.5: Universal Coordinated Time (UTC) following UT1 in integral steps (Data of [IERS C04])

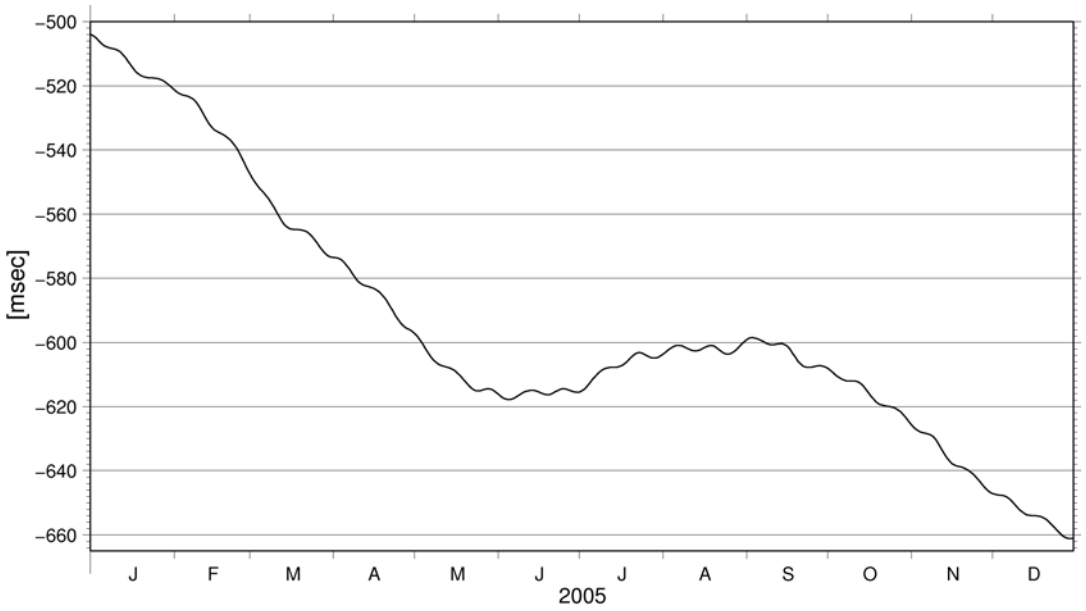

Figure 2.6: Earth rotation variations expressed in UT1-UTC for the year 2005 published in [IERS C04].

For all time-critical applications mentioned above the IERS Rapid/Service Prediction Center provides official EOP values including UT1-UTC on a rapid turnaround basis. Predictions are necessary to fill the time after the last observation. These predictions take all known variations and periodicities of UT1-UTC into account, adequate smoothing methods are applied and short term meteorological forecasts of the Atmospheric Angular Momentum are used. Because the accuracy of predicted UT1-UTC values decreases

with the time-lag to the last observation as specified in table 2.1, contemporary UT1-UTC VLBI results as provided by the *Intensive* series are of primary importance.

Days in Future	σ UT1-UTC $[ms]$	*sigma* UT1-UTC $[cm]$
1	0.130	6.0
5	0.421	19.5
10	0.840	38.9
20	2.53	117.4
30	4.28	198.5
90	8.88	411.9

Table 2.1: Standard Deviation of the differences between the predicted UT1-UTC values of IERS Bulletin A [IERS 2003] and IERS CO4 (considered period March 2003 to February 2004). [Wooden et. al. 2004]

The highest demands on UT1 information in terms of reliability, currency and accuracy are probably made by operators of space craft navigation and communication applications. For example the NASA Deep Space Network requires an EOP accuracy of 30 cm [Oliveau et. al. 1997] for navigation applications, which in case of UT1 corresponds to 0.65 ms. Thus UT1 has to be known with an maximum uncertainty of 0.22 ms ($\hat{=}$ 10 cm), in order to satisfy this requirement with 99.7% of confidence (3-sigma interval). As table 2.1 shows, the uncertainty of a three-day prediction of UT1 is already larger.

Although Very Long Baseline Interferometry is the only geodetic technique that allows a direct measurement of UT1, some other space geodetic techniques can also contribute to combined UT1 series. Satellite techniques like GPS (Global Positioning System) and SLR (Satellite Laser Ranging) allow the determination of the UT1 derivation, called Length of Day (LOD), with a much lower effort than VLBI does. These rapid and close mashed GPS and SLR LOD results are used for a continuous and near-realtime UT1 determination, which cannot be achieved by VLBI.
As the satellite techniques do not have any link to the celestial reference frame, their UT1 results tend to drift away from the nominal values of the earth rotation phase. In e.g. [Thaller 2004] a drift of UT1-UTC derived from GPS LOD estimates relative to VLBI results of about 40 μsec per day was calculated which is equivalent to 1.8 cm per day at the equator (fig. 2.7). For this reason regular VLBI observations are necessary, in order to adjust and maintain the UT1 values derived from LOD measurements.
At the NASA Jet Propulsion Laboratory (JPL) a Kalman-Filter is used for the regular estimation and prediction of UT1-UTC and polar motion components (x_p, y_p) [Oliveau et. al. 1997]. This process is based on measurements of VLBI and SLR and additionally introduces atmospheric angular momentum (AAM) forecasts. The filter uses empirically based stochastic models of the near-term UT1-UTC behavior for interpolation and for short term predictions. The root mean square error of a five day predicted UT1-UTC value compared to UT1-UTC estimates from real observations is stated to be 26 cm [Oliveau et. al. 1997].

2.4 The model of parameter estimation from short term VLBI observations

The basic observing geometry of VLBI observations is depicted in figure 2.8. In the following only the basic concept and the fundamental equations are going to be shortly outlined as far as necessary for a comprehension of this paper. A complete description of the functional model of geodetic VLBI can be

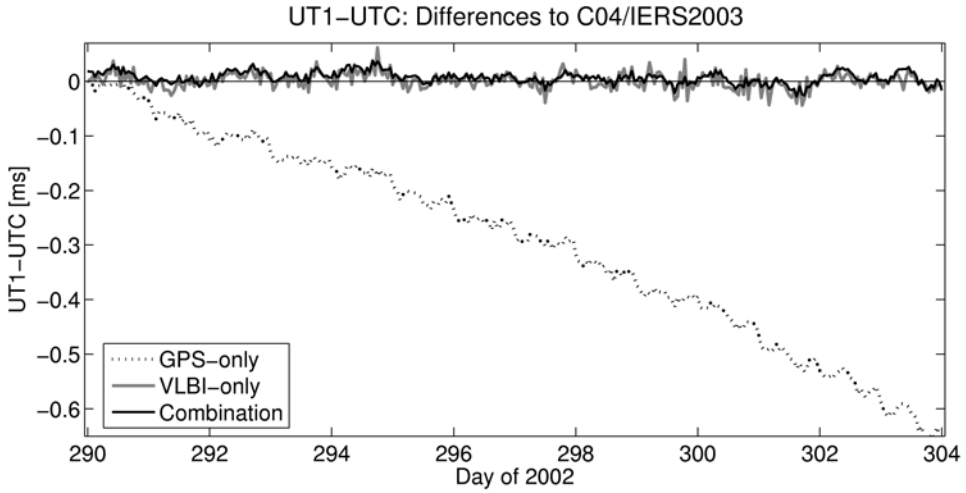

Figure 2.7: Hourly UT1-UTC estimates with respect to IERS C04 [Thaller 2004].

found in e.g. [Schuh 1987]. The stochastic model is discussed in detail in [Tesmer 2004].

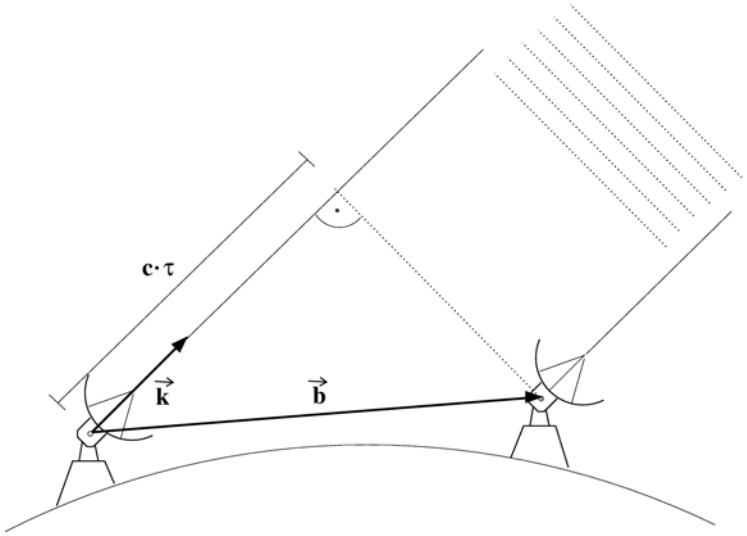

Figure 2.8: Basic observing principle of a single baseline VLBI observation.

The observed time delay τ multiplied by the velocity of light c can be expressed as the scalar product of the baseline vector $\vec{b}$ and the unit vector in source direction $\vec{k}$ and thus

$$\tau = -\frac{1}{c}\vec{b}\,\vec{k}\,. \tag{2.21}$$

The baseline vector $\vec{b}$ is typically given relative to a conventional earth fixed geocentric coordinate system (S_6) while the sources ($\vec{k}$) are usually given in a quasi-inertial celestial reference frame in space (S_2). To express both vectors in the same coordinate system a set of rotations is necessary. Commonly these rotations are divided into precession (matrix P) and nutation (N), earth rotation (S) and the motion of the rotational pole (W) (compare section 2.2.1) so that equation 2.21 turns to

$$\tau_{geom} = -\frac{1}{c}\vec{b_6}\,W\,S\,N\,P\,\vec{k_2}\,. \tag{2.22}$$

In addition to this geometrical part τ_{geom} of the observed time delay, numerous terms need to be added in order to take external and internal effects into account, which influence the measured delay also. These are mainly the time difference between the station clocks (τ_{clock}) and their difference in clock rates (τ_{cl_rates}), the additional time delay due to ionospheric (τ_{ionos}) and tropospheric path delay (τ_{tropo}), deformations of the earth's surface due to earth tides (τ_{tides}) and changing air pressure and water loads (τ_{load}), annual and daily aberration (τ_{abb}), relativistic effects on the radio signal propagation (τ_{rel}) and finally a couple of instrumental error sources (τ_{instr}).
After having applied all these terms the complete geodetic VLBI observation equation looks like

$$\tau_{obs} = -\frac{1}{c}\vec{b_6}\, W\, S\, N\, P\, \vec{k_2} + \tau_{clock} + \tau_{cl\_rate} + \tau_{ionos} + \tau_{tropo} + \tau_{tides} + \tau_{load} + \tau_{abb} + \tau_{rel} + \tau_{instr}\ . \quad (2.23)$$

While the clock parameters as well as the atmospheric path delay has to be estimated from the observations, all other correction terms can be introduced from appropriate models.

The non-linear observation equation has to be linearized in order to estimate the unknown parameters within a Gauss-Markov-Model (e.g. [Koch 1999]). For this purpose partial derivatives are needed for all unknown parameters. Since short term VLBI sessions (see section 3.1) only include a small number of observations only a minimum number of unknowns can be determined. The usual parameterization in the analysis of short term single baseline sessions contains only the compulsory clock offset and its rate, the wet part of the tropospheric path delay per station and of course the UT1-UTC parameter as the main objective. All other parameters need to be known in advance from other observation series or from physical models and are kept fix in the analysis.
The linearized observation equation for the parameter estimation from *Intensive* sessions then is

$$\begin{aligned}(\tau_{obs} - \tau_0) + \epsilon_\tau &= \frac{\partial\tau}{\partial\Delta T_0} d\partial T_0 + \frac{\partial\tau}{\partial\Delta T_1} d\Delta T_1 \\ &+ \frac{\partial\tau}{\partial tropo_A} d\, tropo_A + \frac{\partial\tau}{\partial tropo_B} d\, tropo_B + \frac{\partial\tau}{\partial GAST} d\, GAST\end{aligned} \quad (2.24)$$

with

τ_{obs}		Observed time delay,
τ_0		Time delay calculated from a priori values,
ϵ_τ		Random errors of τ_{obs} (residuals),
ΔT_0	=	$T_{0B} - T_{0A}$ difference between the two station clocks,
ΔT_1	=	$T_{1B} - T_{1A}$ difference between the clock rates of both stations,
$tropo_A$		Tropospheric path delay at station A,
$tropo_B$		Tropospheric path delay at station B,
$GAST$		Greenwich Apparent Sidereal Time, Earth rotation angle.

Partial derivatives for the clock parameters As the clock parameters cannot be estimated as absolute values for each station but only relatively, one station clock is commonly defined as reference clock and its offset and rate are set to zero. For a short term single baseline session the contributions τ_{clock} and τ_{cl_rate} due to the unknown differences in clock offsets and clock rates can be simply expressed by the clock parameters of the second station as

$$\tau_{clock} = T_{0B} - T_{0A} = T_{0B} \quad (2.25)$$

$$\tau_{cl\_rate} = (T_{1B} - T_{1A}) \cdot (t - t_0) = T_{1B} \cdot (t - t_0) \quad (2.26)$$

with

$T_{0A} = 0$	Clock offset of station A as reference,
$T_{1A} = 0$	Clock rate of station A as reference,
T_{0B}	Unknown clock offset of station B,
T_{1B}	Unknown clock rate of station B,
t_0	Reference epoch of T_{0A} .

Consequently the partial derivatives for the unknown clock parameters are

$$\frac{\partial \tau}{\partial \Delta T_0} = \frac{\partial \tau}{\partial T_{0B}} = 1 \quad \text{and} \tag{2.27}$$

$$\frac{\partial \tau}{\partial \Delta T_1} = \frac{\partial \tau}{\partial T_{1B}} = (t - t_0) \, . \tag{2.28}$$

Partial derivatives for the tropospheric path delay The term τ_{tropo} of the observed time delay τ is caused by the refractivity of the troposphere and depends on the temperature, air pressure and humidity. It is useful and common to divide the tropospheric path delay into a hydrostatic and a wet part. Since the larger hydrostatic part can be well calculated from the air pressure and temperature using appropriate atmospheric models only the wet part remains as unknown [NOTHNAGEL 1991].
Using a mapping function (mf) to project the wet delay in zenith direction (zwd) onto the line of sight with elevation angle ϵ the partial derivatives for the tropospheric path delays result as

$$\frac{\partial \tau}{\partial tropo_A} = \frac{\partial \tau}{\partial zwd_A} = -\frac{1}{c} \cdot mf(\epsilon_A) \tag{2.29}$$

$$\frac{\partial \tau}{\partial tropo_B} = \frac{\partial \tau}{\partial zwd_B} = \frac{1}{c} \cdot mf(\epsilon_B) \, . \tag{2.30}$$

Partial Derivative for UT1 As pointed out in section 2.2.1 UT1 is derived from the sidereal time GAST, which is the argument of the rotation matrix S in 2.22. The partial derivative for the estimation of UT1 is (e.g. [NOTHNAGEL 1991], [NOTHNAGEL ET. AL. 1994])

$$\frac{\partial \tau}{\partial UT1} = -\frac{1}{c} \vec{b_6} W \frac{\partial S}{\partial UT1} N P \vec{k_2} \tag{2.31}$$

with

$$S = \begin{pmatrix} \cos(GAST) & \sin(GAST) & 0 \\ -\sin(GAST) & \cos(GAST) & 0 \\ 0 & 0 & 1 \end{pmatrix} \tag{2.32}$$

and therefore with 2.11 and with $\Delta\psi$ = nutation in longitude follows

$$\frac{\partial S}{\partial UT1} = \begin{pmatrix} -\sin(GAST) & \cos(GAST) & 0 \\ -\cos(GAST) & -\sin(GAST) & 0 \\ 0 & 0 & 0 \end{pmatrix} \cdot (C_{sid} + \frac{\partial \Delta\psi}{\partial UT1} \cos(\varepsilon_0)) \, . \tag{2.33}$$

If we express the baseline vector $\vec{b}$ in the true terrestrial (S_5) and the source vector $\vec{k}$ in the true celestial reference frame (S_4)

$$\vec{b_5} = \begin{pmatrix} x_{B_5} - x_{A_5} \\ y_{B_5} - y_{A_5} \\ z_{B_5} - z_{A_5} \end{pmatrix} \quad \text{and} \quad \vec{k_4} = \begin{pmatrix} \cos\delta_4 \cdot \cos h_4 \\ \cos\delta_4 \cdot \sin h_4 \\ \sin\delta_4 \end{pmatrix} \tag{2.34}$$

and neglect the very small term $\frac{\delta\psi}{\delta UT1}$, the partial derivative with respect to UT1 can be given by

$$\frac{\delta\tau}{\delta UT1} = \frac{1}{c}\cdot\vec{b}_5\cdot\frac{\delta S}{\delta UT1}\cdot\vec{k}_4 \tag{2.35}$$

$$= \frac{1}{c}\cdot C_{sid}\cdot\begin{pmatrix} x_{B_5}-x_{A_5} \\ y_{B_5}-y_{A_5} \\ z_{B_5}-z_{A_5}\end{pmatrix}\begin{pmatrix} -\sin GAST & \cos GAST & 0 \\ -\cos GAST & -\sin GAST & 0 \\ 0 & 0 & 0\end{pmatrix}\begin{pmatrix}\cos\delta_4\cos h_4 \\ \cos\delta_4\sin h_4 \\ \sin\delta_4\end{pmatrix}$$

$$= \frac{1}{c}\cdot C_{sid}\cdot\cos\delta_4\cdot[(x_{B_5}-x_{A_5})\cdot(-\sin GAST\cos h_4+\cos GAST\sin h_4) \tag{2.36}$$
$$+(y_{B_5}-y_{A_5})\cdot(-\cos GAST\cos h_4-\sin GAST\sin h_4)]$$

with

h_4	Greenwich hour angle of the radio source,
δ_4	Declination of the radio source transformed by nutation and precession into the true celestial reference frame,
x_5, y_5, z_5	Coordinates of the stations A and B transformed by polar motion into the true terrestrial reference frame.

Statistical quantities as they are used within the following chapters

In order to prevent possible misapprehensions due to the inhomogeneous usage of statistical terminology within different scientific disciplines some statistical quantities as they are used in the following chapters are briefly introduced here.

Simulated sigmas σ Simulated sigmas of the unknown parameters are received from the geometry of the observations as they are predefined within the observing schedule. The matrix of coefficients A containing the partial derivatives for linearizing the functional model is calculated for an *Intensive* session as planned in its schedule. The simulated sigmas then are received by square-rooting the main diagonal elements of the resulting cofactor matrix $Q_{xx} = (A^TA)^{-1}$.
Simulated sigmas are commonly used to compare different schedules for the same session in order to find an observing geometry as best as possible.

Formal errors $\hat{\sigma}$ and correlation coefficients Formal errors are the standard deviations resulting from the process of parameter estimation. The coefficient matrix A now contains all partial derivatives pertaining to the observations as they were really and successfully carried out within the session. Additionally the observations are weighted according to their standard deviations resulting from the correlation process and additional appropriate weighting factors are added in order to receive unity of the estimated variance of unit weight.
The estimated standard deviations, here labeled as *formal errors*, and the estimated correlation coefficients are then taken from the cofactor matrix $Q_{xx} = (A^TPA)^{-1}$. In contrast to the simulated sigmas the formal errors $\hat{\sigma}$ therefore depend on the observing geometry of the real session, on the accuracy of the single delay determinations and on the added reweighting factors.

Weighted Root Means Square For the purpose of comparing two series with each other, the Weighted Root Mean Square (WRMS) after removal of a weighted mean bias is used in the following chapters. The WRMS can be interpreted as a measure of the variability of the calculated differences

between the two compared series about their mean. Its advantage compared to the calculation of a standard deviation is its insensitivity against the choice of weights.

Chapter 3

UT1-UTC observing series

3.1 The two *Intensive* VLBI observing series

Standard VLBI sessions for the determination of earth orientation usually last about 24 hours and involve several globally distributed observing stations. In addition to the earth rotation phase UT1, all other earth orientation parameters (EOP) as well as station coordinates and radio source positions can be determined from these network observations with the drawback, that, at present, data transport limitations inhibit near real-time delivery of the results.
In order to provide VLBI UT1 observations as dense as possible with economic effort and with results as contemporary as possible, short term VLBI sessions, called *Intensives*, have been initiated in early eighties. These special VLBI sessions contain only one single baseline with a large east-west dimension and require only about one hour of observing time with UT1 being their only objective. Thus, these short term single baseline VLBI sessions permit a very quick data transport and postprocessing, and therefore are able to provide UT1 results with a minimized time delay after the observations. A first study on their feasibility and their accuracy was published in [Robertson et. al. 1985].

3.1.1 The observations

Since April 1984 *Intensive* observations are carried out routinely using the baseline Wettzell (Bavaria, Germany) - Westford (Massachusetts, USA), replaced by Wettzell - Green Bank (West Virginia, USA) between March 1994 and June 2000 [Eubanks et. al. 1994]. Since July 2000 the baseline Wettzell - Kokee Park (Hawaii, USA) is regularly used for these short term single baseline *Intensive* sessions instead. These observations (today called INT1) have usually been operated four to five times a week with a special emphasis on a quick data analysis.
Due to the high variability of UT1 and its significance for various applications an independent control as well as a time complement has been aspired to reach more reliability and a dense and complete UT1 series. First investigations in terms of an independent comparison have been carried out in November 1985 using the baseline Wettzell - Kashima (Japan) for a fortnightly project [Yoshino et. al. 1986]. At that time the agreement between the Wettzell - Kashima observations and the results of the regular Wettzell - Westford sessions was calculated to be 0.2 *msec* with a remaining offset of 0.1 *msec*. It was noticed that the agreement between the two *Intensive* baselines highly depends on the accuracy and the consistency of the pole coordinates.
In the years 1989 and 1990 more observations and investigations have been realized using the baseline Wettzell - Shanghai (China) [Nothnagel et. al. 1994] and a mean UT1 agreement between the two single baselines of 50 to 80 μsec was calculated. About ten years later in 1999 a first experiment was carried out using the baseline Wettzell - Tsukuba (Japan) [Nothnagel et. al. 2000]. The formal

errors of the UT1 estimates have been very promising with an average of 12 μsec. An evaluation of the absolute accuracy compared to the Wettzell - Green Banks *Intensives* or to the IERS C04 series was not possible due to an insufficient number of sessions.

Between July and December 2002 twenty Wettzell - Tsukuba *Intensive* sessions were carried out as a pilot project towards a second regular observing routine. In April 2003 the so called INT2 series was launched with regular observations each Saturday using the Wettzell - Tsukuba baseline. In addition regular observations each Sunday are scheduled since August 2004 so that currently six to seven *Intensive* (INT1 and INT2) sessions are operated per week. While the Wettzell - Kokee Park *Intensives* (INT1) are recorded and correlated using the Mark4/5 recording system developed by the National Aeronautics and Space Administration (NASA) [Clark et. al. 1985], [Whitney 2003], the new INT2 sessions use the Japanese K4/K5 recording and correlation system of the Geographic Survey Institute (GSI) [Koyama et. al. 2004].
The time slots of both *Intensive* series have been arranged considering the local time at the observing stations in order to allow the operation during normal working hours. For this reason INT1 sessions are observed between 18:30 and 20:00 UT while the time slot of INT2 sessions is fixed to 07:30 till 09:00 UT. An overview of the current organization of both *Intensive* series is given in table 3.1.

	INT1	**INT2**
Stations	Wettzell (Germany) Kokee Park (Hawaii, USA)	Wettzell (Germany) Tsukuba (Japan)
Length of Baseline	10357.4 km	8445.0 km
East-West-Dimension	10072.3 km	8377.7 km
Observing Days	Monday to Friday	Saturday and Sunday
Time frame of Observations	18.30 to 20.00 UT	07.30 to 09:00 UT
Recording Technique	MARK 4/5	K4/K5 resp. MARK 4/5
Data Transport	e-VLBI	e-VLBI
Correlator	Washington MARK4/5 (NASA)	Tsukuba K4/K5 (GSI)
Scheduler	GSFC Washington D.C.	BKG Leipzig
Avg. Number of Scans per Session (obs./sched.)	16.3 / 17.0	before Aug. 2004 : 18.5 / 19.5 after Aug. 2004: 27.1 / 28.6

Table 3.1: Overview of the current *Intensive* observing routines.

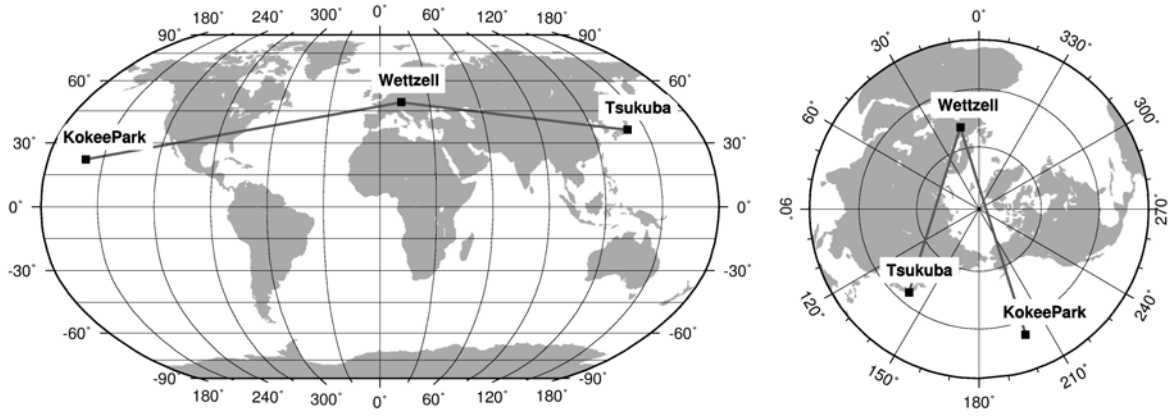

Figure 3.1: Baseline geometry of current *Intensive* observations.

The geometry of the two *Intensive* baselines is depicted in figure 3.1. Both are very long baselines with a large east-west component, which is necessary for a high UT1 sensitivity (cp. section 3.1.2). The INT1 baseline Wettzell - Kokee Park is about one fourth longer than the INT2 baseline Wettzell - Tsukuba and has an about 1700 km longer east-west component so that a higher sensitivity for UT1 can be expected. On the other hand this very large extend of the INT1 baseline limits the simultaneously visible sector of the sky significantly and the observing geometry suffers considerably. Thus, the amount of potentially visible low declination sources for INT1 sessions is much smaller than for INT2. As especially observations of these equatorial sources make the biggest contribution to the estimation of UT1, the advantage due to the larger east-west component is equalized by the limitation of the observing geometry (cp. section 3.1.2).
In the right projection of figure 3.1 it is easy to recognize that the INT1 baseline almost intersects the earth rotation axis and covers 172° of longitudes. Compared to that the INT2 baseline passes the rotation axis in a larger distance and covers only about 127° of longitudes. Additionally it can be seen in the left representation that the INT1 baseline has a north-south dimension which is almost twice as large as for INT2. These geometrical differences may explain parts of the different response of UT1 results to the geometrical input factors like polar motion and nutation (chapter 5).

3.1.2 The observing schedules

The geometrical distribution of the single time delay observations during an *Intensive* VLBI session is predefined in the so called observing schedule. As VLBI radio telescopes are only able to observe unidirectional, single radio sources have to be observed one after the other. Thus, in contrast to GPS observations, VLBI sessions have to be carefully planned in advance in order to reach an appropriate sky coverage. The requirements to an *Intensive* VLBI observing schedule and the impact of the schedule quality on the accuracy of parameter estimation are going to be discussed in the following.

Theoretical considerations on the schedule requirements

The observing schedule is a composition of a number of single quasar observations and only the proper combination of radio sources with different declinations and hour angles and, hence, with changing elevation and azimuth angles allows a successful parameter estimation. From the partial derivatives (section 2.4) of the basic observation equation (equ. 2.23, page 19) some general demands on the design of an *Intensive* observing schedule can be derived and formulated.

From the partial derivation for the **clock offset** (cp. equ. 2.25, page 19) it is apparent that the column of the coefficient matrix connected to ΔT_0 contains constantly ones independently of the observed sources and the used baseline. That means that the accuracy of the clock offset estimation only depends on the number of observations per session and the observing geometry does not have any influence on the clock offset itself.
The column related to the **clock rate** (equ. 2.26) contains the time difference relative to a reference epoch. The estimability of the clock rate therefore improves with the length of the session which is in case of *Intensive* sessions fixed to about one hour. Admittedly, it has to be mentioned that for sessions considerably longer than one hour the stability of the station clocks is not sufficient, so that a second order clock term as additional unknown would be necessary in the case of longer sessions.

From equations 2.29 and 2.30 (page 20) it can be concluded that observations with low elevation angles, which means large values of $mf(\epsilon)$, are essential for the estimation of the **tropospheric path delay**. To be able to distinguish between the elevation dependent tropospheric delay and the clock parameters, which is independent of the elevation, it is necessary to include observations with different elevation angles. Otherwise the correlation between these parameters would be close to one.

From the term $\cos\delta_s$ of equation 2.36 (page 21) it can be anticipated that equatorial sources with low declinations δ_s make the biggest contribution to the estimation of **UT1** while observations of high declination sources do not directly contribute to the UT1 determination. Several tests with *Intensive* observing schedules showed that the inclusion of 20 to 30% low declination sources ($\leq 25°$) in the *Intensive* observing schedules associates with an improvement of the theoretical UT1 sigmas of about 45% in average and 30 to 90 % in total without any significant disadvantage for the other estimated parameters compared to schedules without low declination sources.
Additionally it can be confirmed from equation 2.36 that only the east-west component (differences of the x- and y- station coordinates) of the baseline affects the sensitivity for the earth rotation phase while the difference in the z-coordinates does not have any impact on that. Therefore, the long east-west baselines Wettzell - Kokee Park and Wettzell - Tsukuba are both predestinated for UT1 monitoring.
The other two variables in equation 2.36, $GAST$ and h_4, are predominantly determined by the conditions of *Intensive* sessions itself. The sidereal observing time $GAST$ is, in order to enable a very quick data transport and analysis, limited to a one hour observing window. Because these observing time frames are fixed to Universal Time (UT) for organizational reasons, the respective sidereal time of the *Intensive* sessions varies from day to day by about 4 minutes and by 24 hours during one year. The scheduler itself has no influence on that. In terms of h_4 the scheduler will aim at a lot of different hour angles accompanied by many different declinations in order to induce different values in the design matrix to avoid high correlations between the individual observations. However, this ambition is very much limited by the very small amount of simultaneously visible sources.

General conditions and real procedure of scheduling *Intensive* sessions

General conditions A number of features and basic conditions limit the design of real *Intensive* observing schedules:

- Only a small number of sources is simultaneously visible at both stations of an *Intensive* baseline,
- Only a limited sector of the sky over the observing stations is covered with simultaneously visible sources (fig. 3.2),
- Only a very limited number of low declination sources is available per *Intensive* session,
- The time frame of *Intensive* sessions is fixed to about 1 hour to ensure a contemporary analysis and also with regard to the limited capacities of the observing stations and
- The duration of a single scan is calculated from the flux density of the respective radio source and depending on the sensitivity of the participating telescopes in order to reach the minimum SNR requirements.

Due to the longer extend of the INT1 baseline (10357km), the commonly visible sector of the sky and the amount of sufficiently strong sources is more limited than for INT2 sessions (baseline length 8445km). Especially the availability of equatorial sources, which are essential for the estimation of UT1, is better for INT2 sessions. On the other hand it has to be kept in mind that the sensitivity for UT1 estimation increases with the east-west dimension and therefore with the length of the baseline.

Calculation of scan durations The number of single observations per session is limited by the one-hour duration of the session and by the lengths of the single scans. In order to calculate the necessary scan duration for each radio source, the theoretical SNR has to be determined by [Clark et. al. 1985]

$$SNR = \eta \frac{F_d}{2k} \sqrt{\frac{A_1 \cdot A_2}{T_{S_1} \cdot T_{S_2}}} \cdot \sqrt{2BT} \tag{3.1}$$

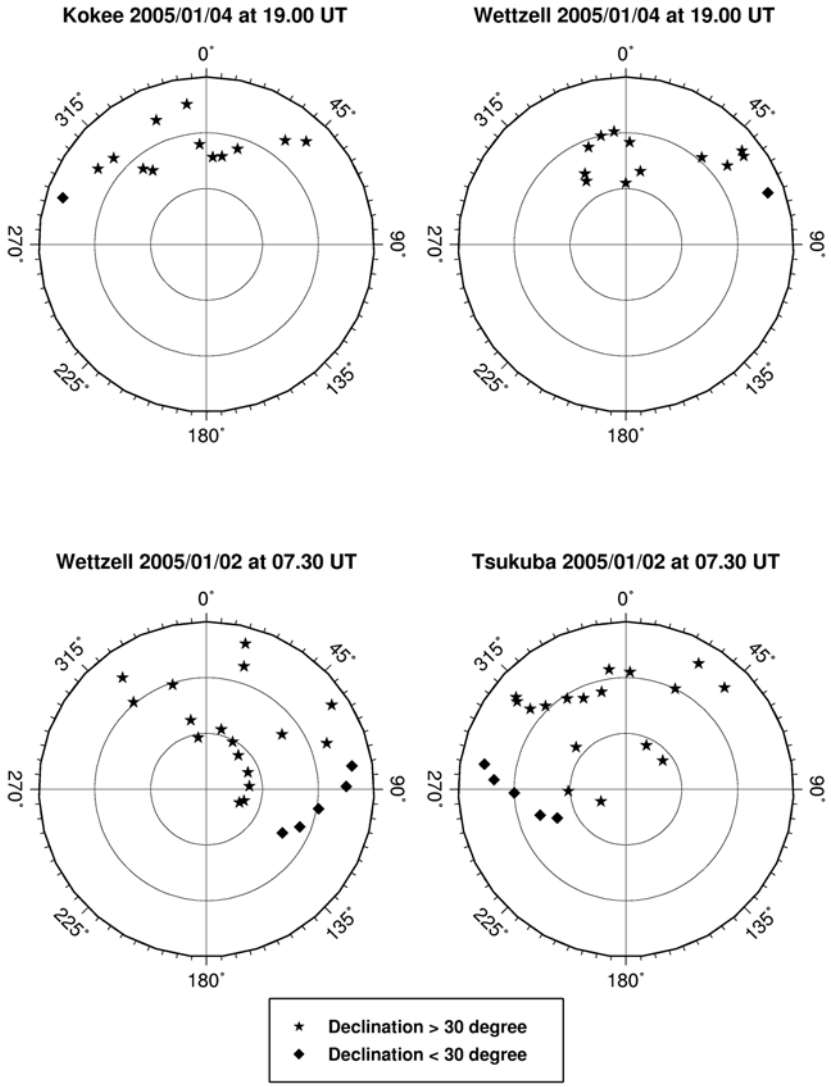

Figure 3.2: Typical situation of simultaneously visible sources at *Intensive* stations for an INT1 (top) and an INT2 (bottom) session. The sources are depicted in skyplots using azimuth and elevation as polar coordinates. The origin of each plot is denoting the zenith direction.

with

η	Loss factor due to digitization,
F_d	Correlated flux density of the observed radio source in Jansky,
k	Boltzmann-constant ($1.38 \cdot 10^{-23} Ws/^\circ K$),
A_1, A_2	Effective areas of the two antennas,
T_{S_1}, T_{S_2}	Noise temperature of the two receiver systems,
B	Effective bandwidth of the registration unit,
T	Coherent Integration Time.

A sufficient SNR has to be required because the standard deviation of the observed time delay τ is

inversely proportional to it:

$$\sigma_\tau = \frac{1}{2\pi \cdot SNR \cdot B} \,. \tag{3.2}$$

The characteristics of both *Intensives* leading to different required integration times are summarized in table 3.2:

	Minimum SNR		Antenna Areas $A_1 \cdot A_2$ $[m^4]$		Bandwidth $[Mhz]$	
	INT1	INT2	INT1	INT2	INT1	INT2
X-Band	20	25	98 696	252 662	680	720
S-Band	15	20			110	120

Table 3.2: Characteristics of both *Intensive* series determining the scan durations.

From equation 3.1 with the numerical values summarized in table 3.2 and under the assumption of similar noise temperatures it can easily be deduced that the integration time of INT1 scans has to be about 2.7 times longer than those of INT2 sessions to reach the same SNR. For that reason INT2 schedules are able to include significantly more single observations within a one-hour session than INT1 schedules. Thus, for INT2 sessions the required minimum SNR can be confidently defined slightly higher than within INT1 sessions because it still can be reached within rather short integration times.

Due to the different basic conditions the two *Intensive* series differ significantly in terms of their schedule design. Additionally two different IVS operation centers currently are in charge of the regular creation of schedules for the two different *Intensive* series, so that the procedures of scheduling are different also.

INT1 scheduling procedure: The observing schedules of the INT1 Wettzell - Kokee Park sessions are created routinely at the U.S. Naval Observatory Operation Center. For that purpose the automatic optimization tool AutoSKED of the SKED software [Vandenberg 1999] is used and the optimization procedure primarily focuses on the sky coverage. Each session lasts one hour and contains 14 to 20 single observations. After the automatic procedure of scheduling the schedules are checked if equatorial sources are included and if necessary and possible low declination sources are manually added. The minimum scan duration is fixed to 40 sec and the SNR requirements are determined to be 20 for X-Band and 15 for S-Band.

INT2 scheduling procedures: The schedules of the Wettzell - Tsukuba INT2 series were created at the Geodetic Institute of the University of Bonn until August 2005 and since then at the Bundesamt für Kartographie und Geodäsie (BKG) in Leipzig (Germany). For the time between April 2002 and Juli 2004 the schedules were prepared manually using the SKED program. The main focus during the manual scheduling procedure was on the sky coverage at both stations and additionally on the inclusion of equatorial sources as well as low elevation observations. The manually created schedules were evaluated and compared using the normal equation matrices created by the SOLVE software [CALC/SOLVE] from the geometry of the schedule. Out of this, (cp. page 2.4) simulated sigmas for the unknown parameters (atmospheric path delays and UT1-TAI) were calculated and different schedules for the same session were compared.
The sessions in this period of time usually lasted about 70 minutes and each contained 20 scans. The minimum scan duration was fixed to 120 seconds in order to avoid any loss of scans during the correlation process. The SNR requirements have been fixed to 25 for X-Band and 20 for S-Band. The sources are selected from a special source catalog for geodetic VLBI sessions provided and regularly updated by the Goddard Space Flight Center.

Reconsideration and improvement of INT2 scheduling routine: In August 2004 the strategy of scheduling INT2 sessions was changed in order to improve the exploitation of the session duration and the sky coverage. Additionally the procedure was changed over to automatic optimization using AutoSKED with manual post-editing in order to reduce the manual work.
A minimum scan duration fixed to 120 seconds is much more than the minimum integration time needed to achieve a SNR sufficient for a reliable delay determination [Clark et. al. 1985] and thus quite often led to an unnecessary high SNR. In order to allow more observations per session it was therefore aimed to a reduction of the individual scan lengths. To evaluate the effect of a reduced scan duration on the delay determination a test correlation of a standard INT2 session was carried out. The integration times of all scans with a SNR higher than 40 for X-band and 30 for S-band were halved and correlated separately. With half of the observing time a decrease of SNR by $\frac{1}{\sqrt{2}}$ has to be expected, which would still satisfy the SNR requirements for a correct correlation. 16 of the 20 scans of the tested database matched these requirements and were halved. In so doing a test database was built with lower SNRs but a higher number of individual scans.

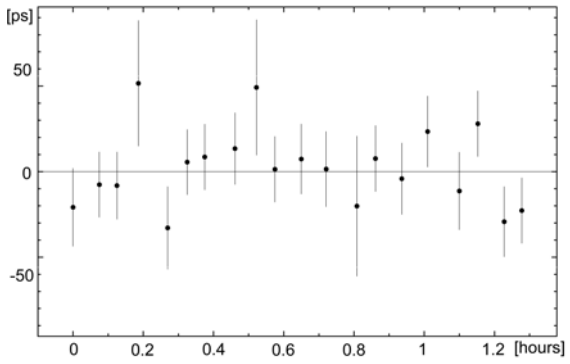

Figure 3.3: Delay residuals of $04APR17XK$ with original scan durations.

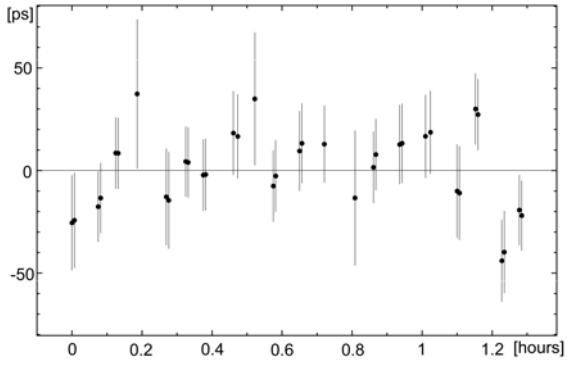

Figure 3.4: Delay residuals of $04APR17XK$ with half scan durations.

The result of the UT1 estimation did not change significantly after the bisection of most of the scan lengths. The difference was only $-0.9\,\mu sec$ which corresponds to $-0.4\,mm$ at the equator and therefore far below the noise level. Fig. 3.3 and fig. 3.4 show the delay residuals after a standard analysis of the original and of the modified database. The depicted error bars represent the standard deviations of the single delay determinations resulting from the correlation process.
It can be seen in figure 3.4 that the residuals and their standard deviations of both parts of each halved scan correspond quite well and the differences are always below $5\,ps$. Thus, the reduced scan duration of each scan does not have a significant impact on the delays resulting from the correlation process. This also shows the very high precision of the correlation procedure because obviously two independent scans observed under almost identical conditions, like the two halves of a split long scan, lead to almost equal delay residuals. An overview of the numerical results of this experiment gives table 3.3.
The standard deviations resulting from an analysis using all 36 observations (second line of table 3.3) show a noticeable improvement compared to the original dataset with 20 observations. This improvement has to be expected from the square root law only in case of uncorrelated observations. Although it has to be assumed that the two observations of each split scan are highly correlated, they apparently improve the parameter estimation noticeably. The results using only the first or only the second halves (third and fourth line) fit quite well to each other and, thus, show that shorter scan durations do not endanger the estimated results.

This analysis has been taken as argument for the practicability of a reduction of the minimum scan

	$\#obs$	$UT1-TAI$ $[msec]$	σ_{UT1} $[\mu sec]$	Atm_{Ts} $[ps]$	σ_{AtmTs} $[ps]$	Atm_{Wz} $[ps]$	σ_{AtmWz} $[ps]$
Full scan lengths	20	-32449.0636	5.55	368.44	5.98	159.35	3.21
All halved scans + 4 unsplit original ones	36	-32449.0627	3.95	368.97	4.48	157.21	2.19
Only first halves + 4 unsplit original ones	20	-32449.0614	5.71	368.94	5.75	157.73	3.21
Only second halves + 4 unsplit original ones	20	-32449.0626	5.51	368.13	5.55	157.70	3.09

Table 3.3: Results of the correlation experiment towards a reduction of the minimum scan lengths.

	MIN SCAN $[sec]$	Scans per Session in average			Standard deviation of UT1	
		Schedule	Measured	Analysis	Simulated from schedules $[\mu sec]$	Estimated from observations $[\mu sec]$
Before Aug. 2004	120	20	19.4	18.4	4.8	11.9
After Aug. 2004	60	28.1	27.6	25.6	4.2	8.8
Improvement		40 %	41 %	39 %	12 %	26 %

Table 3.4: Effect of the scan duration reduction within the INT2 observing schedules since August 2004.

duration from 120 to 60 sec in order to profit from a considerably increased number of single observations per session accompanied by an improved sky coverage. The beneficial effect of this change on the formal errors of the UT1 estimates can also be verified considering the regular INT2 sessions before and after the change (figures 3.9 and 3.8, page 35). While the mean number of scans per session was increased by about 40 % , the mean formal error of UT1 estimates improved by about 26 % (table 3.4).

Operating experiences on scheduling A comparison of the number of scheduled observations of both *Intensive* series with the number of successful scans used in the analysis shows an average loss of 5% (INT1) to 8% (INT2) of the scans. That means that on average 1 to 2 scans of each schedule are lost due to different problems during observation, data recording, correlation or outlier detection. One consequence from that is that the scheduler should ensure, that the very important observations of low declination sources are included in a sufficient quantity, so that a loss of a few scans does not endanger the success of the whole session.

The scheduling procedures are not quite optimal so far (state September 2005) because the usage of the current versions of AutoSKED requires a manual post-editing in order to ensure a sufficient amount of low declination sources. The optimization procedures implemented in AutoSKED are geared to schedule global 24 hour VLBI sessions and therefore are not suitable for the preparation of proper 1 hour single-baseline schedules with an optimized geometry for the estimation of *Intensive* unknowns. Experiences with the regular creation of INT2 schedules showed that the manual substitution of two to four single scans by low declination sources may improve the simulated sigmas (compare page 21) by 15 % to 35 %. Although the schedules derived this way are significantly better than those directly created by AutoSKED, they are still not optimal because no real optimization algorithm is used for the manual

improvements.

The simulation option of SOLVE, used for the evaluation and comparison of different schedules, creates the normal equation matrix from the geometry of the scheduled observations. From its inversion simulated standard deviations for the unknown parameters can be derived and used for evaluation. Considerations on the significance of these simulated sigmas however show no clear correlation between the simulation and the formal errors resulting from the real observations. Neither *Intensive* UT1 results with extraordinary large formal errors or with large deviations can be referred to bad simulations nor very precise UT1 results with very small formal errors are based on schedules with markedly excellent simulations. Such correlations between simulations and real results are not detectable in both *Intensive* series. In order to illustrate this, the simulated and the empirical UT1 standard deviations for one year of INT2 sessions are depicted in figure 3.5.

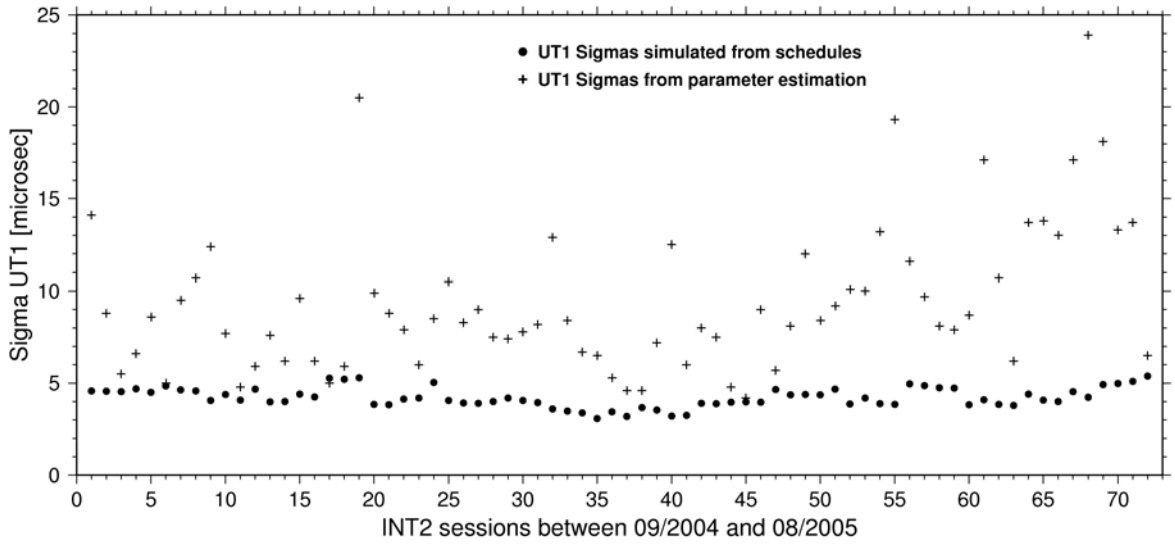

Figure 3.5: Simulated and empirical standard deviations for all INT2 sessions between 2004/09 and 2005/08.

The reason for the missing correlation is, that due to the very low number of observations *Intensive* sessions are highly dependent on each single scan. Any loss of observing data and any low quality delay determination changes the situation significantly and the simulation of the original schedule becomes void. For this reason the simulations are a proper tool to compare different schedules of the same session in order to find the best, but they are not suitable to predict the final absolute accuracy of a sessions.

3.2 Analysis of *Intensive* sessions

3.2.1 Operational analysis procedures

The regular *Intensive* observations are currently analyzed by various institutes and IVS Analysis Centers for diverse applications proceeding different analysis strategies and using different software packages. These individual solutions are used as input data for various combined products of Earth Orientation Parameters satisfying different requirements in terms of currency and accuracy and attending various application areas.
The International Earth Rotation and Reference Systems Service (IERS) is the official institution responsible for the computation and dissemination of earth orientation parameters. Especially for the needs of

time critical applications the IERS operates the IERS Rapid Service/Prediction center hosted by the US Naval Observatory (USNO) in Washington D.C.. Here daily the most current EOP computations and predictions are computed and published as IERS Bulletin A [IERS Bull. A]. It is primarily intended for real-time applications like high-accuracy navigation and positioning and it is used as fundamental information for the transformation of GPS broadcast ephemerids into an earth fixed system. The IERS rapid series is a combination product created from analysis results of VLBI 24 hour network sessions, VLBI *Intensive* sessions, Satellite Laser Ranging (SLR), Global Positioning System (GPS) and Lunar Laser Ranging (LLR).
In terms of the earth rotation component UT1 the situation is rather different because VLBI is the only technique among them which is sensitive to UT1. The results of VLBI 24 hour network sessions currently cannot be available earlier than 14 days after the observation and in order to minimize the time span of prediction the contemporary results of VLBI *Intensive* sessions are of particular importance. With their dense sequence of measurements and the possibility of a fast correlation and analysis with short time delays of three to four days after the observation, the *Intensive* UT1-UTC results are a key contribution to the IERS rapid series. For near-term UT1-UTC predictions the most recent VLBI observations and meteorological forecasts of variations in the Atmospheric Angular Momentum (AAM) are used [Wooden et. al. 2004].
Currently three different Analysis Centers with their individual *Intensive* solutions contribute to this rapid combined series: the Goddard Space Flight Center (GSFC), the US Naval Observatory (USNO) and the St. Petersburg University (SPU). A tabular summary on their current analysis strategies is given in appendix A.1.

In addition to these three solutions a number of other analysis centers and institutes calculate and provide *Intensive* UT1-UTC solutions for different scientific or public requirements. All these solutions differ in terms of analysis strategy, software, geophysical models and reference frames. If some of these solutions are taken as input data for a combination process, usually the different input series are adjusted by removing offsets and rates relative to each other and possibly by detecting and excluding outliers. In so doing the consistency with reference frames is lost and the reasons for these removed systematic differences are ignored. Additionally the two different types of *Intensive* observations are treated as one single consistent UT1 series without any check.
In this context the question arises for the impact of different basic conditions on the UT1 results of *Intensive* sessions with special regard to the differences between the two *Intensive* baselines (INT1 and INT2).

As an example the results of the standard solutions of GSFC and SPU for a three months period (2005 May 1st to July 31st) are represented in figure 3.6. It can be seen that even within one single solution systematic differences up to a few tens of microseconds (GSFC) between the UT1 results of the two *Intensive* baselines may appear in certain intervals, while the results of the same interval may look totally different in another solution (SPU).
A measure of the quality of the different solutions is given in section 4.1 on the basis of the consistency of the results of the two *Intensive* series.
To find possible inconsistencies affecting the *Intensive* UT1 results of the two different baselines, the impacts of solution features have to be investigated separately (chapter 5).

3.2.2 Precision of both *Intensive* observation series

The precision or uncertainty of an experimental result measures the quality of the parameter determination. It also specifies the repeatability of the experiment.
A measure of the precision is the estimated standard deviation $\hat{\sigma}$ of an estimated parameter (e.g. [Koch 1999], p. 96). The standard deviation of an unknown parameter is a result of the parame-

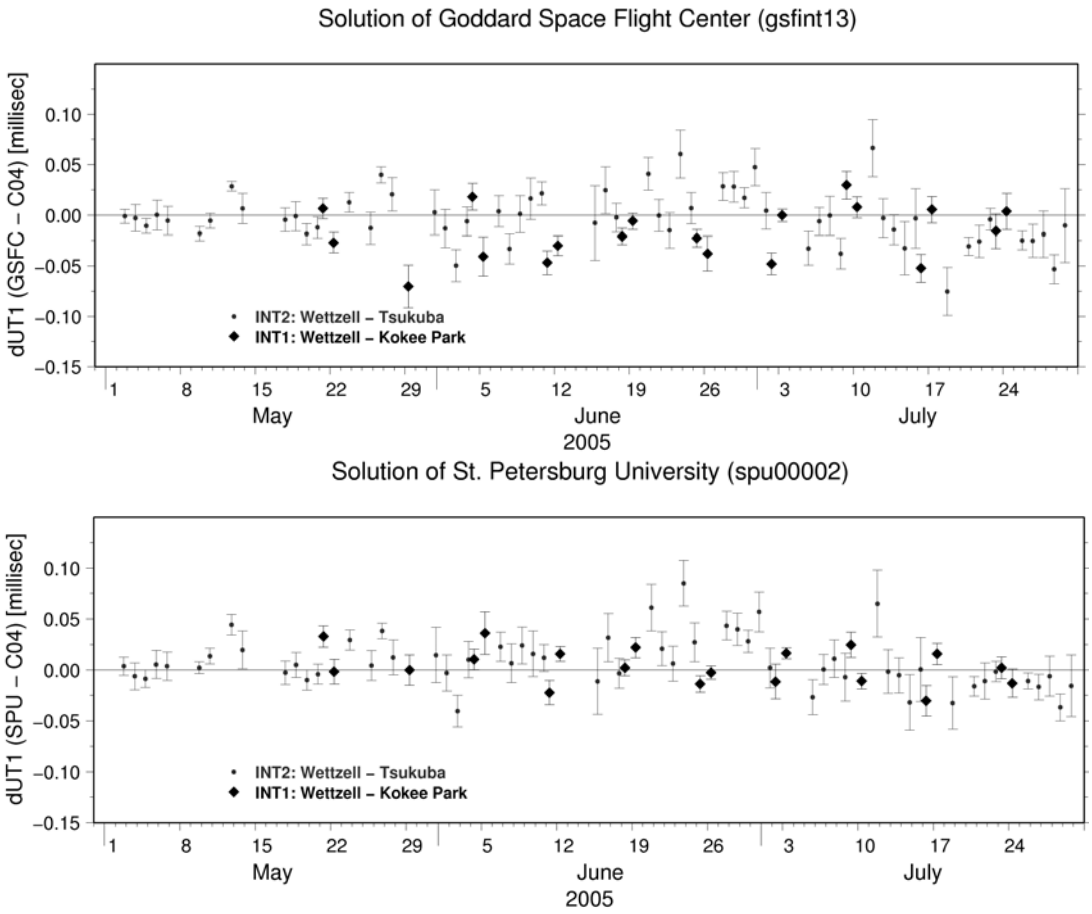

Figure 3.6: Solutions of GSFC (top) and SPU (below) of *Intensive* sessions exemplarily for the period between 2005, May 1st and July 31st. For the purpose of presentability the results are depicted with respect to a quadratic interpolation of C04 [IERS C04].

ter estimation from an overdetermined system (e.g. [Koch 1999], p. 163) and it depends on the scatter of the individual observations, their number and weights and on the quality of the physical modeling.
Within the analysis of VLBI sessions generally a reweighting procedure is carried out in order to achieve conformity of theoretical (usually =1) and empirical variances of unit weight. For that purpose a reweight noise is computed and added in quadrature to the standard deviation of the determined time delays such that the resulting empirical variance of unit weight is approximately equal to 1. The main diagonal of the inverse normal equation matrix then directly contains the variances of the estimated parameters. Their square-roots are the standard deviations customarily also named *formal errors* (cp. page 2.4).
A comparison of the estimated standard deviations of UT1 results of the two *Intensive* series INT1 and INT2 is shown in fig. 3.7. For this overview a total of 580 *Intensive* sessions in periods with coexistence of INT1 and INT2 observations was analyzed. In these time frames (08/2002 - 12/2002 and 04/2003 - 04/2005) 458 INT1 and 122 INT2 sessions are available.
These charts show that both *Intensive* UT1 series have similar levels of standard deviations averaged over the considered time frames, both being appropriate for the determination of UT1. It is also noticeable that over 70% of the results of the INT2 sessions have a standard deviation below 10 μsec while only about 33% of INT1 results are precise like this. A large part of this fact can be explained by the number of observations per session which on average is higher within the INT2 sessions than within INT1. The num-

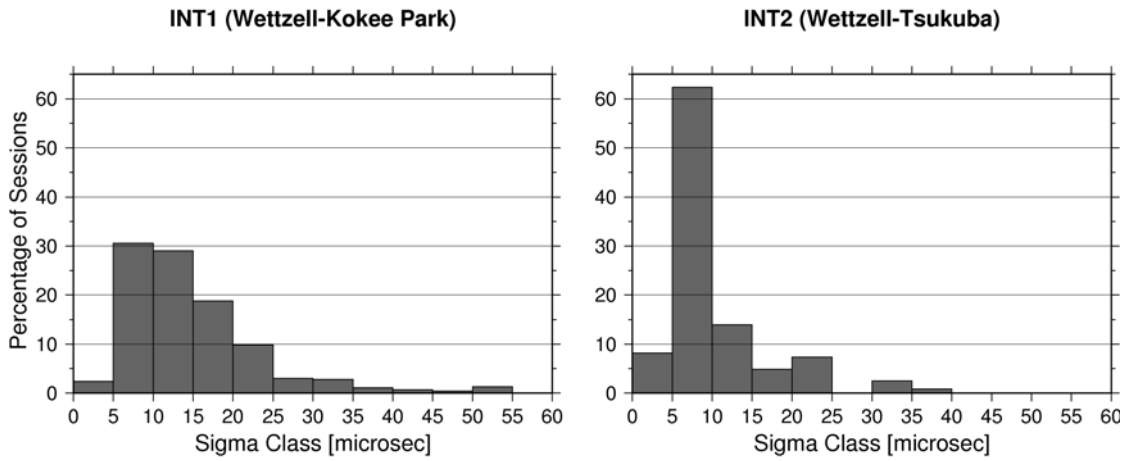

Figure 3.7: Histogram of the estimated standard deviations of UT1 results (Used Data: 08/2002 - 12/2002 and 04/2003 - 04/2005).

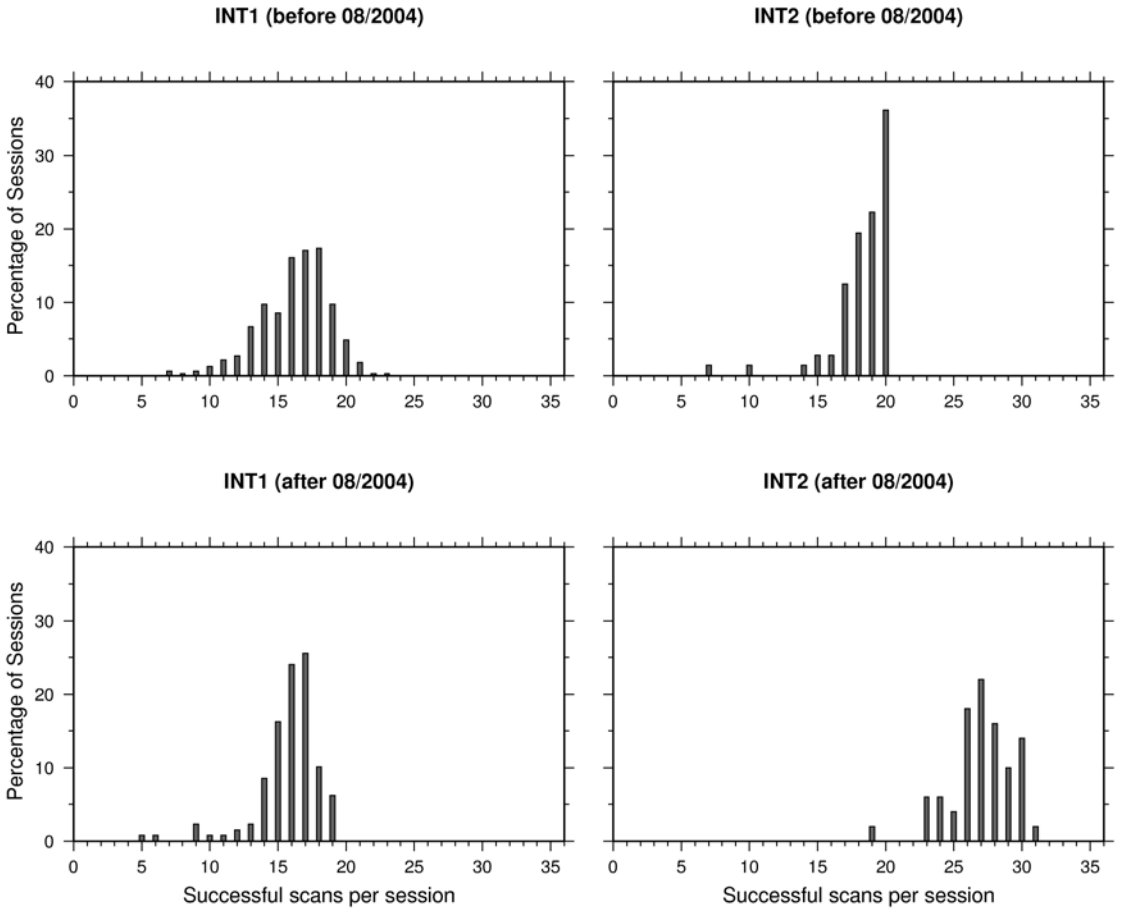

Figure 3.8: Histogram of the number of observations per session (Used Data: 08/2002 - 12/2002 and 04/2003 - 04/2005).

ber of single observations per 1-hour session is mainly dependent on the required scan durations needed to reach a minimum signal to noise ratio (SNR) (see also equation 3.1 on page 26 and table 3.2 on page 28).

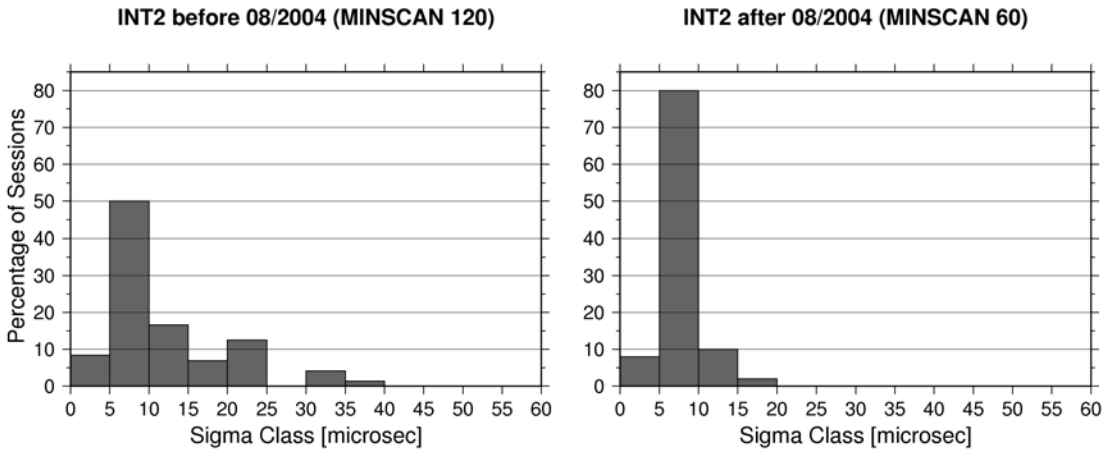

Figure 3.9: Histogram of estimated UT1 standard deviations before and after changing the INT2 scheduling procedure.

In 08/2004 the procedure of scheduling INT2 sessions (section 3.1.2, page 29) has been changed in such a way that the required minimum scan duration has been halved and thereby the number of observations per sessions is increased by about 50 % (fig. 3.8). As a consequence the precision of the INT2 results expressed by their formal errors has been improved considerably (fig. 3.9). The general setup of the INT1 observing schedules and consequently the average of the standard deviations has not been changed.
Considering all sessions after the INT2 scheduling improvement, the new *Intensive* series INT2 using the baseline Wettzell - Tsukuba shows a significantly lower level of formal errors than the long-dated Wettzell - Kokee Park INT1 series. After August 2004 almost 90% of the INT2 UT1 results have formal errors lower than $10\mu sec$ which is achieved only for 30% of the INT1 sessions. 90% of the formal errors of INT1 UT1 results are below 30 μsec. A UT1 difference of $10\mu sec$ is equivalent to 4.6 mm at the equator.

Correlations between estimated parameters In addition to the formal errors also the correlation coefficients as a measure of separability between the estimated parameters are a quality feature for the session performance and for the reliability of the results. As an example the correlation coefficients of the Multi-Intensive sessions (description section 3.3) for both single baseline series are listed in appendix B.
Since UT1 is the only objective of *Intensive* sessions, solely the correlations between UT1 and the auxiliary parameters are of prior interest, while the correlations among the auxiliary parameters are rather uncritical. It turns out that the correlations connected to UT1 generally are on an uncritical low level. Nevertheless, in few sessions single UT1 correlation coefficients appear, that are rather large. For example session no. 9 in table B.1 has extraordinary high correlations between UT1 and the atmospheric path delay, as well as UT1 versus the clock offset. This session has only 14 successful scans of 17 originally scheduled ones and, unfortunately, two of the three lost scans are low declination sources. It can be expected that this loss of data causes the remarkable high correlations.
As almost all correlation coefficients related to UT1 are fairly low, it can be followed that UT1 is sufficiently separable from the other unknown parameters and most of the sessions summarized in the tables B.1 and B.2 have a suitable observing geometry. This conclusion is also valid for the regular *Intensive* sessions, because the Multi-Intensive sessions conform with normal *Intensive* sessions equally distributed

over one year (cp. section 3.3.1).

3.3 The Multi-Intensive projects

In order to study the accuracy and consistency of UT1 results of short term VLBI sessions two extra experimental VLBI sessions were carried out in June and July 2004 which were specially set up for research purposes. The observations of these two sessions form a compact and representative dataset and an ideal basis for empirical studies.

3.3.1 The observations

The so called Multi-Intensive sessions (short names: MIN01 and MIN02) are composed of a 24 hours series of consecutive usual *Intensive* sessions each one lasting about 1 hour and using the baselines Wettzell - Kokee Park (MIN01) and Wettzell - Tsukuba (MIN02) respectively. At the same time independent 24 hour VLBI sessions including five (MIN01) or six (MIN02) globally distributed observing stations were carried out in parallel. An overview of both Multi-Intensive sessions is given in table 3.5 and figures 3.10 and 3.11.

	MIN01	**MIN02**
Date	2004.06.16	2004.07.07
Intensive	Wettzell - Kokee Park	Wettzell - Tsukuba
Multi baseline	Algopark, Fortaleza, Gilcreek, Tsukuba, Westford	Algopark, Fortaleza, Gilcreek, Ny Alesund, Kokee Park, Westford

Table 3.5: The Multi-Intensive sessions MIN01 and MIN02.

The schedules of the consecutive one hour *Intensive* sessions were created following the identical procedures and conditions as in usual INT1 and INT2 sessions (cp. section 3.1.2). The 24 hour schedules of the simultaneous network sessions were created using AutoSKED with the sky coverage as primary optimization parameter. That way a representative data set of *Intensive* sessions of both single baselines was generated and simultaneous global network sessions suitable for comparisons are available.

As the time frames of the standard regular *Intensive* sessions are fixed to Universal Time (cp. section 3.1.1), their respective sidereal observing time shifts by approx. 4 minutes from day to day and thus by 24 hours during one year. Consequently the consecutive one hour sessions of the Multi-Intensive projects geometrically represent 24 (for MIN01) and 21 (for MIN02) *Intensive* sessions equally distributed over one year. Therefore they provide together with the simultaneous global network sessions different possibilities of analysis and so various objectives:

1. The series of consecutive usual 1-hour single baseline *Intensive* sessions spanning 24 hours can give information about the reliability of UT1-UTC results of short term sessions. As the variations of UT1-UTC within one hour are restricted by laws of nature, larger and erratic steps between the UT1 results of two successive sessions can be interpreted as an error in measurement or analysis.

2. The geometries of the consecutive 1-hour sessions may be taken as a sample representing regular *Intensive* sessions evenly distributed over one year. This is because the sidereal observing times of regular *Intensive* sessions varies during one year by 24 hours due to the difference between solar and sidereal time (compare figure 2.2, page 10). For this reason the Multi-Intensive single baseline sessions provide a representative data pool to study the impact of deficiencies of models and a priori values on the UT1 results and their dependency on the sidereal epoch (chapter 5).

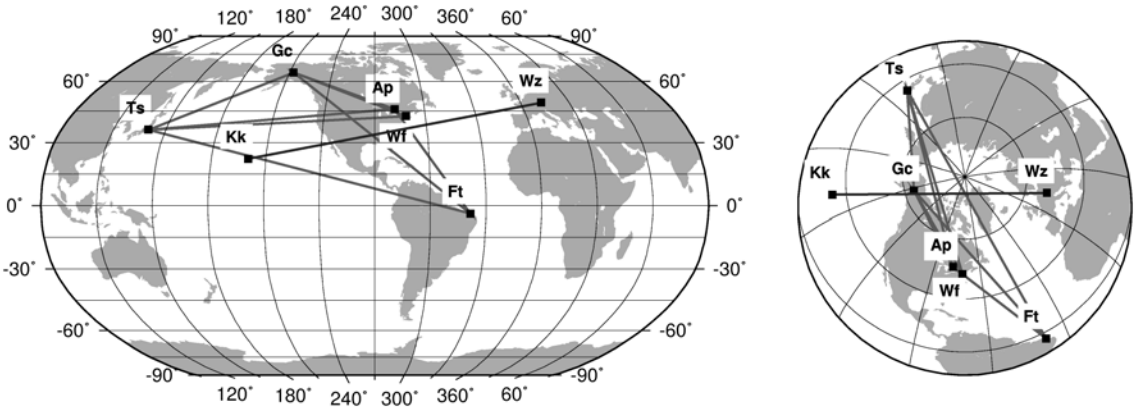

Figure 3.10: Stations involved in the Multi-Intensive project MIN01.

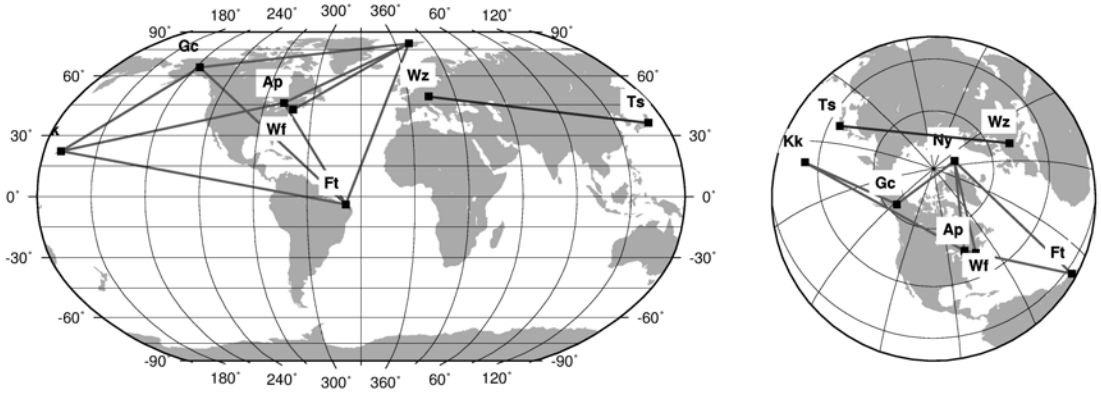

Figure 3.11: Stations involved in the Multi-Intensive project MIN02.

3. The accuracy of UT1 estimates from a 24 hour multi-baseline session is expected to be better than the accuracy of UT1 from a 1-hour single-baseline session. The differences between the UT1 angles derived from the 1 hour *Intensive* sessions and UT1 from a global network session derived at the same epoch can therefore be considered to be dominated by the errors of the short term sessions (section 4.2).

4. The continuous dataset of consecutive *Intensive* sessions is an ideal basis for investigations on the impact of different methods of correcting subdaily EOP variation on the UT1-UTC results (section 5.4).

3.3.2 Analysis procedure and results

The general conditions of the analysis procedures applied to the global network and *Intensive* sessions of the Multi-Intensive experiments are summarized in table 3.6. The fixed pole position within the *Intensive* analysis has been adapted to the estimates of pole components from the corresponding global network session in order to ensure identical intermediate reference frames. The terrestrial and the celestial reference frames have been kept identical as well as the used models for nutation and precession. In order to exclude the different influences of high frequency EOP corrections from these investigations no

correction has been applied during this analysis.

	24 hour network sessions	**1 hour single baseline sessions**
No. of stations	5 (MIN01) ; 6 (MIN02)	2
Software	CALC / SOLVE	CALC / SOLVE
Adjust. method	Least Square	Least Square
Parameterization:		
Polar Motion	Segmented offsets in 1 hr intervals Constraints: 1 mas/day # 50	-
UT1-UTC	Segmented offsets in 1 hr intervals Constraints: 0.67 ms/day # 25	One offset per session No constraints # 1
Zenith Wet Delay	Segmented offsets per station in 1 hour intervals Constraints: 40 ps/hour # 125 (MIN01); 150 (MIN02)	One offset per station per session No constraints # 2
Clock	Global rate and 2nd order terms and segments in 1 hr intervals Constraints: 0.02 psec/sec Ref. Clock: WESTFORD # 108 (MIN01); 135 (MIN02)	Offset and rate per session No constraints Ref. Clock: WETTZELL # 2
Total no. of parameters	308 (MIN01); 360 (MIN02)	5
No. of observations	1176 (MIN01); 843 (MIN02)	14 to 21
Tropos. Mapping	Niell Map. Funct.	Niell Map. Funct.
Dry Tropos.	Modif. Saastamoinen	Modif. Saastamoinen
Gradients	No	No
TRF	VTRF2005	VTRF2005
CRF	ICRF	ICRF
Apriori Polar Motion	usno_finals.erp	usno_finals.erp adapted to estim. of network sess.
Nutation	IERS96	IERS96
Precession	IERS96	IERS96
Hi-Frequ. EOP	NONE	NONE

Table 3.6: Analysis Strategy of Multi-Intensive sessions. (# $\hat{=}$ Number of unknowns)

The results of the single baseline *Intensive* observations from this analysis of MIN01 and MIN02 are depicted in figures 3.12 and 3.13.
Directly noticeable is a subdaily signal overlaying a smooth long term progress. Additionally it is visible that the formal errors of the single UT1-UTC estimates vary significantly from session to session. Furthermore, especially in MIN01, steps between two consecutive sessions appear which are larger than it has to be expected. [Hefty et. al. 2000] calculated a maximum UT1 amplitude of 7.5 μsec for 6 hour periods and about 15 μsec for 12 hours. Thus, maximum subdaily differences of about 45 μsec have to be expected.

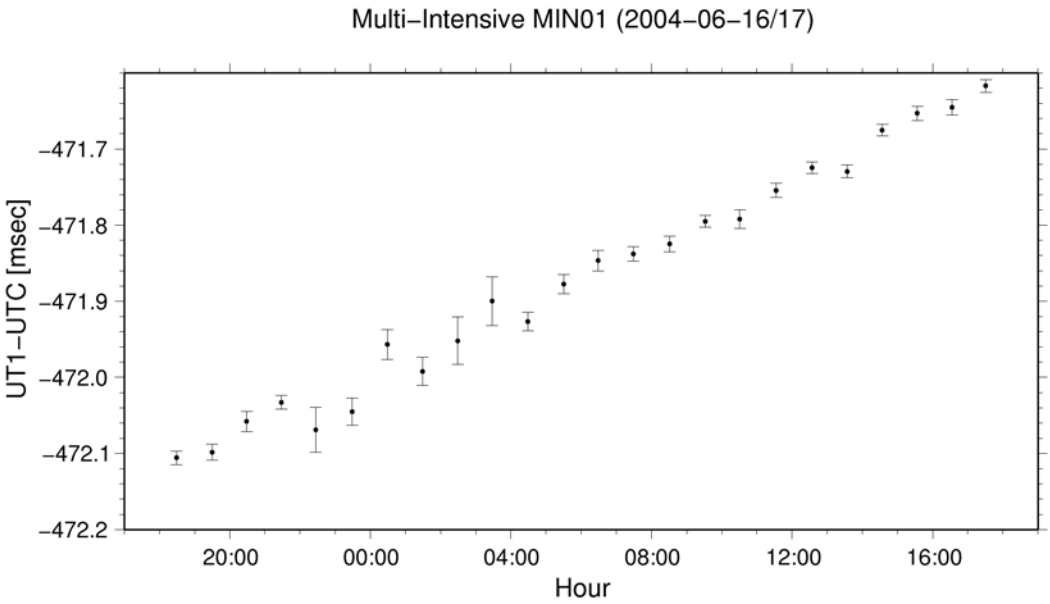

Figure 3.12: Standard Solutions of the single baseline sessions of MIN01.

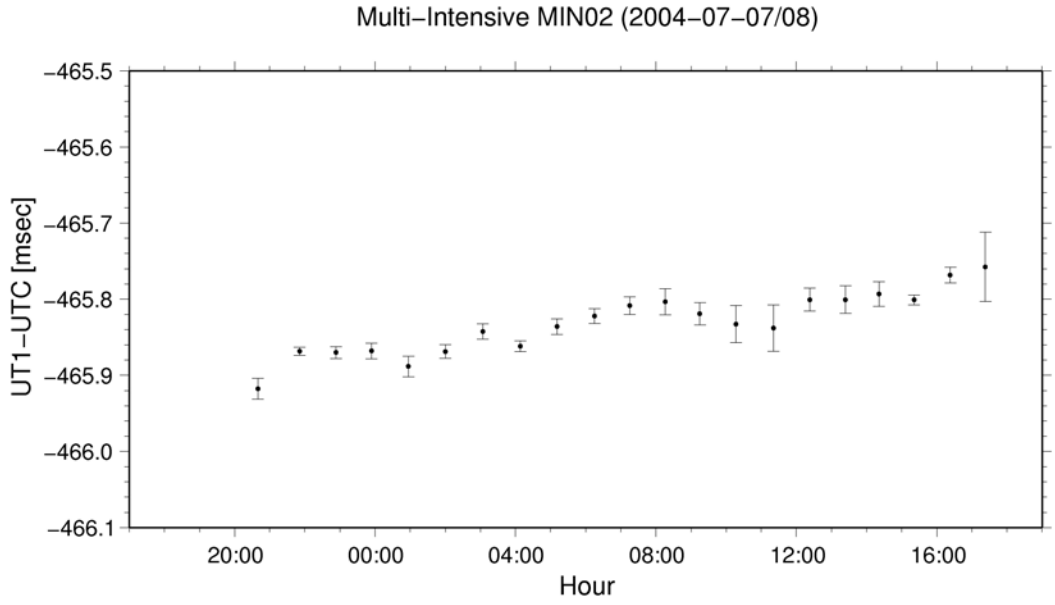

Figure 3.13: Standard Solutions of the single baseline sessions of MIN02.

Chapter 4

Quality of *Intensive* UT1 estimates

In order to analyze the quality of short term VLBI sessions we need to distinguish between the accuracy of the results and their precision. The accuracy measures the correctness of the results and qualifies how good the values represent the unknown truth. Significantly different is the meaning of precision which is a measure of how well the results are determined internally.
Therefore, if we want to describe the quality of the *Intensive* observation series we need to look at both, accuracy and precision. While precision can be determined from the observations themselves (section 3.2.2), adequate reference data are necessary for the determination of the accuracy. These reference data should be determined by an independent and ideally more accurate observing method. In terms of daily UT1 values no adequate independent reference data are available for a comparison. For this reason, only the agreement between the two independent *Intensive* baselines (section 4.1) and the consistency of *Intensive* UT1 results with those of global VLBI network sessions (section 4.2) can serve as indicators characterizing the quality of *Intensive* UT1 results.

4.1 Comparison of different standard solutions with regard to the consistency of both *Intensive* baselines

The agreement between the UT1 results of two independent *Intensive* baselines can be regarded as a quality factor characterizing the suitability of the respective solution strategy. It can be expressed by a weighted root mean square (WRMS) calculated from differences between the UT1 results of the two baselines referred to equal reference epochs.
Because the reference epochs and the number of sessions are different for the two baselines, an appropriate interpolation or approximation procedure is necessary in order to transform the UT1 values to common reference epochs as precondition for the calculation of differences. In general, INT1 observations are carried out on three to five days a week between Monday and Friday, whereas INT2 sessions solely cover the weekend days. Therefore it is reasonable to apply a proper interpolation or approximation method continuing the INT1 UT1 series over the weekends and to compute offsets of the INT2 values with respect to this INT1 curve.

Transforming the INT1 series to the epochs of INT2 sessions: In search of an appropriate curve continuing the INT1 series during the weekends, several possibilities have been tested. Interpolating splines of different degrees are forced to follow exactly each of the INT1 data points ignoring different formal errors and possible inaccuracies, which may be included in the UT1 results. Therefore an approximating piecewise polynomial approach has to be preferred instead of a simple interpolation. Additional aggravating factors are the inhomogeneous time intervals of INT1 values and the existence of data gaps,

which complicates a proper predefinition of uniformly spaced connection points for an approximating spline.
Tests using a fourth-degree spline approximation covering time periods of 14 days and using different restrictions of differentiability at the connection points showed that degree four is not sufficient for an appropriate approximation of the UT1 behavior within a two weeks interval. This experience also agrees with the periods of UT1 variations induced by earth tides, being the major part of UT1 variations. [YODER ET. AL. 1981] specifies significant tide-induced UT1 amplitudes for periods down to five days and, thus, a polynomial of lower degree than five cannot be sufficient wihtin a 14 days interval.
A shortening of the time intervals for each polynomial is also not efficient, because then an unsatisfying high number of intervals has not enough nodes for an approximation. Increasing the degree of the polynomials leads to bad condition numbers of the normal equation matrix and, thus, to numerical problems during matrix inversion.
In order to overcome these problems with a reasonable effort, individual and independent pieces of fifth-degree polynomials each one covering a period of twelve days have been calculated without any smoothness restrictions connecting it to its neighbor polynomial.
This way the INT1 nodes between Monday and Friday before and after each INT2 weekend are used for the estimation of six unknown coefficients of the fifth-degree polynomials and their standard deviations. Using these estimated coefficients and their estimated standard deviations INT1 UT1 values and their uncertainties can be calculated corresponding to the epochs of the INT2 sessions.
Intervals with less than eight INT1 data points have been excluded from the consideration. The run of the estimated curve is most uncertain in cases with a local extremum exactly during the weekend gap, especially if the curve has very steep flanks before and after the weekend. In order to achieve results as reliable as possible all intervals with a local extremum during the weekend gaps have been excluded from the considerations also.
As an example a short section including two INT2 weekends with their corresponding approximated INT1 polynomials are plotted in figure 4.1.

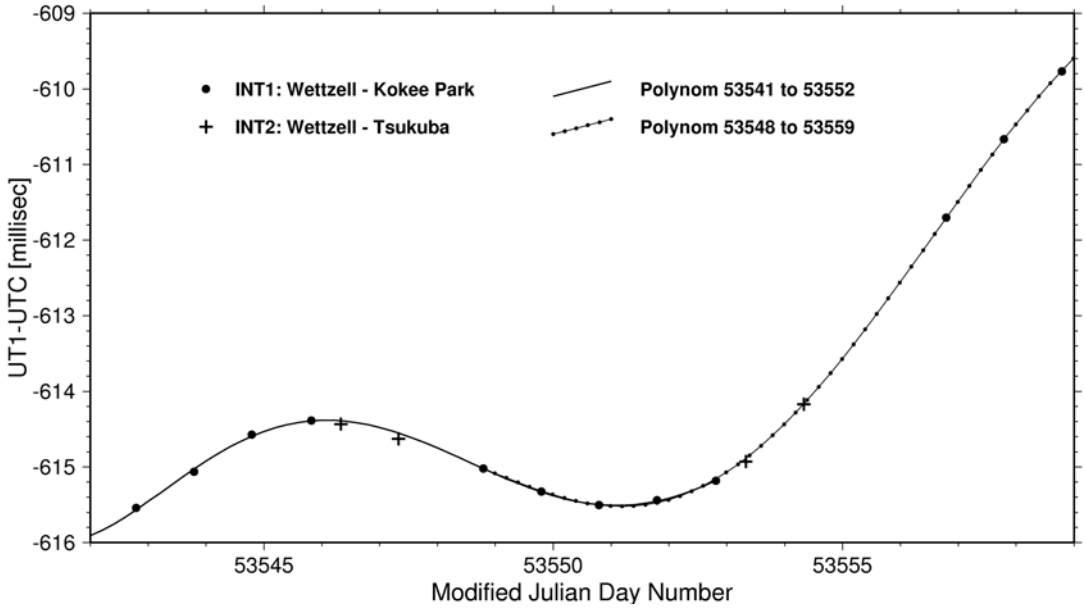

Figure 4.1: Part of the fifth-degree polynomial approximation of the *Intensive* solution of St. Petersburg University (SPU).

Differences between these approximating fifth-degree polynomials and the UT1 values of INT2 sessions

have been calculated from the three solutions contributing to the IERS rapid series described in section 3.2.1. From these differences displayed in figure 4.2 and their formal errors, derived by error propagation of the INT2 formal errors and those of the respective INT1 polynomial value, a weighted mean offset and a weighted root mean square (WRMS) have been derived for each solution series. These numbers can be interpreted as measure of the internal consistency of a UT1 series from both *Intensive* baselines. The weighted mean offsets and WRMS are summarized in table 4.1. As the Analysis Centers started at different epochs to include the INT2 sessions in their analysis procedure, only the period of time (April to December 2005) in which both series were analyzed by all three centers can be used for a comparison.

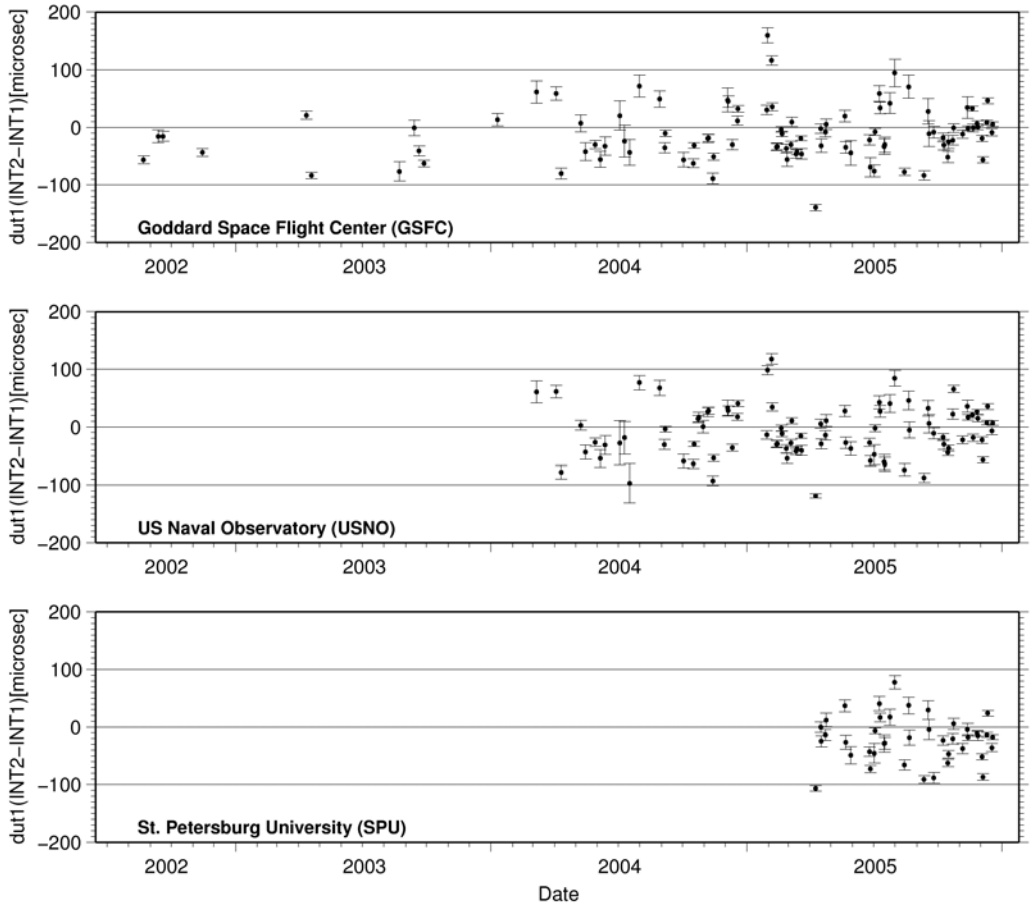

Figure 4.2: Differences of the UT1 results of INT2 sessions with respect to the polynomial approximation of INT1 results depicted for the three input solutions of the IERS rapid EOP product.

	Using all avail. differences			Only April to December 2005		
[μsec]	**GSFC**	**USNO**	**SPU**	**GSFC**	**USNO**	**SPU**
Weighted mean offset	-13.0 ± 4.1	-12.6 ± 4.5	-29.4 ± 6.1	-5.6 ± 5.0	-3.1 ± 5.2	-24.7 ± 5.6
WRMS	39.7	42.2	38.3	31.3	32.8	34.3
No. of differences used	97	90	41	40	41	38

Table 4.1: Offset and scatter for the differences between INT1 and INT2 results calculated for the three solutions contributing to the IERS rapid EOP product (gsfint15.eopi, usn2005c.eopi, spu00002.eopi).

These results show that the solutions of GSFC and USNO contain no significant offset between the two baselines, which indicates the use of highly consistent reference frames as well as polar motion and nutation information. In contrast to that a distinct offset between the two types of *Intensive* observations can be detected in the series of SPU. The most likely reason for this differences is the usage of a less precise terrestrial reference frame within the analysis. A UT1 difference of about 25 μsec corresponds to 1.1 cm at the equator.
The scatter expressed by the WRMS after removal of the weighted mean offset is of equal order of magnitude for all three solutions. Being about 30 μsec the WRMS representing the internal precision of a joint *Intensive* series is considerably worse than the precision pretended by the formal errors of the parameter estimation of each individual observing session (compare figure 3.7 on page 34).
In 2002 Working Group 2 of the IVS aspired a UT1 accuracy from *Intensive* sessions of 5 to 7 μsec to be reached until 2005 [IVS Working Group 2]. The consideration above shows that current *Intensives* are still quite far away from reaching that goal.

4.2 Consistency of *Intensive* UT1 results with global network sessions

The accuracy of a measured quantity indicates its agreement with the true value. Even very precise results with small scatter and small error bars are useless if their accuracy is unknown. Since true values of UT1 are inaccessible and, thus, a comparison of *Intensive* results with nominal values is impossible, an analysis of the conformance with the UT1 results of global VLBI network sessions is of particular interest. The observations of a global network session are completely independent and its UT1 estimates are at least as precise as the single baseline results. It can be assumed that the global network UT1 results are significantly less dependent on a priori polar motion components, because those don't have to be fixed within the analysis, but can be estimated from the observations. Due to their global observing geometry, the network sessions are also much less sensible to nutation insufficiencies as well as small incorrectnesses of station and source positions.

The observations of the Multi-Intensive projects MIN01 and MIN02 (section 3.3) provide an excellent dataset for such investigations. Due to the simultaneously measured single baseline and network sessions, a direct comparison of UT1 results is possible without large interpolation intervals.
In order to compare the UT1-UTC estimates of the hourly *Intensive* sessions with the results of the network session it has to be ensured that the compared UT1-UTC values correspond to identical reference frames defined through station coordinates, source positions, polar motion, nutation and precession models. In terms of the polar motion components the pole coordinates estimated from the respective global network session have been adopted and fixed within the analysis of the short term single baseline *Intensive* sessions. Furthermore both kinds of UT1 estimates have to be referred to identical reference epochs, wherefore a proper interpolation method has to be applied to overcome small differences of epochs. After the separate analysis of the *Intensive* and the network sessions, as described in section 3.3.2 and summarized in table 3.6, differences between the *Intensive* results and those of the global sessions are calculated. In order to assimilate the reference epochs, a quadratic interpolation of the network results onto the epochs of the *Intensive* sessions has been applied. The results of the analysis and the differences are depicted in figures 4.3 and 4.4.

A small weighted mean offset has been removed from the *Intensive* results (table 4.2) and the formal errors of the *Intensive* values have been rescaled in order to reach a realistic proportion of the variance levels. Therefore it has been assumed, due to the characteristics described before, that the UT1-UTC results of the network sessions are at least twice as accurate as those of the *Intensive* sessions. In order

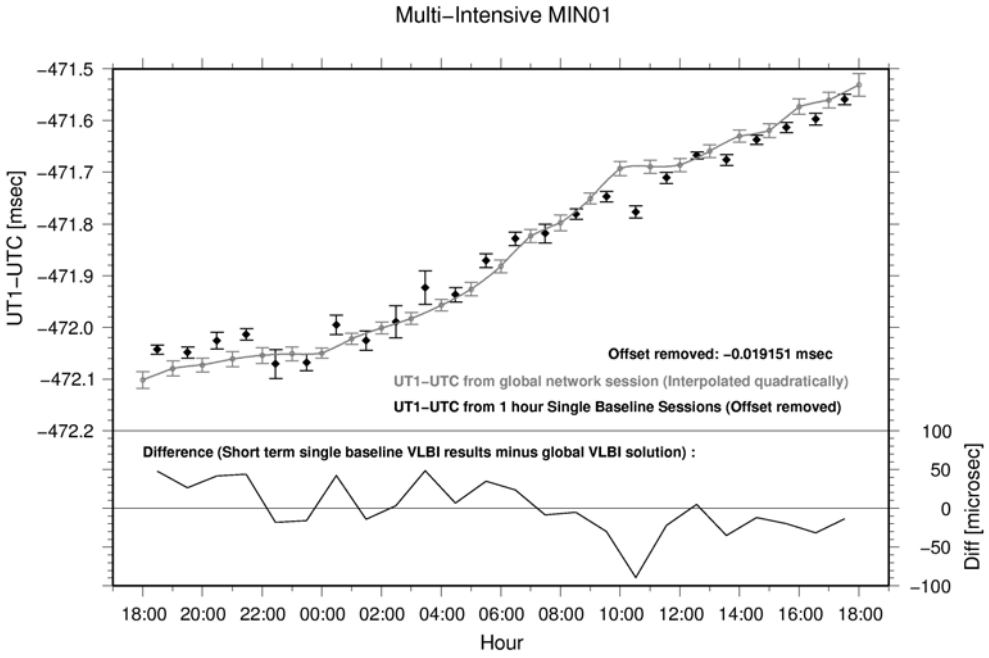

Figure 4.3: Comparison of the *Intensive* UT1 results and the results of the simultaneous 24 hours network session (MIN01).

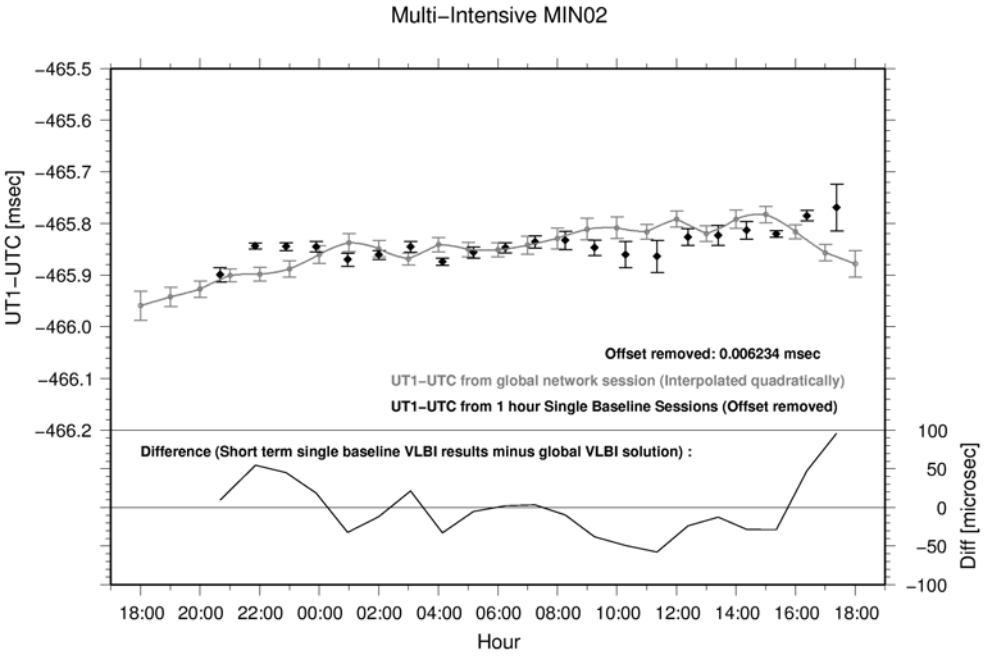

Figure 4.4: Comparison of the *Intensive* UT1 results and the results of the simultaneous 24 hours network session (MIN02).

to meet this assumption a scaling factor $f_{\sigma_{INT}}$ has been applied to the formal errors of the *Intensive* sessions.

$$f^2_{\sigma_{int}} = \frac{2 \cdot \bar{\sigma}^2_{net}}{\bar{\sigma}^2_{int}} \quad \text{with} \quad \bar{\sigma}^2_{int} = \frac{\sum_{i=1}^{n_{int}} \sigma^2_{int_i}}{n_{int}} \quad \text{and} \quad \bar{\sigma}^2_{net} = \frac{\sum_{i=1}^{n_{net}} \sigma^2_{net_i}}{n_{net}} \,. \tag{4.1}$$

A doubled weighted root mean square deviation was calculated by

$$DWRMS = \sqrt{\frac{\sum_{i=1}^{n} p_i \, d_i d_i}{\sum_{i=1}^{n} p_i}} \tag{4.2}$$

where n is the number of differences d_i and p_i is the weight factor calculated as

$$p_i = \frac{1}{\sigma^2_{d_i}} = \frac{1}{(f_{\sigma_{int}} \cdot \sigma_{int_i})^2 + \sigma^2_{net_i}} \,. \tag{4.3}$$

Here $\sigma^2_{int_i}$ denotes the original variance of the respective *Intensive* UT1-UTC value and $\sigma^2_{net_i}$ stands for the variance of the interpolated UT1-UTC value from the network session estimated in 1 hour intervals. The calculated $DWRMS$ includes all variabilities of both compared UT1-UTC series and can give a measure for their conformance. To receive a $WRMS$ for one of the two series the $DWRMS$ has to be divided by $\sqrt{2}$ in the case of equal qualities and absence of correlations or in appropriate portions taking into account the assumed ratio of accuracies of 1:2.
A more accurate quantification cannot be given this way but a qualitative statement is still justified using this rough estimate which means an allocation of the total deviations in the form of 67% caused by the series of *Intensive* results and 33% assigned to the network session estimates. The resulting numbers are listed in table 4.2. The last *Intensive* session of MIN02 has been omitted due to an inexplicable large difference.

$[\mu sec]$	**Offset removed**	$DWRMS$	**Network Sess.** $WRMS = DWRMS * \sqrt{\frac{1}{3}}$	**Intensive** $WRMS = DWRMS * \sqrt{\frac{2}{3}}$
MIN01	19.2	33.7	19.5	27.5
MIN02	6.2	32.3	18.6	26.3

Table 4.2: Comparison of UT1-UTC results of *Intensive* sessions with those of VLBI global network sessions.

Both *Intensive* series show a similar conformance with the UT1 results of their respective simultaneous global network session. That means that the two *Intensive* series can be assumed to be equally accurate and, therefore, both routine series are equivalent in terms of suitability for UT1-UTC determination.
A comparison with the averaged formal errors of the UT1 results of Multi-Intensive global network and *Intensive* sessions (table 4.3) shows that the random variations of the *Intensive* series expressed with their $WRMS$ (table 4.2) is significantly larger than it has to be expected from their formal errors. The other way round this implys that the formal errors derived from the parameter estimation are too optimistic and not sufficient to describe the total budget of random errors. This gives reason to have a closer look onto the complete error budget of *Intensive* sessions.

$[\mu sec]$	**Network Sess.** $\bar{\sigma}_{net}$	**Intensive** $\bar{\sigma}_{int}$	**Differences** $\bar{\sigma}_d$ (Int-Net)	**WRMS Net.** Network	**WRMS Int.** Intensive
MIN01	7.6 ± 2.1	14.6 ± 7.0	16.5 ± 6.3	19.5	27.5
MIN02	10.0 ± 2.4	13.3 ± 9.4	16.6 ± 7.7	18.6	26.3

Table 4.3: Averaged UT1 formal errors of the Multi-Intensive Sessions.

A weighted root mean square of the differences between the *Intensive* and the network session UT1 results ($DWRMS$) of about 33 μsec corresponds to approx. 1.5 cm at the equator.

Remark on this consideration The considerations above are afflicted with the fact that the observing schedules of the two global network sessions have not been optimized for the estimation of hourly UT1 values, but were just created as normal VLBI sessions optimized for sky coverage over 24 hours and for the estimation of one set of EOP parameters per 24 hours.
As a consequence, the assumption has to be mistrusted, that the results of the global session are at least twice as accurate as the single baseline ones. This lack of the considerations carried out here is also confirmed due to the fact that the resulting differences and WRMS between global and single baseline session results are of the same order of magnitude as the calculated differences between the UT1 results of the two single baselines (cp. figure 4.2 and table 4.1, page 42).
In order to generate reliable UT1 values with a real higher-ranking accuracy, it is recommended to repeat these two Multi-Intensive experimental sessions with optimized schedules for the estimation of hourly high precision UT1 values from the global network sessions. The comparison of *Intensive* UT1 results with those of global network sessions is still of prior interest in order to estimate their absolute accuracy without any access to real true values.

Chapter 5

Impact factors on *Intensive* UT1-UTC estimates

The transformation between a terrestrial and a celestial reference system is traditionally expressed using the concept of a rotation axis of diurnal rotation described in both systems (cp. section 2.2.1). The rotations are subdivided into precession, nutation, polar motion and diurnal rotation (equ. 2.2, p. 9). If only the diurnal rotation is object of estimation and all other EOP and the reference frames are fixed to a priori values, as it is necessary in *Intensive* analysis, the UT1 results are directly dependent on this a priori information.
For this reason the dependencies of *Intensive* UT1 estimates on the a priori values of polar motion and nutation have to be analyzed with a special emphasis on the baseline dependent differences. Additionally, the impact of small inconsistencies of the reference frames is considered here. Geometrical and analytical considerations are evaluated and compared to empirical results.

5.1 The impact of polar motion

5.1.1 Theoretical considerations

Pure geometrical consideration

At first, a brief depiction of the pure geometrical interrelations between the earth rotation phase UT1 and the components of polar motion is given here. As the UT1 results of VLBI sessions are always estimated within an adjustment process and every individual radio source observation has its own geometry in terms of hour angle and declination, a rigorous and universal relation between polar motion variations and UT1 estimates cannot be successful. Thus, the geometrical formulations given here are not sufficient to explain the full reaction of UT1 estimates on changes of polar motion components in its entirety but nevertheless they can explain a big part of the effect.
The components of polar motion x_p and y_p describe the direction of the current rotation axis (z_5) relative to the conventional terrestrial reference system (S_6), which is realized by the station coordinates (x_6, y_6, z_6). For historical reasons the y_p axis is defined to point to the reverse direction of the terrestrial y_6-axis. The coordinates of the observing stations are transformed from the conventional (S_6) into the current true earth fixed system (S_5) by

$$\begin{pmatrix} x_5 \\ y_5 \\ z_5 \end{pmatrix} = R_x(y_p) \cdot R_y(x_p) = \begin{pmatrix} 1 & 0 & -x_p \\ 0 & 1 & y_p \\ x_p & -y_p & 1 \end{pmatrix} \cdot \begin{pmatrix} x_6 \\ y_6 \\ z_6 \end{pmatrix} \tag{5.1}$$

[Mueller 1969]. Thus, a small change or mismodeling of the components of polar motion causes a small rotation of the *Intensive* baseline with respect to the axes of the conventional terrestrial reference system. Such a small baseline rotation is directly connected to a change of the estimated earth rotation phase. For the determination of UT1, which represents the rotation phase about the z-axis, only the baseline projection into the equatorial plane matters and has to be considered.
The x, y-direction of a baseline with respect to the system S_6 can be expressed by

$$\alpha = \arctan \frac{y_2 - y_1}{x_2 - x_1} \tag{5.2}$$

where the station coordinates x_1, x_2, y_1, y_2 are given in the mean conventional terrestrial reference system S_6 and the indices stand for the eastern (index 1) and the western (index 2) station of the baseline (compare fig. 5.1).

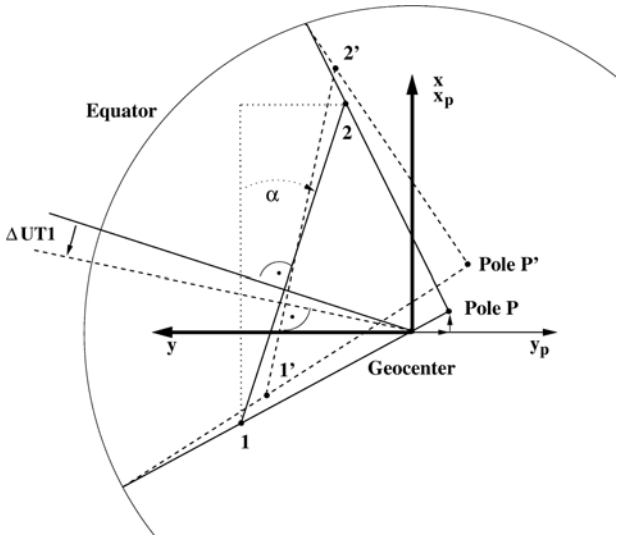

Figure 5.1: Rotation of an *Intensive* baseline projection in the equatorial plane due to small corrections of polar motion components.

If the pole P of the rotation axis is displaced to P' due to an inadequate a priori information on the pole components, the coordinates of the observing stations and thus the x, y-direction α (eq. 5.2) of the baseline is affected. The partial derivatives of equation 5.2 characterize the interrelation between the baseline direction and small changes of the station coordinates

$$\frac{\partial \alpha}{\partial x_1} = \frac{y_2 - y_1}{(y_2 - y_1)^2 + (x_2 - x_1)^2} \quad \text{and} \quad \frac{\partial \alpha}{\partial x_2} = -\frac{y_2 - y_1}{(y_2 - y_1)^2 + (x_2 - x_1)^2}, \tag{5.3}$$

$$\frac{\partial \alpha}{\partial y_1} = -\frac{x_2 - x_1}{(y_2 - y_1)^2 + (x_2 - x_1)^2} \quad \text{and} \quad \frac{\partial \alpha}{\partial y_2} = \frac{x_2 - x_1}{(y_2 - y_1)^2 + (x_2 - x_1)^2}. \tag{5.4}$$

The station coordinates are influenced by small changes dx_p, dy_p of the pole components according to equation 5.1 by

$$d\,x = -z \cdot d\,x_p \quad \text{and} \quad d\,y = z \cdot d\,y_p \tag{5.5}$$

and, thus, inserting into the equations 5.3 and 5.4 leads to the dependency of the baseline direction α on dx_p and dy_p:

$$\frac{d\,\alpha}{d\,x_p} = \frac{(y_2 - y_1) \cdot (z_2 - z_1)}{(y_2 - y_1)^2 + (x_2 - x_1)^2} \quad \text{and} \tag{5.6}$$

$$\frac{d\,\alpha}{d\,y_p} = \frac{(x_2 - x_1)\cdot(z_2 - z_1)}{(y_2 - y_1)^2 + (x_2 - x_1)^2}\,. \tag{5.7}$$

A rotation $d\,\alpha$ of the baseline projection can also be interpreted as a rotation of the coordinate axes in opposite direction. Therefore, the influence of dx_p and dy_p on the UT1 estimates will be $d\,UT1 = -d\,\alpha$ and thus

$$\frac{d\,UT1}{d\,x_p} = -\frac{(y_2 - y_1)\cdot(z_2 - z_1)}{(y_2 - y_1)^2 + (x_2 - x_1)^2} \quad \text{and} \tag{5.8}$$

$$\frac{d\,UT1}{d\,y_p} = -\frac{(x_2 - x_1)\cdot(z_2 - z_1)}{(y_2 - y_1)^2 + (x_2 - x_1)^2}\,. \tag{5.9}$$

It stands out, that the theoretical impact of polar motion on UT1 estimates is equal to zero, if both stations are of equal latitude ($z_1 = z_2$). Thus, a baseline's UT1 result is the more affected by polar motion components, the bigger its north-south component is. Additionally the denominators of equations 5.8 and 5.9 show, that baselines with very large east-west dimensions are more robust against polar motion insufficiencies than shorter ones. Consequently, it has to be expected from geometry that a small change in the components of polar motion results in a change of UT1 as listed in table 5.1.

	INT1 Wz-Kk $[\frac{rad}{rad}]$	**INT2** Ts-Wz $[\frac{rad}{rad}]$	**INT1** Wz-Kk $[\frac{\mu sec}{mas}]$	**INT2** Ts-Wz $[\frac{\mu sec}{mas}]$
$\frac{dUT1}{dx_p}$	-0.07	0.04	-4.74	2.40
$\frac{dUT1}{dy_p}$	-0.23	-0.12	-15.26	-8.12

Table 5.1: Linear dependency of UT1 on the components of polar motion deduced from geometrical considerations.

These dependencies are derived geometrically and, therefore, they only describe the apparent angular response of an interferometer geometry observing an equatorial radio source. In a real observing situation a shift in polar motion and, thus, in α affects the observation equation by means of the momentary orientation of the baseline vector $\vec{b_5}$ (compare equation 2.23 on page 19) :

$$\tau_{obs} = -\frac{1}{c}\vec{b_5}\,S\,\vec{k_4} + \tau_{clock} + \tau_{cl\_rate} + \tau_{ionos} + \tau_{tropo} + \tau_{tides} + \tau_{load} + \tau_{abb} + \tau_{rel} + \tau_{instr}\,. \tag{5.10}$$

The shift in the baseline vector affects the whole set of observation equations and, consequently, the estimate of UT1. As the source direction ($\vec{k_4}$) is different for each individual observation of a session, the total effect on the final UT1 estimate will be dependent on the sessions's observing schedule. As a consequence it has to be expected that the response of the UT1 estimates on changes in the polar motion components is only an indirect one and cannot be completely predicted.

Analytical consideration on the impact of polar motion on UT1

The impact of a small, polar motion induced baseline rotation on the individual observed time delays highly depends on the specific geometrical situation of each single scan observation of a session. This geometry differs in terms of hour angle and declination of the radio source from scan to scan. Therefore, the partial derivatives of the linearized observation equation (equ. 2.24) vary significantly from scan to scan. The final UT1 estimation is subject to an adjustment process containing about 15 to 30 different scan observations, each one carried out under different geometrical conditions and, thus, differently influenced by small polar motion variations. For these reasons a general analytical formulation of the impact of polar motion variations on the parameter estimates is not reasonable here.

5.1.2 Empirical considerations

In order to confirm and refine the conclusions of the geometrical considerations an empirical test has been setup. The full impact of fixed pole information on the estimated parameters of *Intensive* VLBI sessions is empirically explored by using the single baseline sessions of the Multi-Intensive projects MIN01 and MIN02. As depicted in section 3.3, these datasets form a representative substitution of *Intensive* sessions geometrically well distributed over one year and the changing schedule conditions are completely included.

	MIN01 INT1	**MIN02** INT2
Stations	Wettzell - Kokee Park	Wettzell - Tsukuba
Number of 1-hour sessions	24	21
Scans per session	14 to 22	17 to 27
Parameterization	Clock offset Clock rate Zenith wet delay per station UT1-TAI	
Zenith troposph. dry delay	Modified Saastamoinen [Davis 1986]	
Mapping of Dry Atm.	Niell Dry Mapping Function [Niell 1996]	
Partial deriv. for Wet Atm.	Niell Wet Mapping Function [Niell 1996]	
Nutation	IERS Convent. 1996 [McCarthy 1996]	
A priori UT1	[IERS Bull. A]	
Polar Motion	[IERS Bull. A]	
TRF	VTRF2005 [Nothnagel 2005]	
CRF	ICRF (glo.crf)	

Table 5.2: The basic conditions of the empirical investigations on the impact of polar motion components on UT1 estimates.

The solution setup for this investigation is summarized in table 5.2. For the analysis of the reaction of the five estimated parameters on variations of the pole components, the x- and the y-pole coordinates were increased separately by steps of 0.1 *mas*, 0.5 *mas*, 1.0 *mas* and 3.0 *mas*.
In order to understand the dimension of these steps: the precision of the a priori pole information [IERS Bull. A] is quoted to be 100 μas which accords to 3 mm on the earth surface. The precision of a pole value predicted for five days decreases to 2.6 *mas* or 8 *cm* which is somewhat below the last step of 3.0 *mas*.
The response of the UT1 estimates to variations of the pole components is charted in figure 5.2. The numbers in the individual diagrams stand for the respective sessions within the Multi-Intensive projects. From the diagrams it is directly visible that the UT1 estimates react on changes of the fixed pole components in a linear way. The factors of proportionality are different for the two *Intensive* baselines and in addition vary from session to session due to the differences in observing geometries. Table 5.3 gives an overview of the proportionality factors obtained from this analysis of the Multi-Intensive data.

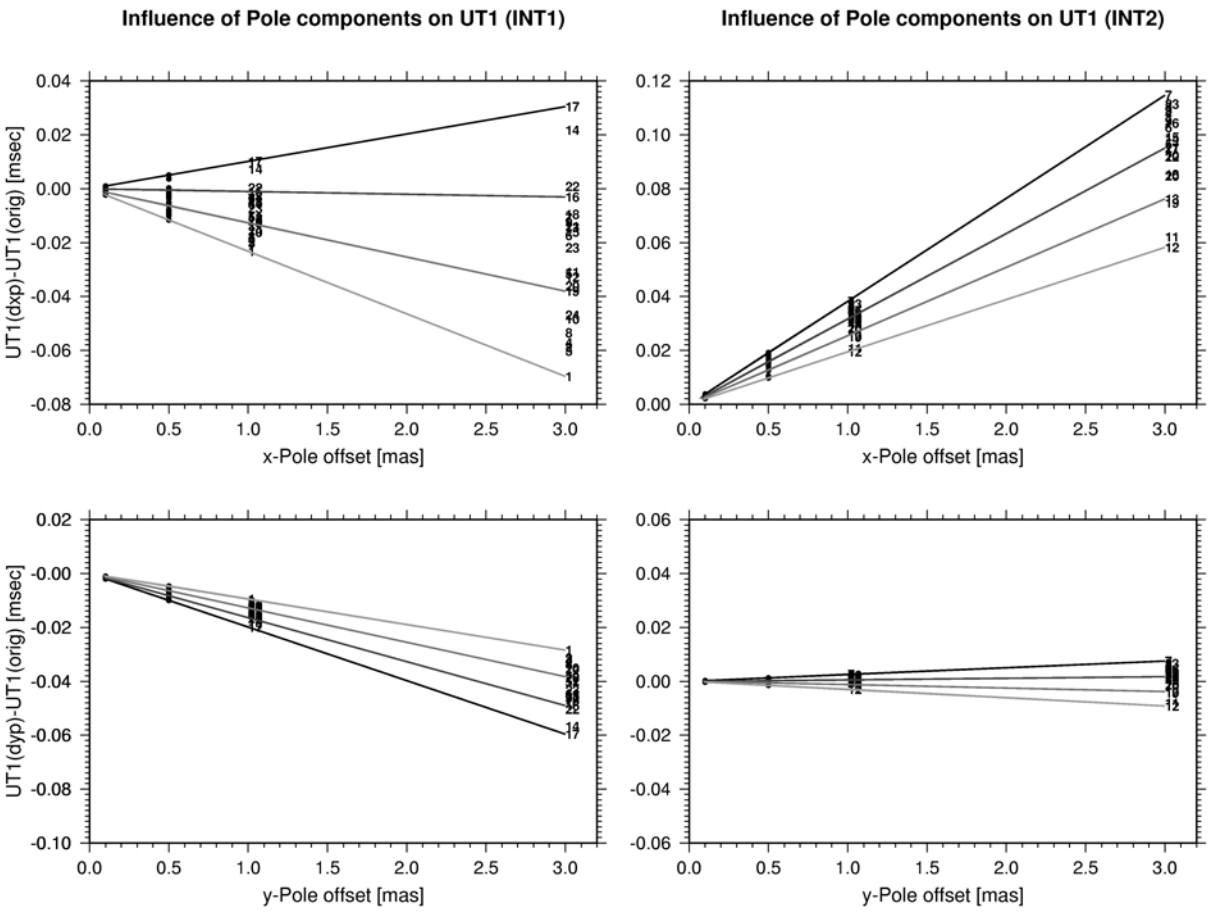

Figure 5.2: Impact of pole variations on UT1 estimates from *Intensive* sessions derived from empirical tests using the Multi-Intensive observations.

	INT1 $[\frac{\mu sec}{mas}]$			**INT2** $[\frac{\mu sec}{mas}]$			Weighted Means **INT1** $[\frac{\mu sec}{mas}]$	Weighted Means **INT2** $[\frac{\mu sec}{mas}]$
$\frac{dUT1}{dxpol}$	-23.2	to	10.1	19.4	to	38.2	-8.7	30.8
$\frac{dUT1}{dypol}$	-19.9	to	-9.5	-3.0	to	2.5	-14.0	0.3

Table 5.3: Reaction of *Intensive* UT1 results to variations of the pole components (empirical results from Multi-Intensive observations).

Conclusions from the empirical test The following major qualitative conclusions can be derived from the empirical tests (cp. figure 5.3):

- INT1: The bigger the factor of proportionality for the impact of x-pole variations, the smaller is the factor for the impact of y-pole.
- INT2: The bigger the factor of proportionality for the impact of x-pole variations, the bigger is the factor for the impact of y-pole.
- INT1: The influence of both pole components on the UT1 estimates is of equal order of magnitude.

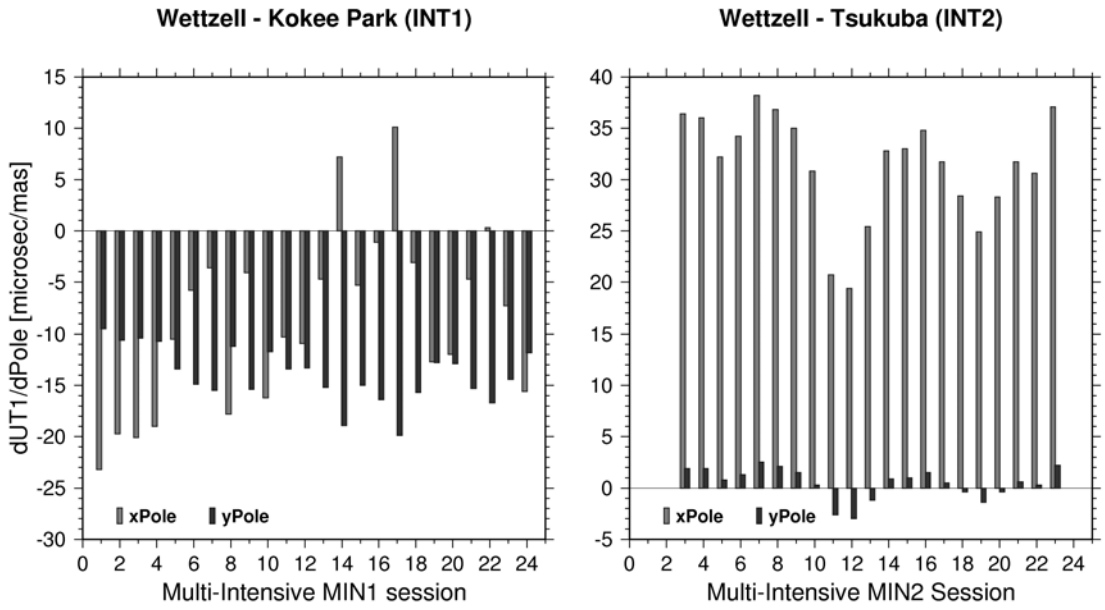

Figure 5.3: Comparison of x- and y-pole impacts on UT1 estimates of both *Intensive* baselines derived from Multi-Intensive observations.

- INT2: The influence of x-pole variations on UT1 estimates is about 10 times larger than the influence of the y-pole.
- INT1 & INT2: The influence of x-pole variations is significantly more spread and thus more session dependent than the influence of the y-pole.

In order to visualize the relation between the slopes for the x_p- and the y_p-dependencies the values are depicted relative to each other for each session in figure 5.4.
All tested sessions satisfy the following relations:

$$\textbf{INT1:} \quad \frac{dUT1}{dx_p} = -3.2 \cdot \frac{dUT1}{dy_p} - 53.6 \frac{\mu sec}{mas} \tag{5.11}$$

$$\textbf{INT2:} \quad \frac{dUT1}{dx_p} = +3.4 \cdot \frac{dUT1}{dy_p} + 29.7 \frac{\mu sec}{mas} \tag{5.12}$$

Interrelation between empirical and theoretical results The impacts resulting from geometrical considerations, depicted as crosses in figure 5.4, satisfy very well the equations 5.11 and 5.12 deduced from the empirical tests. In case of the INT1 baseline Wettzell - Kokee Park the anticipated geometrical polar motion impacts (table 5.1) comes out within the limits of the empirically derived reactions listed in table 5.3, while it does not in case of the INT2 baseline Wettzell - Tsukuba. Looking at the positions of the crosses compared to those of the dots in figure 5.4, this becomes also visible . A possible reason is that the INT2 baseline passes the rotation axis in a certain distant (cp. figure 3.1 on page 24) and thus the simple geometrical relations may not be exhaustive. In contrast to that, the INT1 baseline almost intersects the rotation axis and consequently it is more obedient to the geometrical considerations.
In figure 5.4 it is visible that the geometrically expected values of the ratio of x-pole versus y-pole impact exactly tags that point of the empirically derived straight lines (equations 5.11 and 5.12), that has the shortest distance to the origin. This fact supports the assumption that the geometry can only explain parts of the effect of polar motion differences on UT1 estimates. The real behavior of individual sessions

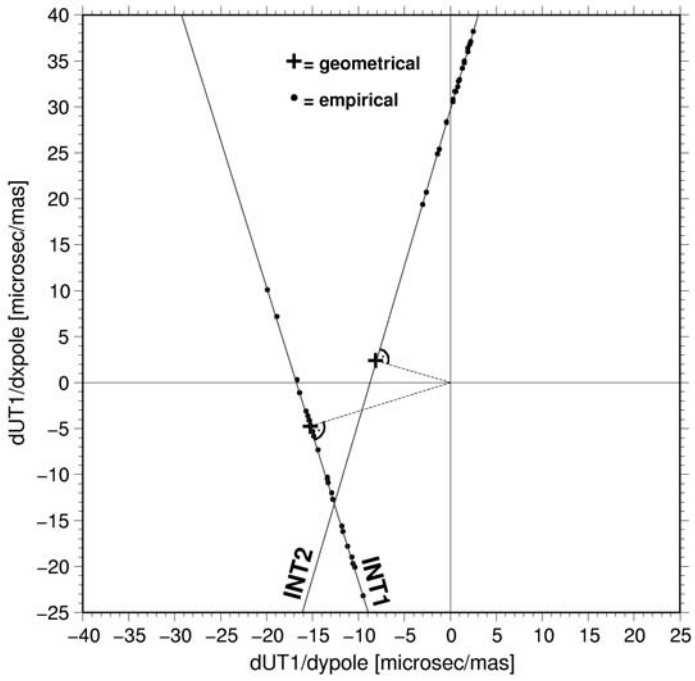

Figure 5.4: Impacts of x-pole relative to y-pole variations on the UT1 estimates as obtained from the Multi-Intensive observations. The values marked with a + represent the results of the geometrical consideration.

cannot be anticipated from simple geometrical considerations alone, because of the varying observing geometries and the inevitable asymmetry of observing schedules.

In order to gain a better understanding of the impact of pole components on the parameter estimation, in the following the empirical tests are additionally analyzed with regard to the other estimated parameters, clock offset and atmospheric path delay. Here it is of special interest, if these auxiliary parameters also follow similar regularities as the UT1 parameter, in the cases when the a priori pole information is biased.

The impact of polar motion on the estimation of clock offsets

The estimates of the auxiliary parameters derived during the empirical test described above with increments of pole coordinates of 0.1 *mas*, 0.5 *mas*, 1.0 *mas* and 3.0 *mas* have been analyzed. It turns out, that the estimated clock offsets are also biased by variation of the pole components in a linear way. In figure 5.5 the differences of the clock estimates are depicted. Again the numbers in the diagrams stand for the respective sessions within the Multi-Intensive project. Identical shades are used as in figure 5.2 on page 51 to display the same exemplary sessions. In order to reach a comparable setup for both *Intensive* baselines, in both cases the station clock of the eastern station was taken as reference clock.
Some qualitative conclusions can be identified for the estimated clock offsets (cp. also figure 5.6) similar to those derived for UT1:

- INT1: The bigger the factor of proportionality for the impact of x-pole variations, the smaller the factor for the impact of y-pole.
- INT2: The bigger the factor of proportionality for the impact of x-pole variations, the bigger the factor for the impact of y-pole.

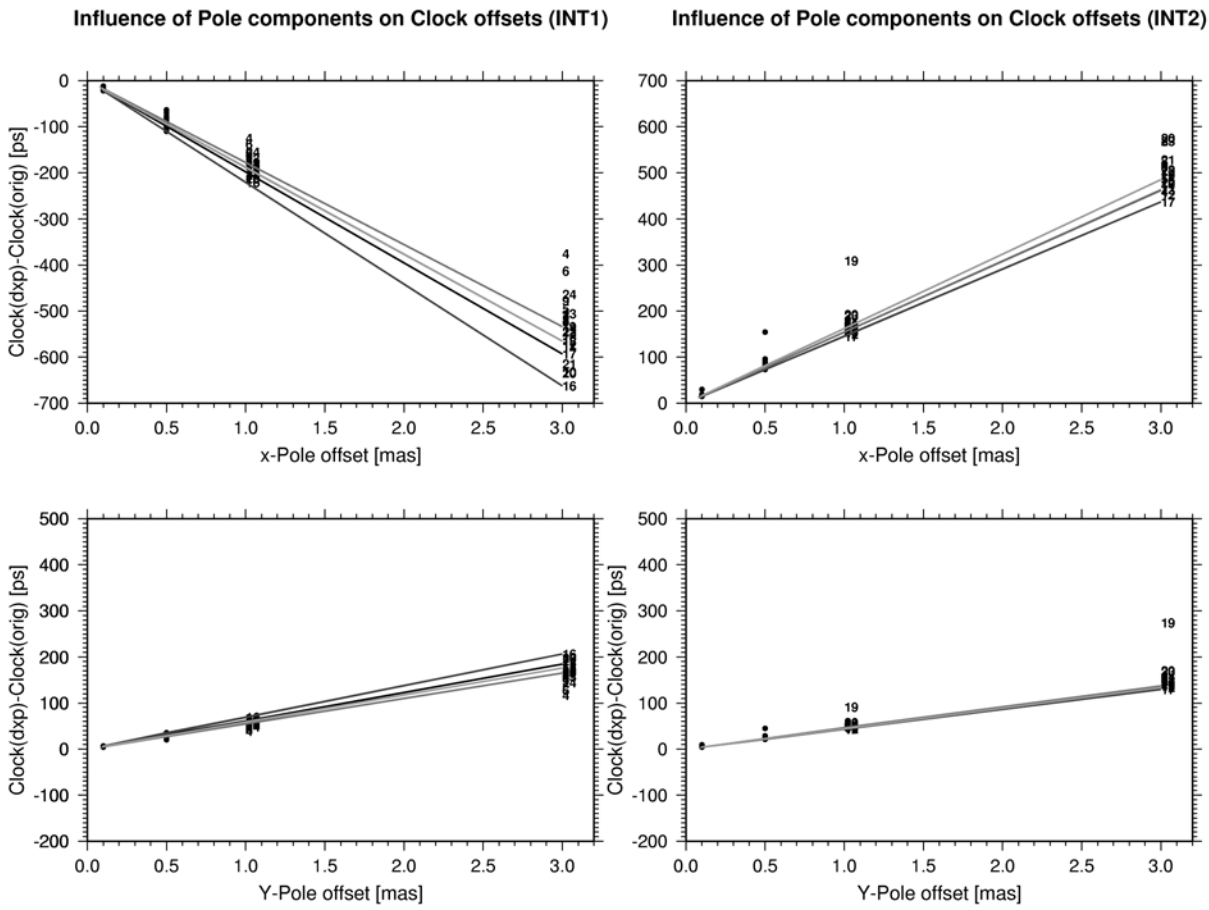

Figure 5.5: Impact of pole variations on the estimated clock offsets of the Multi-Intensive sessions. Identical gray tones are used to flag the same exemplified sessions as in figure 5.2.

	INT1 $[\frac{ps}{mas}]$			INT2 $[\frac{ps}{mas}]$		
$\frac{dClock}{dxpol}$	-221	to	-125	-309	to	-145
$\frac{dClock}{dypol}$	39	to	69	-91	to	-43

Table 5.4: Ranges of slopes of *Intensive* clock offsets dependent on variations of the pole components (empirical results from Multi-Intensive sessions).

- INT1: The influences of x-pole and of y-pole have opposite signs.
- INT2: The influences of both pole components have the same sign.
- INT1 & INT2: The absolute values of the x-pole impact are about three times larger than the impact of y-pole.
- INT1 & INT2: The absolute values of impacts of equal pole components are of equal order of magnitude for both *Intensive* baselines.

The proportionality factors between the estimated clock offsets and the manipulated pole components are depicted in figure 5.6 for each session of the empirical test separately. Table 5.4 summarizes the

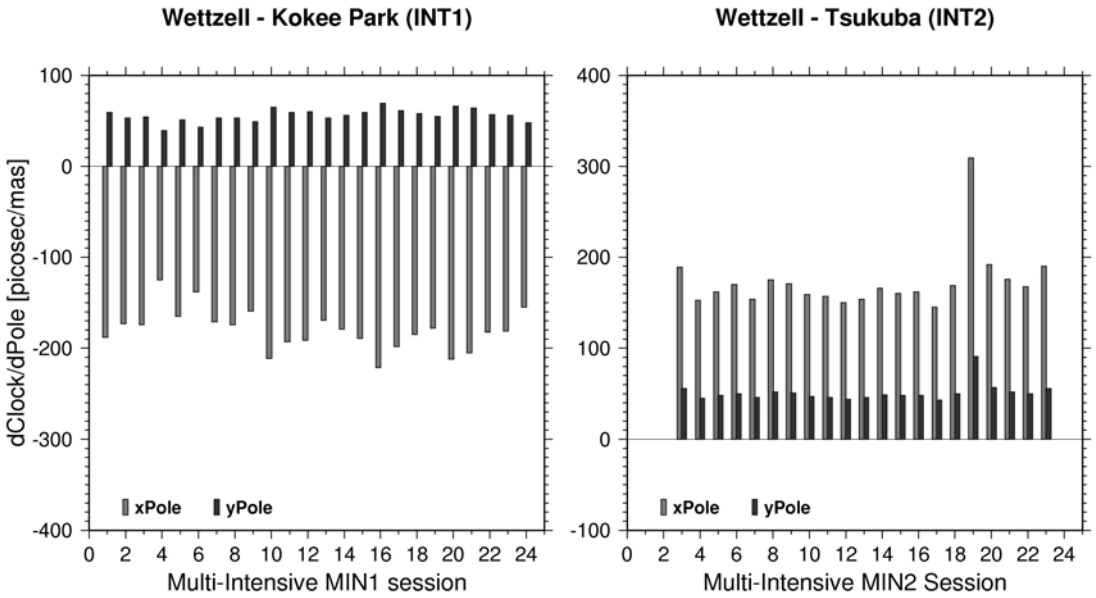

Figure 5.6: Comparison of x- and y-pole impacts on clock estimates of both *Intensive* baselines derived from Multi-Intensive observations.

spectrum of slopes derived from the empirical test.
Again the relationship between x-pole and y-pole impacts show a uniform linear dependency, which all sessions comply with. The linear relation of the changing of clock estimates depending on x-pole variations versus its changing depending on y-pole is depicted in figure 5.7.
The impact of pole components on the estimates of clock offsets satisfies for all tested sessions the following relations:

$$\textbf{INT1:} \quad \frac{dClock}{dx_p} = -3.2 \cdot \frac{dClock}{dy_p} - 1.7 \frac{psec}{mas} \tag{5.13}$$

$$\textbf{INT2:} \quad \frac{dClock}{dx_p} = +3.4 \cdot \frac{dClock}{dy_p} + 1.6 \frac{psec}{mas} \tag{5.14}$$

The slopes of these linear equations are equal to those of the respective relations for UT1 estimates (cp. equations 5.11 and 5.12, page 52) and it has to be expected that these characteristic slopes will also be valid for the atmospheric path delays, which is considered in the following.

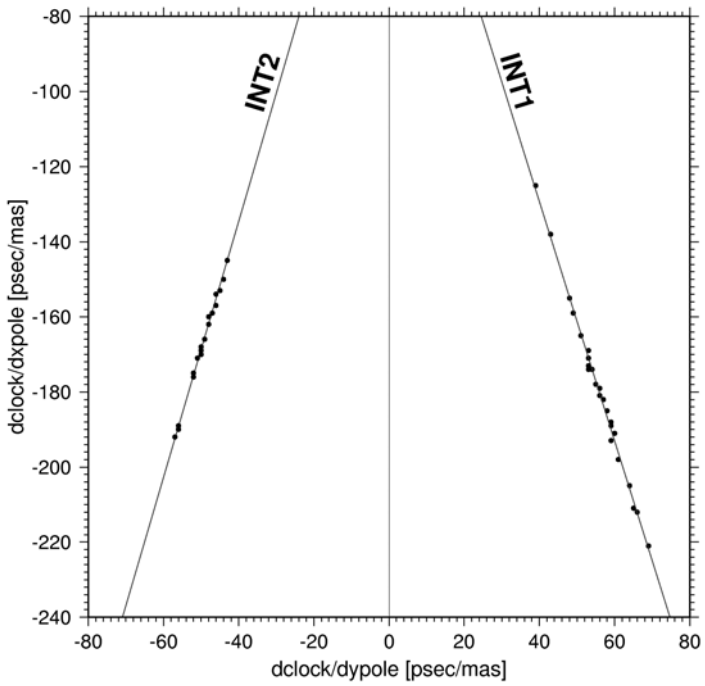

Figure 5.7: Relation between the impact of x-pole and y-pole on the estimation of clock offsets as obtained from the Multi-Intensive observations.

The impact of polar motion on the estimation of atmospheric path delays

Variations of the fixed pole components also influence the estimation of the tropospheric path delay at both stations of a baseline. The full impact on the tropospheric path delay is composed of the impacts on the estimates at the two stations and thus in total it can be expressed by

$$\Delta\tau_{Atm}(INT1) = \Delta\tau_{Atm2} - \Delta\tau_{Atm1} = \Delta\tau_{Kk} - \Delta\tau_{Wz} \text{ and} \quad (5.15)$$

$$\Delta\tau_{Atm}(INT2) = \Delta\tau_{Atm2} - \Delta\tau_{Atm1} = \Delta\tau_{Wz} - \Delta\tau_{Ts}\,. \quad (5.16)$$

Here the eastern station of a single baseline again was chosen as reference station in analogy to the parameterization of the clock offsets. Looking at the results (figure 5.8) it becomes obvious that, as well as the estimates of UT1 and of the clock offset, also the estimated tropospheric path delay is affected in a linear way. The factors of proportionality are listed in table 5.5. The slopes again are depicted in figure 5.9 for each session separately.

	INT1 $[\frac{ps}{mas}]$			**INT2** $[\frac{ps}{mas}]$		
$\frac{dAtm}{dxpol}$	-35.8	to	1.8	-36.7	to	-17.1
$\frac{dAtm}{dypol}$	-0.5	to	11.1	-10.7	to	-5.1

Table 5.5: Ranges of slopes of *Intensive* atmospheric path delays on variations of the pole components (empirical results of Multi-Intensive sessions).

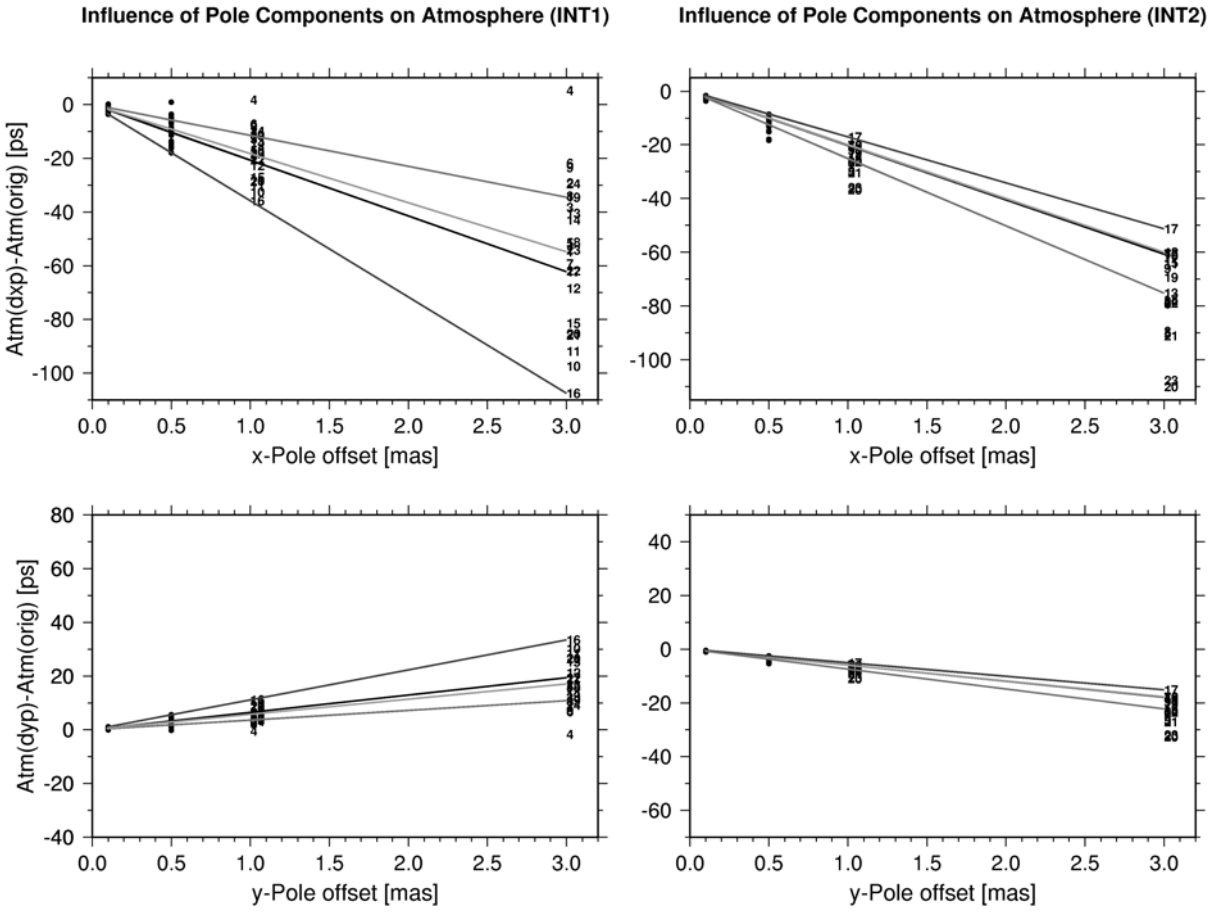

Figure 5.8: Impact of pole variations on estimated atmospheric path delays obtained from Multi-Intensive sessions (identical gray tones are used displaying the same sessions as in figures 5.2 and 5.5).

As depicted in figure 5.10 all tested sessions satisfy the following relations

$$\textbf{INT1:} \quad \frac{d\,Atm}{d\,x_p} = -3.2 \cdot \frac{d\,Atm}{d\,y_p}, \tag{5.17}$$

$$\textbf{INT2:} \quad \frac{d\,Atm}{d\,x_p} = +3.4 \cdot \frac{d\,Atm}{d\,y_p}. \tag{5.18}$$

The slopes again are identical to those found for UT1 and for the clock offsets. From the plots it is obvious that again the reaction of estimated atmospheric path delays to variations of the pole components is highly dependent on the session and therewith presumably on the schedule geometry. The influence of y-pole is for both baselines lower and less dependent on the session than the x-pole influence.
Different from the straight lines for UT1 (figure 5.4) and for the clock offsets (figure 5.7) the respective lines in figure 5.10 for the ratio of x-pole versus y-pole impact to the atmosphere exactly intersect the origin.

5.1.3 Summary and conclusions on the impact of pole components

The first and somewhat surprising fact discovered by the empirical tests is, that the impact of polar motion components on all estimated parameters is strictly linear. Although the reaction of the estimates

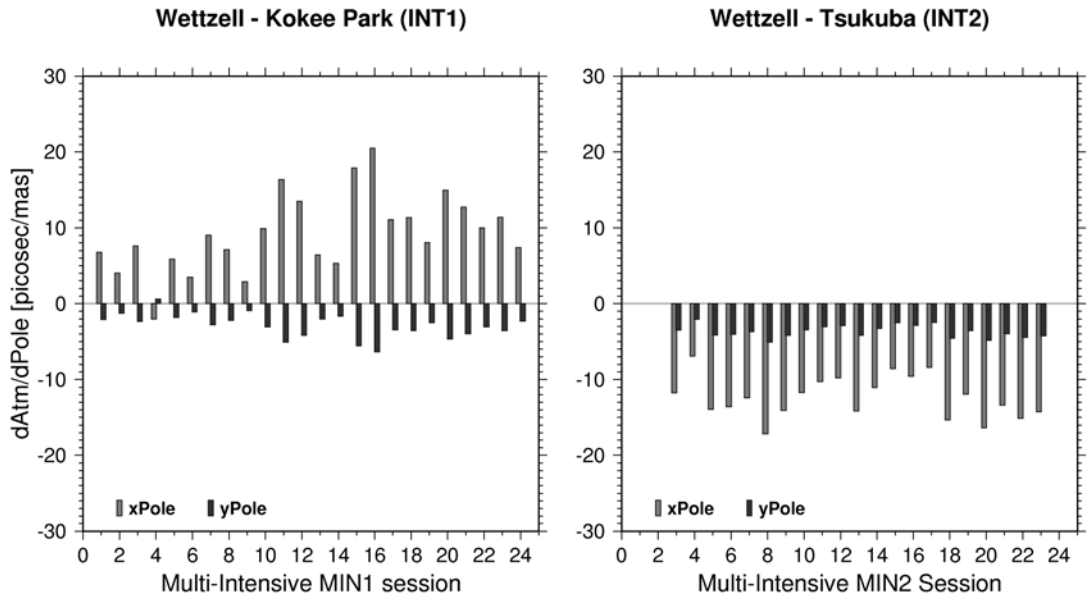

Figure 5.9: Comparison of x- and y-pole impacts on the estimation of tropospheric path delays derived from Multi-Intensive observations.

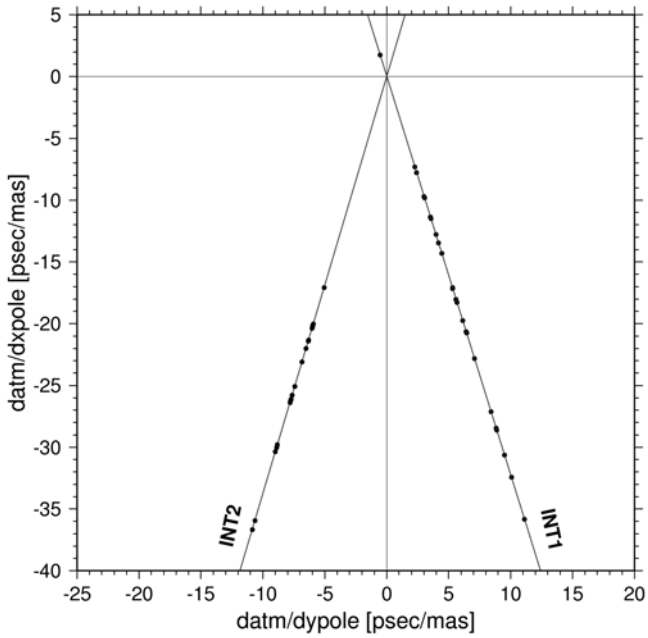

Figure 5.10: Relation between the impact of x-pole and y-pole on the estimation of atmospheric path delays as resulted from Multi-Intensive observations.

to variations of the a priori pole information is very much dependent on the scan geometries of each individual session, it is always linear and only the respective slopes vary from session to session. Linked to that the tests reveal, that for all sessions the polar motion impact on the estimated clock offset is about one order of magnitude larger than its influence on the atmospheric path delays.

In order to get an impression on the dimension of the sensitivity of clock- and atmosphere-parameters to polar motion variations compared to UT1 a rough estimate may help:

> A 1-*ps*-delay within τ_{tropo} or τ_{clock} of equation 2.23 (page 19) multiplied with the velocity of light results in a dilatation of about 0.3 mm in source direction. Assuming a line of sight almost perpendicular to the baseline these 0.3 mm correspond to a baseline rotation and, thus, to a UT1 difference of

$$\text{INT1:} \qquad \Delta\alpha = \frac{b}{r} \cdot \rho = \frac{0.3\,mm}{10072.3 \cdot 10^6\,mm} \cdot \frac{180 \cdot 60 \cdot 60 \cdot 10^6\,\mu as}{\pi} = 6.1\,\mu as \quad (5.19)$$

$$\hat{=} \qquad \Delta UT1 \approx 0.4\,\mu sec$$

$$\text{INT2:} \qquad \Delta\alpha = \frac{b}{r} \cdot \rho = \frac{0.3\,mm}{8377.7 \cdot 10^6\,mm} \cdot \frac{180 \cdot 60 \cdot 60 \cdot 10^6\,\mu as}{\pi} = 7.4\,\mu as \quad (5.20)$$

$$\hat{=} \qquad \Delta UT1 \approx 0.5\,\mu sec.$$

> with r denoting the baseline length and b as the arc length corresponding to 1 ps (0.3 mm).

Applying these roughly estimated scaling factors to the values of tables 5.4 and 5.5 and comparing them to the UT1 values of table 5.3 it becomes obvious that, by far, the estimated clock offsets make up the largest part of all parameters in terms of absorbing a motion of the fixed pole.

The second outstanding phenomenon found from these tests is, that a constant ratio exists between the impacts of x-pole and y-pole. This ratio is valid for all of the estimated parameters and specific for each baseline:

$$\frac{\frac{d\,param}{d\,x_p}}{\frac{d\,param}{d\,y_p}} = \frac{d\,y_p}{d\,x_p} = const.. \quad (5.21)$$

The absolute term *const.* is individually given for each baseline.
In order to explain this, we assume an ideal *Intensive* baseline with stations of equal latitude. In this case, geometrically a rotation of the baseline about an axis parallel to itself does not change the observing geometry at all and, thus, does not have any impact on the observed time delays. Such a rotation corresponds to a component of polar motion perpendicular to the baseline (figure 5.11, left).
In contrast to that, a rotation about an axis perpendicular to the baseline and parallel to the equatorial plane has full impact on the geometry and, thus, influences the observed time delays depending on the position of the individual observed source. The respective component of polar motion describing such a rotation points into the direction of the baseline (figure 5.11, right).
For this reason only the projection of the vector of polar motion components onto the equatorial direction of the baseline has any impact on the observing geometry and, thus, on the estimated parameters. Therefore the ratio between x-pole and y-pole impacts is defined by the direction of the baseline relative to the conventional reference system of the polar motion components. In case of the real *Intensive* baselines the assumed equal latitudes of stations are not completely fulfilled, but the differences are negligible in this context because they are small compared to the lengths of the baselines.

The respective ratios between x-pole and y-pole impacts (equ. 5.21) for the two *Intensive* series are -3.2 for INT1 and 3.4 for INT2, which represent the slopes of the straight lines in figures 5.4, 5.7 and 5.10. These numbers agree with the direction of the respective baseline relative to the reference system of pole components (S_p):

$$m \quad = \quad \frac{\overset{p}{x}_2 - \overset{p}{x}_1}{\overset{p}{y}_2 - \overset{p}{y}_1} = \frac{x_2 - x_1}{-y_2 + y_1}, \quad \text{thus} \quad (5.22)$$

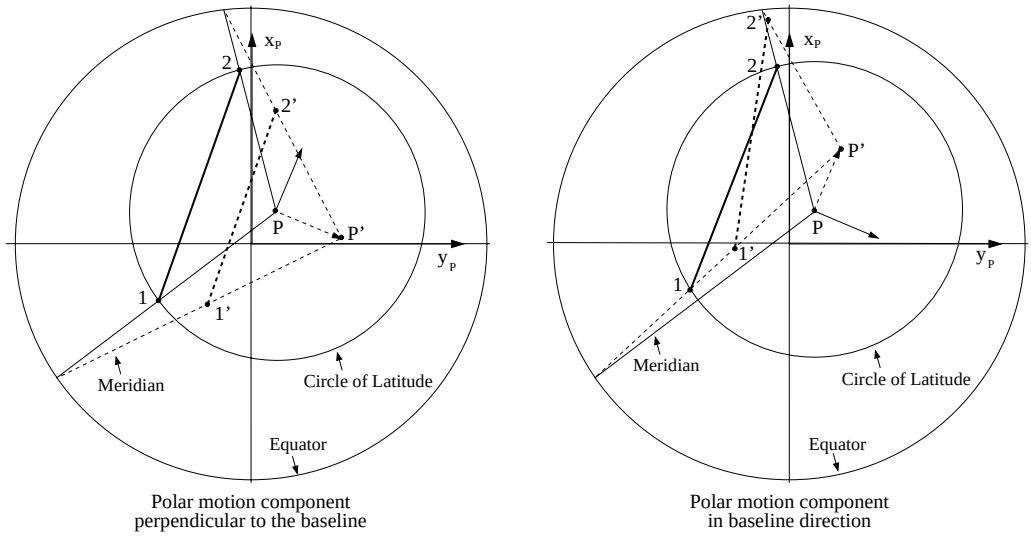

Figure 5.11: Rotation of a baseline induced by polar motion. 1, 2: station positions according to the instantaneous pole of rotation (P) and 1', 2': station positions according to a different pole (P') due to incorrect components of polar motion. *Left:* The polar motion component perpendicular to the baseline causes no baseline rotation. *Right:* The polar motion component parallel to the baseline direction corresponds with a rotation of the baseline.

$$
\begin{aligned}
INT1 \,:\, m_{Int1} &= \frac{x_{Kk} - x_{Wz}}{-y_{Kk} + y_{Wz}} = \frac{-5\,543\,837.70 - 4\,075\,539.77}{-(-2\,054\,567.42) + 931\,735.38} = -3.2 \quad \text{and} \\
INT2 \,:\, m_{Int2} &= \frac{x_{Wz} - x_{Ts}}{-y_{Wz} + y_{Ts}} = \frac{4\,075\,539.77 - (-3\,957\,408.79)}{-931\,735.38 + 3\,310\,229.43} = 3.4\,.
\end{aligned}
\tag{5.23}
$$

Here again the index 1 stands for the eastern and 2 for the western station of the baseline. p tags the reference system of pole components, which is a left-handed system in contrast to the right-handed conventional terrestrial reference system.

Conclusions on the significance of the impact of polar motion Since *Intensive* sessions deliver the very time critical parameter UT1, the analysis of sessions has to be carried out as soon as possible after the observations, which means currently about 3 days later. Therefore the analyst cannot revert onto pole information based on longterm observing series from all techniques, but in fact, has to rely on rapid or predicted pole information. For example the IERS specifies a standard deviation of pole components calculated from observations of $0.1\,mas$ for the Bulletin A rapid series [IERS Bull. A]. If the analyst has to rely on predicted values, the standard deviation of x_p and y_p increases to $0.5\,mas$ for a one day prediction and up to $1.6\,mas$ for a prediction four days after the last observation.
The empirical investigations show that a mismodeling of $1\,mas$ of the x-pole component may cause a difference in the UT1 results between the two *Intensive* baselines of up to $61\,\mu sec$. A $1\,mas$ mismodeling of the y-pole component in the worst case may cause a difference of $22\,\mu sec$. In other words to ensure a consistency of the UT1 results of both *Intensive* series of better than $10\,\mu sec$ the modeling of the pole components has to be better than $0.2\,mas$.

5.2 The impact of nutation

As pointed out in section 2.4, it is necessary to introduce the current nutation angles as a priori information into the analysis of *Intensive* sessions and it is impossible to estimate any nutation corrections from one-hour sessions. Within the standard analysis procedures, e.g. those solutions summarized in appendix A, geophysical models are used to realize the nutation angles. The conclusions on the impact of polar motion components derived in section 5.1 give rise to the supposition that imperfections of the nutation model may again lead to differences between the UT1 series of the two independent *Intensive* baselines. Additionally the question arises how differences between the nutation models used by the different analysis centers influence the UT1 results. [Titov 2000] already showed significant differences between *Intensive* solutions (Wettzell - Green Bank) based on two different models.
In the following, the sensitivity of *Intensive* UT1 results to small changes of the nutation angles is determined and tested using *Intensive* observations of 2005.

5.2.1 Theoretical Considerations

The nutation in longitude specifies the relation between the true and the mean vernal equinox (cp. figure 2.1) and, thus, the conversion of the observed apparent sidereal time into the mean sidereal time. Due to the derivation of UT1 from GMST by a fixed formula (equ. 2.7) a change or insufficiency of the used nutation model therefore directly influences the definition of UT1.
Additionally also the nutation in obliquity has a certain impact on the results of *Intensive* sessions because VLBI observations in principle are sensitive to the complete rotational position of the earth relative to the space fixed celestial reference system.
Only within long duration VLBI sessions, with at least close to 24 hours duration, it is possible to estimate all components of earth rotation separating polar motion and nutation [Nothnagel 1991]. In contrast to that, a short one-hour single-baseline session does not provide a sufficient basis to distinguish between polar motion and nutation. For this reason, within *Intensive* sessions the impact of nutation on UT1 estimates is geometrically identical to the impact of polar motion. In other words, small changes of nutation angles can also be expressed as changes of pole components, whose impact on UT1 is already known from section 5.1.

Changes of the nutation model in general associates with changes of the pole components, which can be expressed by [Zhu et. al. 1983]

$$dx_p = d\Delta\epsilon \cdot \sin\Theta + d\Delta\psi \cdot \sin\epsilon \cdot \cos\Theta \tag{5.24}$$

$$dy_p = -d\Delta\epsilon \cdot \cos\Theta + d\Delta\psi \cdot \sin\epsilon \cdot \sin\Theta\,. \tag{5.25}$$

Here dx_p, dy_p are the changes of pole components related to small nutation differences $d\Delta\epsilon$ and $d\Delta\psi$. ϵ means the mean obliquity of the ecliptic and Θ stands for the Greenwich Apparent Sidereal Time (GAST).
If the small changes of nutation angles $d\Delta\epsilon$ and $d\Delta\psi$ associate with the changes of pole components dx_p and dy_p as expressed by equations 5.24 and 5.25, they will affect UT1 estimates like $-dx_p$ and $-dy_p$, because the pole components are fixed and, thus, cannot absorb the small rotations caused by $d\Delta\epsilon$ and $d\Delta\psi$.
Therefore the impact of nutation angles on the estimates of UT1 can be formulated as

$$\frac{dUT1}{d\Delta\epsilon} = \frac{dUT1}{(-dx_p)} \cdot \frac{dx_p}{d\Delta\epsilon} + \frac{dUT1}{(-dy_p)} \cdot \frac{dy_p}{d\Delta\epsilon} \tag{5.26}$$

$$= -\frac{dUT1}{dx_p} \cdot \sin\Theta + \frac{dUT1}{dy_p} \cdot \cos\Theta \tag{5.27}$$

$$\frac{dUT1}{d\Delta\psi} = \frac{dUT1}{(-dx_p)} \cdot \frac{dx_p}{d\Delta\psi} + \frac{dUT1}{(-dy_p)} \cdot \frac{dy_p}{d\Delta\psi} \tag{5.28}$$

$$= -\frac{dUT1}{dx_p} \cdot \sin\epsilon \cos\Theta - \frac{dUT1}{dy_p} \cdot \sin\epsilon \sin\Theta\,. \tag{5.29}$$

It is incidental that the impact of a change of the nutation model on the UT1 estimates varies periodicly with a cycle duration of a sidereal day. Due to the fact that INT1 sessions are observed between 18.00 and 20.00 UT and INT2 sessions between 07.30 and 09.00 UT a mismodeling of the nutation would affect the UT1 estimates with a phase difference of about 10 hours.
Furthermore it has to be taken into account that the observing times of the *Intensives* are fixed to solar time and thus the sidereal time of the sessions varies from day to day by the difference between a solar and a sidereal day, which is about 4 minutes per day. Therefore the influence of the nutation depends on the day of the year.
Assuming mean values for $\frac{dUT1}{dx_p}$ and $\frac{dUT1}{dy_p}$ according to section 5.1, the theoretical impact of $d\Delta\epsilon$ and $d\Delta\psi$ can be assessed. As the theoretical considerations concerning the polar motion impact (table 5.1 on page 49) have not completely matched the empirical results, here mean values derived from the empirical test (table 5.3 on page 51) are used instead.
The nutation impacts on *Intensive* UT1 results, anticipated this way, are depicted in figures 5.12 and 5.13.

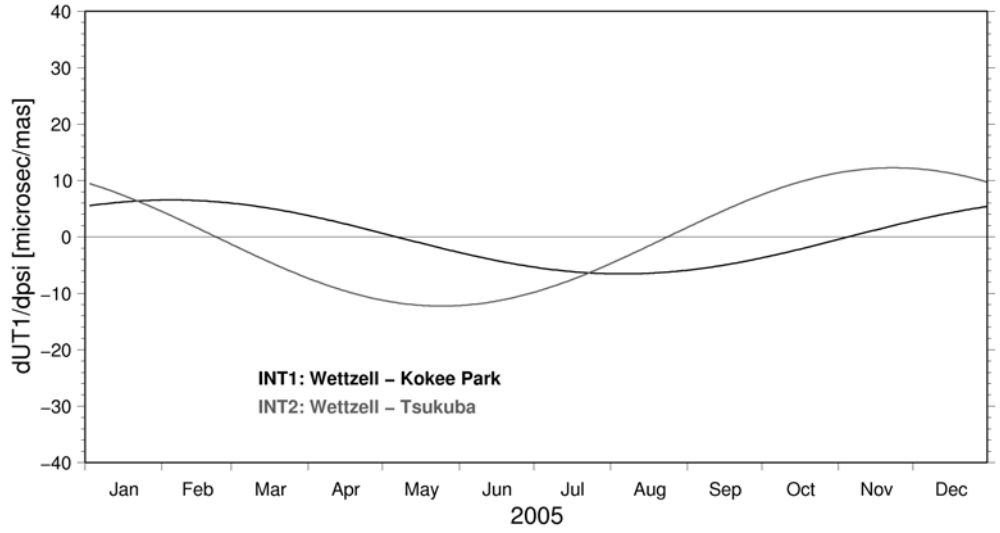

Figure 5.12: Theoretical impact of a fictitious constant 1 *mas* change of the nutation in longitude on UT1 estimates of 2005 *Intensive* sessions.

The plots show the expected phase difference of the nutation impact on the UT1 estimates between the two *Intensive* series. Thus, a change or a mismodeling of the nutation angles will lead to differences between the two series depending on the day of the year. Due to fact that the nutation modeling itself is a composition of numerous individual harmonic oscillations, a possible incorrectness of the model would have a certain periodic behavior also, which superposes with the annual period of the UT1 impact displayed. This periodicity of the nutation terms themselves is disregarded in the diagrams and in the investigations, because only their impact on UT1 estimates is of interest here.

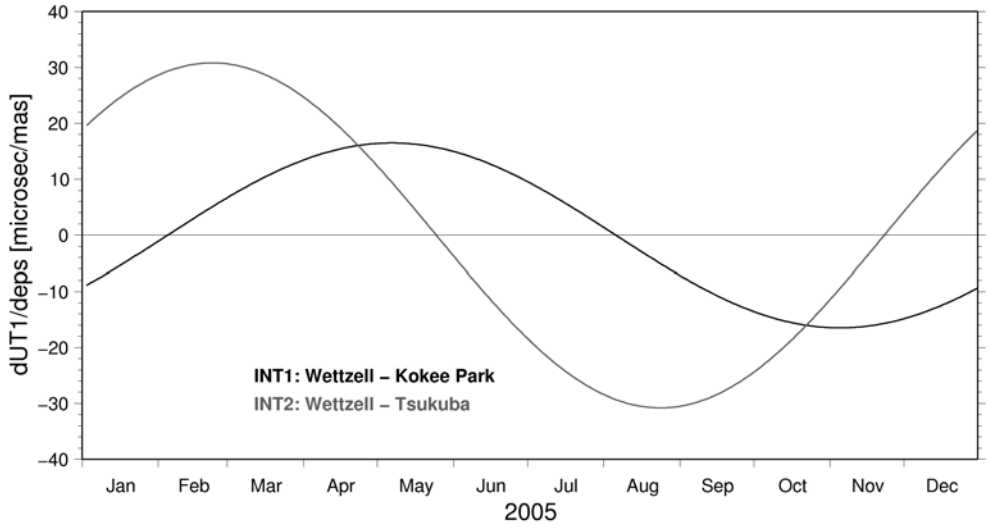

Figure 5.13: Theoretical impact of a fictitious constant 1 *mas* change of the nutation in obliquity on UT1 estimates of 2005 *Intensive* sessions.

5.2.2 Empirical Considerations

Using the complete data set of *Intensive* sessions of the year 2005 an empirical test has been carried out in order to support the theoretical conclusion derived before. A constant offset of 1 *mas* has been added separately to $\Delta\psi$ and $\Delta\epsilon$ of the IERS 1996 nutation model [McCarthy 1996], which is used in CALC/Solve by default.
Figures 5.14 and 5.15 show the UT1 differences induced by the enforced nutation offsets. In order to compare these empirical results with the theoretical conclusions, the curves of the theoretical impacts (fig. 5.12 and 5.13) are added again in the diagrams.

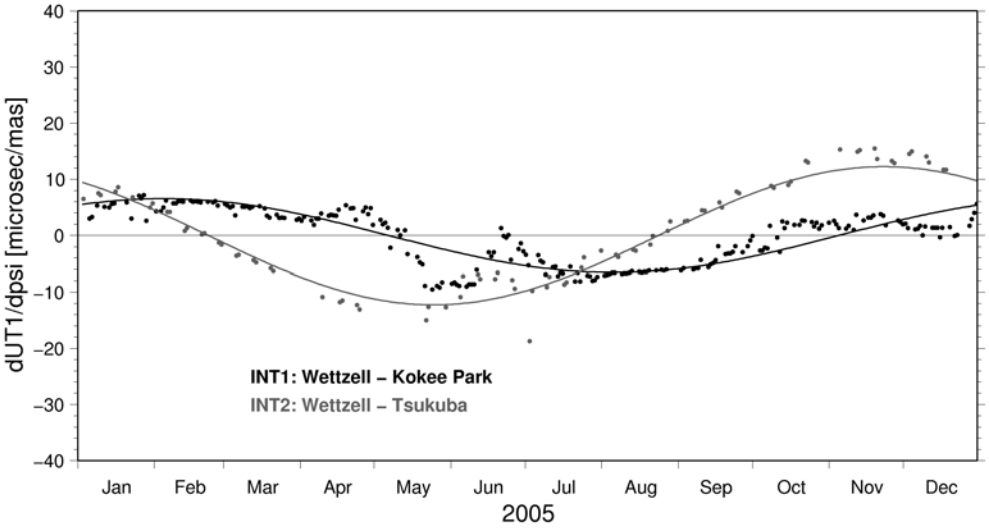

Figure 5.14: Differences of UT1 results induced by an enforced constant 1 *mas* difference of the nutation in longitude (dotted). The solid lines denote the theoretically expected impacts (cp. section 5.2.1).

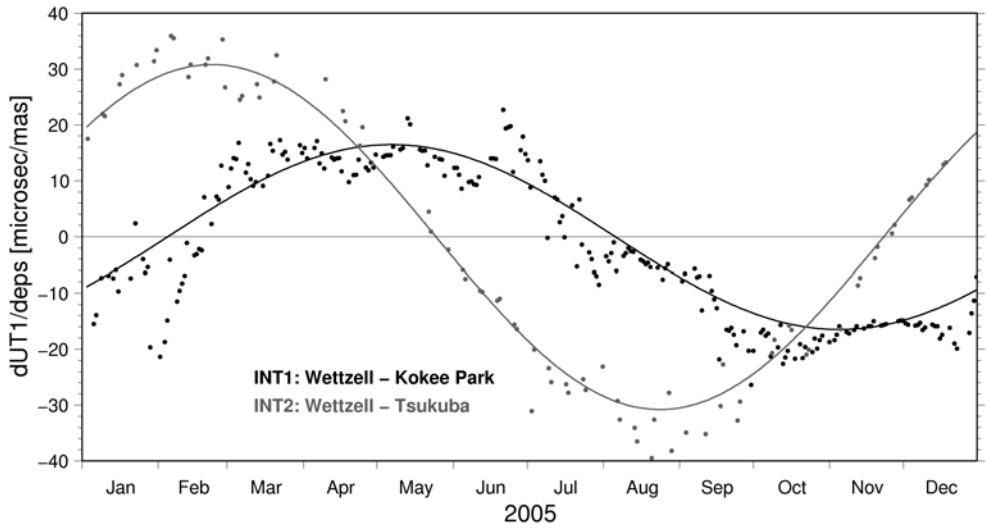

Figure 5.15: Differences of UT1 results induced by an enforced constant 1 *mas* difference of the nutation in obliquity (dotted). The solid lines denote the theoretically expected impacts (cp. section 5.2.1).

It can be seen that the results of the empirical test support the theoretical assumptions very well. Nevertheless again certain variations are visible among the reactions of the individual sessions. The reason for that is, that the factors $\frac{dUT1}{dx_p}$ and $\frac{dUT1}{dy_p}$ in equations 5.28 and 5.29 are session dependent as shown in section 5.1.2 and explained on page 49. That means that the full reaction of an individual UT1 result to nutation changes again depend on the schedule geometry of the individual session.

5.2.3 Conclusions on the significance of the impact of nutation

The empirical results of section 5.2.2 show that inaccuracies of the nutation model may lead to varying differences between the UT1 results of the two different *Intensive* baselines. These differences depend on the geometry of the baselines as well as on the Greenwich Apparent Sidereal Time of the observation epoch.

In order to assess the quality of the IERS 1996 nutation model, which is currently still used as standard a priori nutation model within the CALC/SOLVE software, the offsets between the modeled nutation components and their estimates from regular global VLBI network sessions are depicted in figure 5.16. The respective mean offset and WRMS are summarized in table 5.6 as they are calculated from all global VLBI sessions of the year 2004 analyzed using the standard EOP solution strategy of BKG (*Bundesamt für Kartographie und Geodäsie*) (correspondent to bkg00007.eops). Combination studies have shown that all nutation series of IVS analysis centers coincide to each other within 0.03 mas [IVS Analysis Coordinator], which is negligible compared to their offset with respect to the IERS 1996 model. For this reason, the numbers solely assessed from the BKG solution and presented in table 5.6 allow a reasonable assessment of the quality of the IERS 1996 nutation model.
Assuming a constant mismodeling of about -0.3 *mas* for both nutation components according to table 5.6, the resulting UT1 bias, which has to be expected, varies between -10 and 10 μsec for INT2 and even less for INT1. In worst case a maximum mismodeling of the nutation components of 1 *mas* according to figure 5.16 has to be expected. Thus inconsistencies between -30 and +30 μsec are possibly induced by the used nutation model.
These nutation induced variations are slightly larger than the mean formal errors of INT1 UT1 results (cp. table 3.7, page 34) but significantly larger than the formal errors of INT2 sessions.

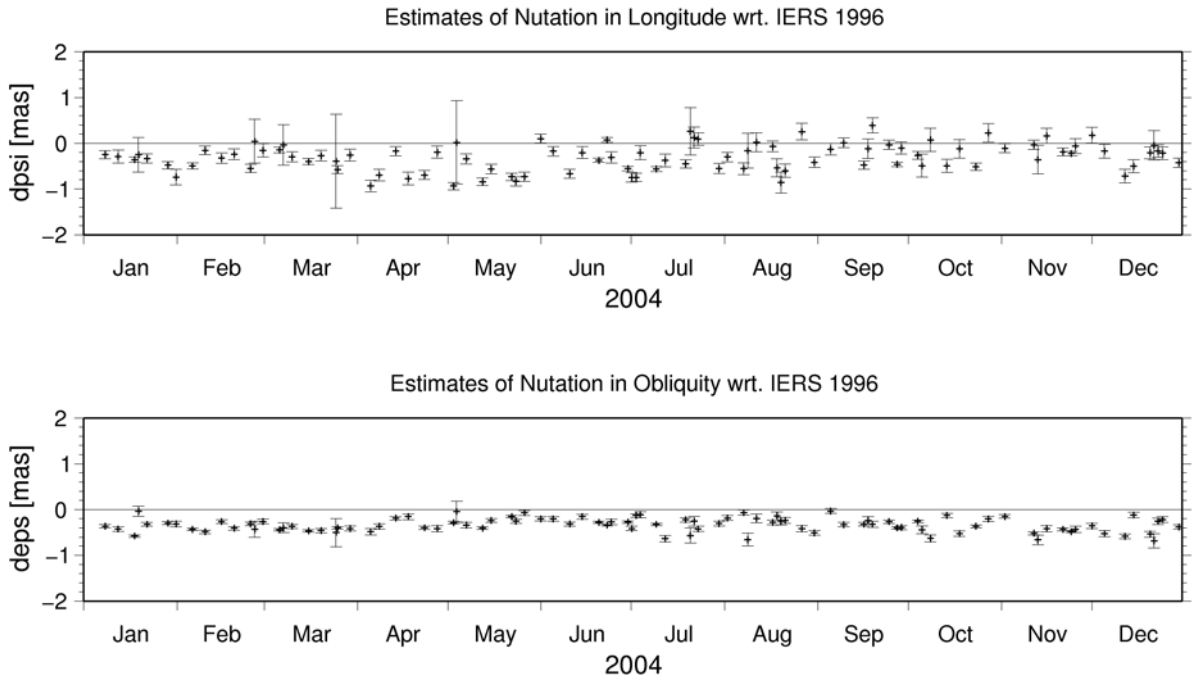

Figure 5.16: Agreement of IERS 1996 nutation model with results of VLBI global network sessions (bkg00007.eops).

	$\Delta\psi$ $[mas]$	$\Delta\epsilon$ $[mas]$
Weighted Offset	-0.33	-0.39
WRMS	0.25	0.14

Table 5.6: Agreement of IERS 1996 nutation model with results of VLBI global network sessions representative for the year 2004.

In order to have a short look at the improvements, which have to be expected from the implementation of the new nutation model IAU2000A [IAU 2000] in the Analysis Software, the respective offsets between modeled values and their estimates are depicted in figure 5.17. Again the BKG solution strategy has been used. The respective statistics received therefrom are summarized in table 5.7.

	$\Delta\psi$ $[mas]$	$\Delta\epsilon$ $[mas]$
Weighted Offset	0.23	-0.14
WRMS	0.29	0.13

Table 5.7: Agreement of IAU2000A nutation model with results of VLBI global network sessions representative for the year 2004.

It can be seen that the weighted mean offsets between estimates and modeled values are noticeable reduced when using the new nutation model. Therefore in terms of *Intensive* UT1 accuracy it is strongly

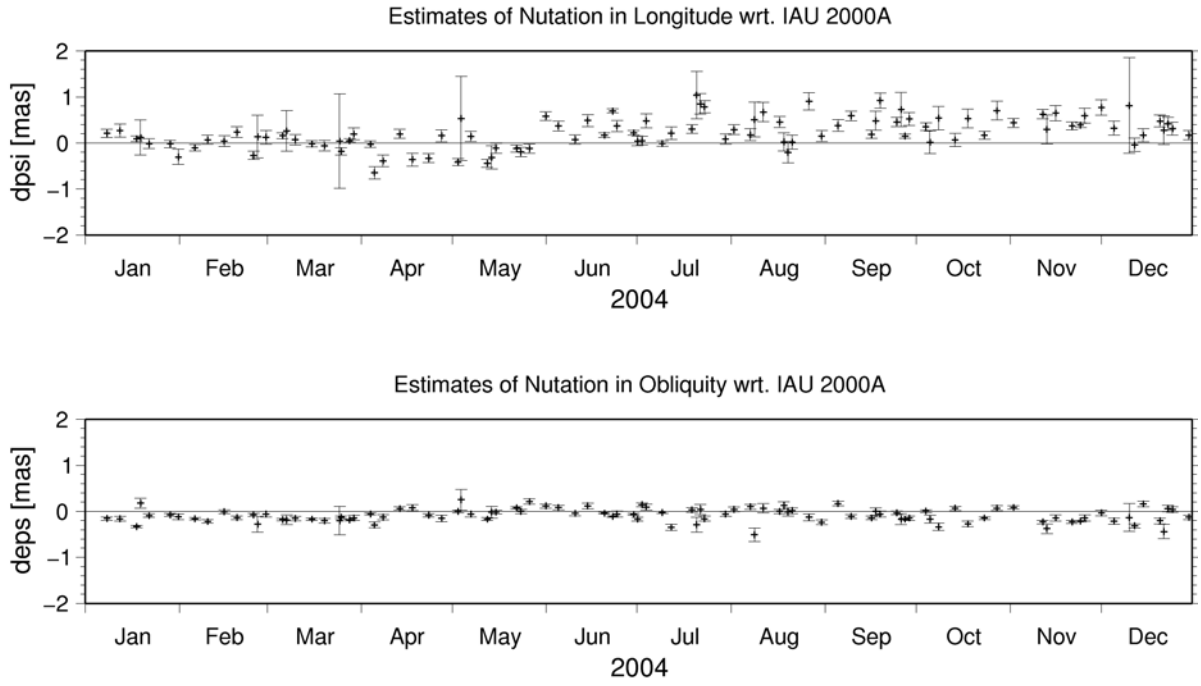

Figure 5.17: Agreement of IAU2000A nutation model with results of VLBI global network sessions (correspondent to bkg00007.eops) calculated from global network sessions of the year 2004.

recommendable to shift over to the new model of nutation for all regular standard *Intensive* solutions.

5.3 The impact of the terrestrial reference frame on UT1 estimates

The axes of the terrestrial reference system are fixed to the earth's surface and represent the real earth. The system is realized by the coordinates of globally distributed observing stations that form the terrestrial reference frame (TRF). That means that within the analysis of *Intensives* the reference system is realized by the coordinates of only two stations. An unmodeled movement of one of these two station positions can easily cause a significant change of the represented reference system and therefore changes of the UT1 results. In other words if a station moves unnoticed or unaccounted, the observed VLBI time delay will not lead to UT1 results consistent with the station coordinates of the used TRF.

The two different *Intensive* baselines can only contribute to a joint UT1 series if they are based consistently on an identical terrestrial reference system. Therefor the station coordinates of all three *Intensive* stations need to be known in one common and consistent reference system. Unknown small local site displacements or incorrect global coordinates would breach this condition and would lead to discrepancies between the two UT1 series. These induced differences depend on direction and size of the displacement and on the direction of the baseline. As an unknown local movement of a station as well as an incorrectness in the global station's coordinates affect the situation in the same way, both cases are subsumed by the word *displacement* in the following considerations.

5.3.1 Theoretical considerations

A displacement of one or both observing stations of an *Intensive* baseline causes a three-dimensional rotation of the baseline. This angular deviation of the baseline direction can be interpreted directly as a change of the axis orientation of the reference system in reverse direction. As the z-axis is nearly aligned to the earth rotation axis, only the projection of the baseline onto the equatorial plane has to be considered when we are looking at the impact on the earth rotation phase. However, a change or mismodeling of the z-coordinate of one or both stations of an *Intensive* baseline will influence the estimation of the clock offset and of the atmospheric path delay and will therefore also influence the UT1 estimates.

Correspondent to equations 5.3, 5.4, 5.8 and 5.9 (pages 48 and 49) a change of UT1 due to small variations of the station coordinates can be formally derived from the accompanied change of the baseline direction in the x, y-plane

$$\frac{dUT1}{dpos} = -\frac{d\alpha}{d\,pos} = -\frac{d}{d\,pos}\arctan(\frac{y_2 - y_1}{x_2 - x_1}) \tag{5.30}$$

with $dUT1$ (= change of UT1 estimates) induced by $dpos$ (= change of one of the station coordinates x_1, x_2, y_1 or y_2). For a 1-cm-change of station positions the resulting numerical values are listed in table 5.8.

	Tsukuba		**Wettzell**		**Kokee Park**	
$[\frac{\mu sec}{cm}]$	dx	dy	dx	dy	dx	dy
INT1	-	-	4.1	-13.0	-4.1	13.0
INT2	4.7	15.7	-4.7	-15.7	-	-

Table 5.8: Geometrical impact of small changes of station positions on UT1 estimates (theoretical consideration).

As already mentioned the z-component of a station position will also have a certain impact on the UT1 estimates because it influences the estimation of the auxiliary parameters. To approve the geometrical considerations on the influence of x- and y-coordinates and in order to find the impact of the z-coordinates empirical tests have been carried out.

5.3.2 Empirical Considerations

The behavior of UT1 estimates after station displacements is expected to be dependent on the individual observing geometry of each session. Therefore again the Multi-Intensive sessions provide an ideal opportunity to investigate the TRF impact empirically. The station positions have been separately modified by 5 mm, 1 cm and 3 cm successively and the respective UT1 reactions are depicted in figure 5.18.

Again the resulting impacts are completely linear, different for the two baselines and session dependent. The impact of displacements of the two stations of a baseline are of equal size but with opposite signs. The weighted mean slopes, visualized by the straight lines and summarized in table 5.9, confirm the values expected from geometry (table 5.8) very well. Especially the derived values for the INT1 sessions fit perfectly to the geometrical expectations.

For both *Intensive* baselines the impact of the y-coordinates is about three times larger than that of the x-component. The reason for this effect becomes directly obvious by looking at the equatorial directions of the baselines depicted in figure 5.19. A change of the x-coordinates of a station mostly influences the length of the baseline while the y-coordinates primarily causes a rotation of the baseline, which is directly connected with a change of UT1.

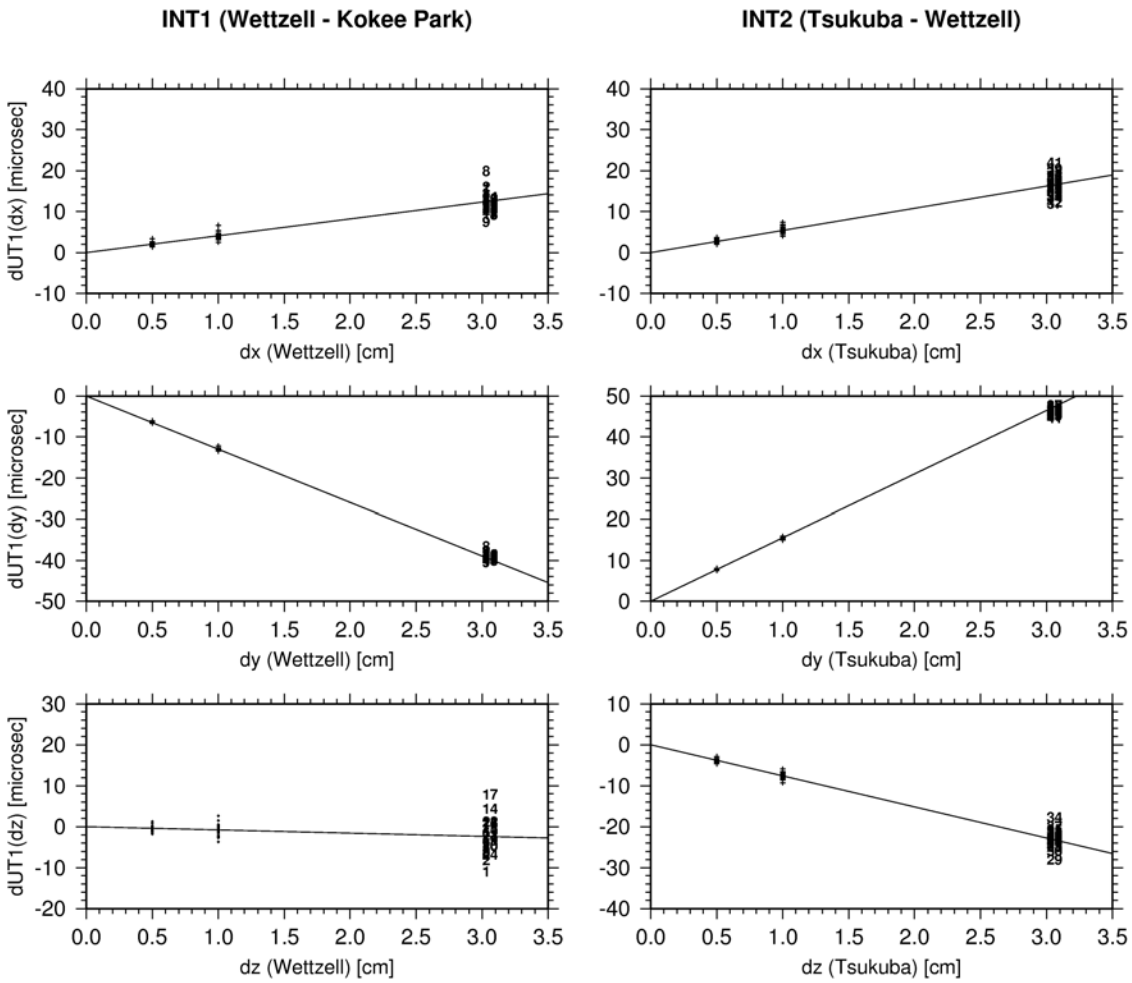

Figure 5.18: *Intensive* UT1 reaction to variations of the station position; depicted for the eastern station of each baseline. Weighted mean slopes are visualized by the straight lines.

	Tsukuba			**Wettzell**			**Kokee Park**		
$[\frac{\mu sec}{cm}]$	dx	dy	dz	dx	dy	dz	dx	dy	dz
INT1	-	-	-	4.1	-13.0	-0.8	-4.1	13.0	0.8
INT2	5.4	15.5	-7.6	-5.4	-15.5	7.6	-	-	-

Table 5.9: Mean impact of small changes of station positions on UT1 estimates (empirical test).

Also interesting is the impact of the z-coordinates. While the INT1 baseline shows only a marginal impact of the stations' z-coordinates, the INT2 sessions are significantly more influenced by them. That means that a 1-cm change or mismodeling of the z-coordinate of Wettzell would cause a difference in the UT1 results of both *Intensive* series of about 8 μsec.

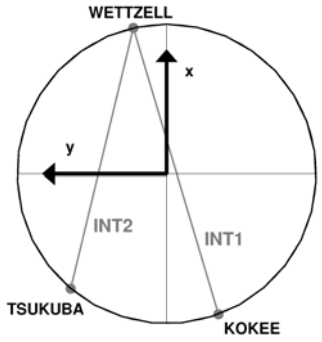

Figure 5.19: *Intensive* baseline directions projected into the equatorial plane and the x- and y-coordinate axes.

5.3.3 Conclusion on the significance of station displacements

Currently available realizations of the terrestrial reference system have an internal accuracy of station positions of smaller than 2 *mm*. For example the standard deviations of station positions and velocities in the vtrf2005 [NOTHNAGEL 2005] are listed in table 5.10.

	Positions 1997.0			**Velocities**			**Positions 2002.0**			**Positions 2006.0**		
$[mm]$	σx	σy	σz	σV_x	σV_y	σV_z	σx	σy	σz	σx	σy	σz
Tsukuba	1.3	1.3	1.9	0.3	0.3	0.3	1.5	1.5	2.0	1.6	1.6	2.1
Wettzell	0.7	0.2	1.0	0.1	0.0	0.2	0.7	0.2	1.1	0.8	0.2	1.2
Kokee Park	0.8	0.4	0.5	0.2	0.1	0.1	0.9	0.5	0.5	1.0	0.5	0.6

Table 5.10: Internal accuracy of station positions and velocities of vtrf2005 [NOTHNAGEL 2005].

Thus, a mismodeling of the station positions in the range of centimeters does not have to be expected. Any internal inaccuracies of the global terrestrial reference frame can be eliminated from the list of possible sole reasons for significant differences between the two *Intensive* series.

A different matter in this context may be unmodeled periodic or episodic local site displacements. Since any unknown horizontal station movements in the range of centimeters are unlikely and do not have to be expected, mainly seasonal height changes should be considered here.

Impact of station heights

Depending on its direction relative to the direction of the baseline a station displacement has different impacts to the UT1 estimates. In this regard especially the impact of height changes is of important interest, because the station heights may be dependent on seasonal factors like the ground water level. Therefore height changes of the three *Intensive* stations have been transformed into x, y and z- components and using the results displayed in table 5.9 the impact of station heights on the UT1 estimates can be derived. Additional empirical tests verified, that this procedure gives correct results. The impact of station heights on UT1 estimates of *Intensive* sessions is listed in table 5.11.

$[\frac{\mu sec}{cm}]$	**Tsukuba** $\frac{dUT1}{dH}$	**Wettzell** $\frac{dUT1}{dH}$	**Kokee Park** $\frac{dUT1}{dH}$
INT1	-	0.3	-0.6
INT2	0.6	-0.2	-

Table 5.11: Impact of station heights on UT1 estimates.

It is incidental that variations of station heights of realistic order of magnitude will not have any significant impact on the estimated UT1 results. For example the station height of Tsukuba varies over the year depending on the ground water level. The maximum height difference between the lowest and the highest level is about 1 cm [MUNEKANE ET. AL. 2004]. From the results presented above it can be definitely eliminated that a significant signal caused by these height changes may be found in the *Intensive* UT1 results.
Also variations of station heights caused by imperfect modeling of loading effects do not have to be expected in a relevant order of magnitude. [SCHERNECK 1993] has estimated position errors for stations near the ocean coast below 1 *mm* induced by errors of the tidal ocean loading model. Also the effect of unmodeled atmospheric loading effects are in the range of a few millimeters for stations closer than 500 km to the coast [MCCARTHY ET. AL. 2003]. The current standard model of station displacements due to solid earth tides is accurate to 1 *mm* [MCCARTHY ET. AL. 2003] and, thus, deficiencies of the earth tide model also do not affect the UT1 results of *Intensive* sessions significantly.

5.4 The impact of high frequency EOP correction on the UT1 estimates

Daily and subdaily variations of earth orientation are induced by different geophysical phenomena like ocean tides, luni-solar gravitational tides, non-tidal oceanic angular momentum and atmospheric tides e.g. [HAAS ET. AL. 2004]. Conventionally, nutation does not include diurnal and subdiurnal terms and the a priori information of polar motion used within *Intensive* analysis is commonly given in one-day steps and, thus, can also not contain high-frequency variations with periods of one day and less. The Universal Time UT1 is defined to be smoothed for these daily and subdaily frequencies and therefore it is necessary to remove the signal of high-frequency EOP variations from the observed VLBI time delays in order to estimate the UT1 of interest. Different models are available to account for these high-frequency variations of polar motion components as well as of UT1.

5.4.1 Theoretical Considerations

In the context of short term single baseline *Intensive* sessions, two aspects of high frequency EOP correction affect the UT1 estimates. At first there is a direct correction of UT1 which covers the daily and subdaily variations of the diurnal earth rotation. This correction is used in order to correct the observed single time delays for its contribution due to the high frequency parts of UT1. Thus the finally estimated UT1 values represent spots of the smoothed UT1 curve not including subdaily frequencies. The amplitudes of the daily and subdaily variations of UT1 are up to 100 μsec [SCHUH ET. AL. 2004].
The second effect of high frequency EOP variations within the analysis of *Intensive* sessions is the corresponding correction of polar motion components. Due to the interrelation of *Intensive* UT1 results with the fixed pole coordinates as depicted in section 5.1, this correction also affects the UT1 estimates. The order of magnitude of the daily and subdaily pole variations is up to 1 *mas*. Thus, according to the considerations in section 5.1, summarized and refined in tables 5.1 (page 49) and 5.3 (page 51), a

significant and baseline dependent impact on the *Intensive* UT1 results has to be expected.
Especially due to the second aspect it also has to be expected that the UT1 results of *Intensive* sessions are significantly more dependent on the model of high-frequency EOP corrections used than UT1 estimated together with all other components of earth orientation from a 24 hour global VLBI network session. Thus, inconsistencies between the UT1 results of the two *Intensive* baselines and those of global network sessions may be induced by any inaccurate high frequency EOP model.

5.4.2 Empirical Considerations

In order to get an idea of the relevance of the diurnal and subdiurnal EOP variations for *Intensive* UT1 results, three different empirical tests have been carried out with different objectives:

1. All *Intensive* sessions of 2005 are analyzed using one of the standard high frequency correction models as an example. Here the model hf1102a [GSFC] has been used for this purpose, which is regularly used within the routine analyses of GSFC and USNO (compare appendix A). The UT1 differences with respect to the results derived without any high frequency correction represent the complete contribution of the correction to the final UT1 results and can help to receive an impression on its relevance.

2. Solutions of the 2005 *Intensives* using the three most common models of high frequency EOP corrections are compared to each other. The UT1 differences between these three solutions give information on the equivalence of the three models in terms of their impacts on *Intensive* UT1 results.

3. The sessions of the Multi-Intensive projects (cp. section 3.3) are used to compare the impact of high frequency corrections on results of *Intensive* and of global network sessions.

The full impact of high frequency EOP correction within *Intenisve* UT1 analysis (item 1) In order to get an impression of the order of magnitude and thus of the relevance of the high frequency EOP correction, the UT1 results of an *Intensive* standard analysis using the correction model hf1102a of GSFC are reduced by the results of an identical analysis but without any high frequency correction. The differences are depicted in figure 5.20 and represent directly the full impact of the correction model to the UT1 results.
With amplitudes up to $\pm 55\ \mu sec$ the significance of the high frequency EOP correction for UT1 estimation is obvious. The UT1 results of the two baselines are affected differently and with varying amplitudes during the year. Consequently the usage of a model of high frequency EOP corrections for the analysis of single baseline observations is essential for the accuracy and consistency of the UT1 results.

Differences between the most common models of high frequency variations (item 2) At present the most common correction models used within routine VLBI analyses are

hf1102a Calculated at the Goddard Space Flight Center from VLBI observations until December 1998 [GSFC],

jmg1996 Calculated by John Gipson from 15 years of VLBI data [Gipson 1996] and

hfray_iers Including the integral Ray model (71 tidal waves) [Ray et. al. 1994] and the Brzezinski-Mathews-Bretagnon-Capitaine-Bizouard model (10 lunisolar waves) of semidiurnal/diurnal variations in the earth's orientation as recommended in the IERS 2003 Conventions [McCarthy et. al. 2003].

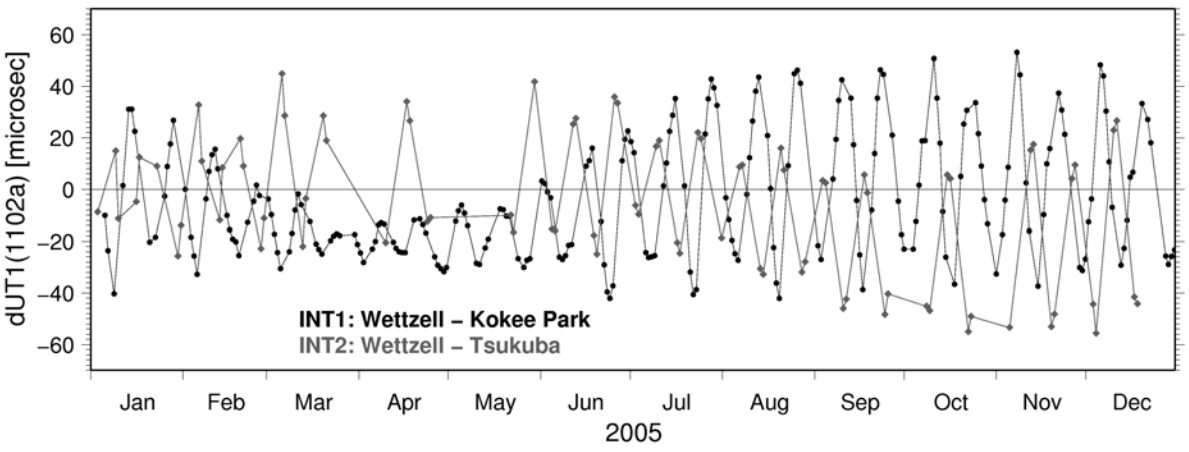

Figure 5.20: Impact of high frequency EOP correction (hf1102a) on UT1 estimates from single baseline *Intensive* sessions during one year.

Here in the context of *Intensive* UT1 estimation not the absolute values of the correction terms are of interest, but only their impact on the final UT1 estimates is considered and compared.
Using these different models of high frequency earth orientation variations three solutions for the year 2005 have been calculated and the differences between their UT1 results are depicted in figure 5.21. Respective RMS values of these differences are summarized in table 5.12.

$[\mu sec]$	**INT1**		**INT2**	
	Offset	RMS	Offset	RMS
JMG96 - HF1102A	0.5	1.6	-0.7	1.5
JMG96 - RAY	-0.2	5.7	-0.7	7.4
HF1102A - RAY	-0.7	5.6	0	7.4

Table 5.12: RMS of UT1 differences induced by different models of high frequency EOP (calculated from *Intensive* sessions of 2005).

As it has to be expected, the usage of different high frequency EOP models does not induce any long term UT1 offsets (table 5.12) but may cause significant time dependent differences. The two series *hf1102a* and *jmg1996* deduced from VLBI observations show very similar effects on the *Intensive* UT1 estimates and thus the respective UT1 differences are all below 5 μsec (1st diagram of figure 5.21). In contrast to that, the third correction model *hfray_iers* causes significantly larger UT1 differences with respect to solutions using one of the other two models (2nd and 3rd diagram of figure 5.21). This fact is also expressed by the respective RMS values of table 5.12. Thus differences between two *Intensive* solutions of up to 15 μsec maybe caused only by the usage of two different correction models of high frequency earth orientation variations.
Corresponding to the results of sections 5.1 and 5.2 the two different *Intensive* baselines are affected in a different way and in worst case additional inconsistencies between the UT1 results of the two baselines of up to 25 μsec may be induced only by using a different high frequency correction model.

As a second aspect, it has been studied in this context which one of the three models has the most beneficial effect on the consistency between the results of the two *Intensive* baselines. For this purpose the mean differences between INT1 and INT2 results and the respective WRMS have been calculated

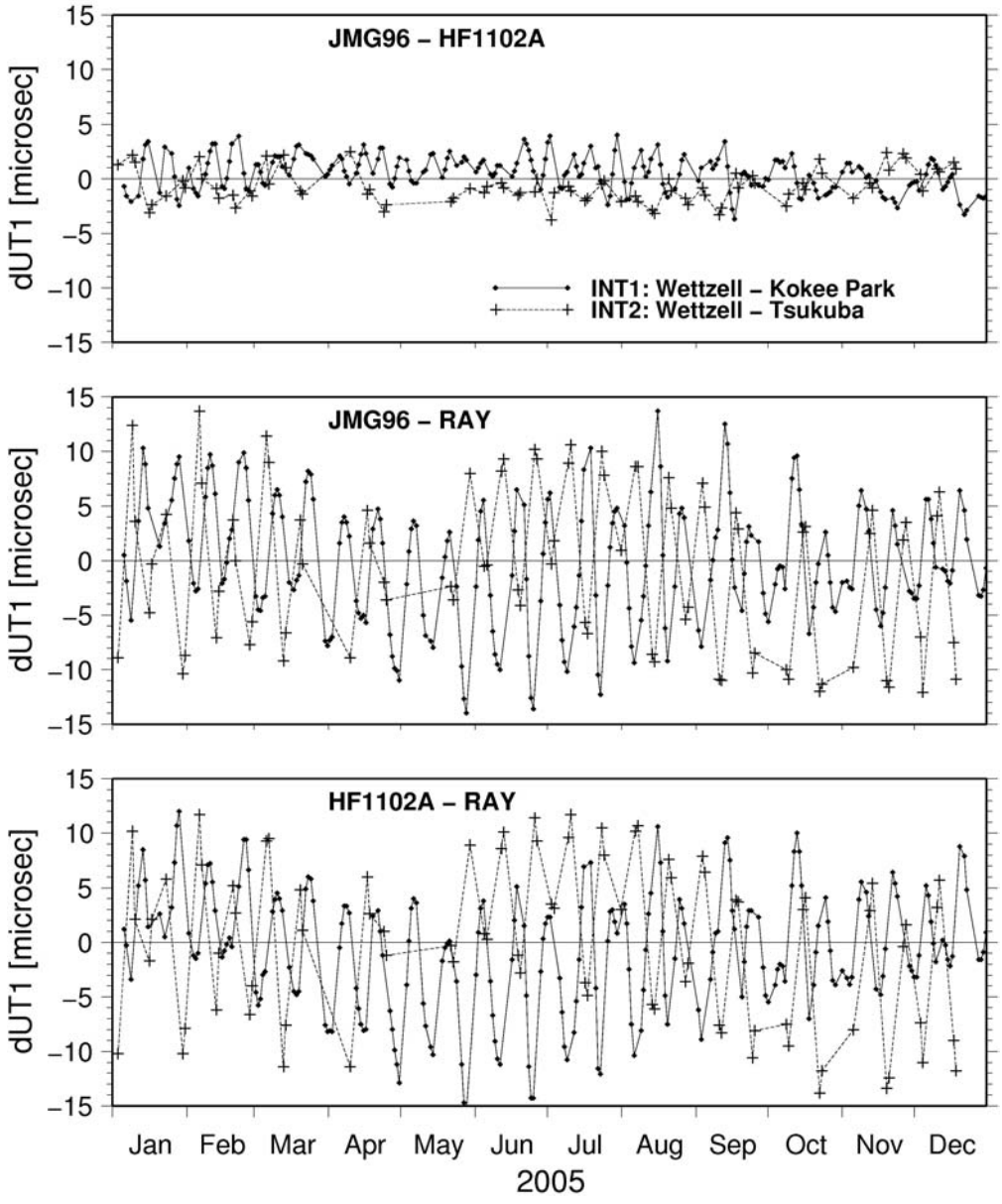

Figure 5.21: Differences of *Intensive* UT1 results caused by the usage of different correction models of high frequency earth orientation variations.

for each of the solutions using the method of piecewise approximating polynomials (cp. section 4.1, page 40). The results are summarized in table 5.13.

$[\mu sec]$	**Without**	**hf1102a**	**jmg1996**	**hfray_iers**
Weighted Mean Difference (INT2-INT1)	-24.0	-16.3	-15.3	-15.2
WRMS after removal of bias	52.7	40.7	39.9	38.1

Table 5.13: Impact of different high frequency EOP correction models on the consistency of UT1 results of the two different baselines. The numbers are based on all *Intensive* sessions of year 2005.

These numbers primarily show that, as it has to be expected, the usage of a high frequency EOP correction model improves the consistency of the results of the two *Intensive* series significantly. The resulting offsets and WRMS for the three corrected solutions do not differ significantly, although in figure 5.21 differences between the models are obvious.

Comparison of the impact of high frequency EOP corrections on *Intensive* UT1 estimates and on results of a global network session (item 3) As already mentioned, the UT1 results of *Intensive* sessions are expected to be significantly more dependent on the correction model of high frequency EOP than the results of a global network session mainly due to the fixed pole components within the analysis and its very weak geometry.

The observations of the Multi-Intensive sessions (cp. section 3.3) are particularly suitable for considerations concerning the high frequencies EOP corrections because they cover a time frame of 24 hours in evenly distributed intervals and, thus, the effects of subdaily EOP variations are directly identifiable. The respective global network session observed at the same time allows a direct comparison between the impact on *Intensive* results and on UT1 received from the network session. In order to isolate the pure effect of the high-frequency EOP correction, again simple differences are calculated between the UT1 results of identical solutions with and without corrections. Exemplarily the results are depicted in figures 5.22 and 5.23 for the often used correction model *hf1102a*.

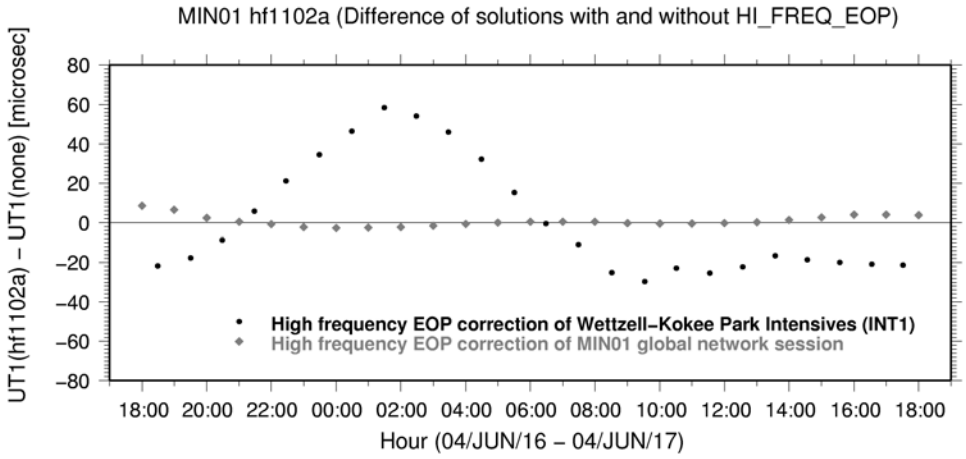

Figure 5.22: Impact of HF1102A high frequency EOP correction on UT1 estimates from single baseline *Intensive* (INT1) and global network sessions. Data of Multi-Intensive (MIN1) project.

As expected in both cases the UT1 results of the global network sessions are not seriously affected by the high frequency correction and the results of the *Intensive* sessions are obviously much more biased. Especially the INT1 baseline, used within the MIN01 sessions, shows a very large reaction to the respective EOP correction (figure 5.22). On the basis of this consideration it is not possible to decide if the different response of the *Intensive* UT1 results to the high frequency correction is due to the two different baseline geometries or caused by the different absolute correction terms at the two different observing days. A direct comparison of the behavior of the two baselines is not possible and not intended here. Only the direct comparison with the reaction of the respective simultaneous global network session is meaningful. Nevertheless the test shows that if we consider the consistency of *Intensive* UT1 results with those of 24 hour global network sessions we have to keep in mind the different effect of high frequency EOP corrections on UT1.

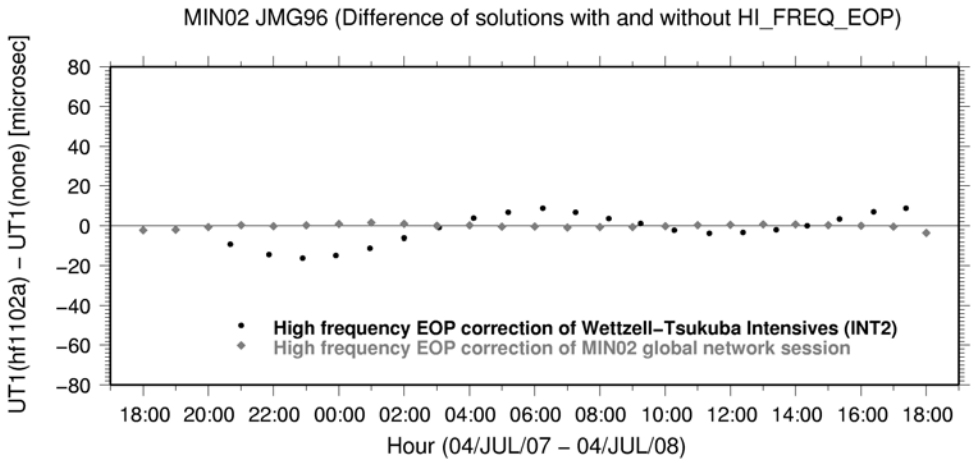

Figure 5.23: Impact of HF1102A high frequency EOP correction on UT1 estimates from single baseline *Intensive* (INT2) and global network sessions. Data of Multi-Intensive (MIN2) project.

5.4.3 Conclusion on the significance of high frequency EOP correction

In terms of single baseline *Intensive* sessions, the impact of a high frequency EOP model on UT1 estimates is always composed of two different aspects: on the one hand the direct correction of subdaily UT1 variations and on the other hand the indirect influence caused by high frequency variations of the pole position. As figure 5.20 shows, the usage of a high frequency correction model within the analysis of *Intensive* sessions is absolutely necessary. The results presented in table 5.13 underline this requirement. The differences between the impacts of the models used on the *Intensive* UT1 estimates are, as presented in figure 5.13, all below 15 μsec. Additionally, because the two baselines are affected differently, inconsistencies between INT1 and INT2 results depending on the correction model used are induced. Their magnitude is up to 25 μsec. Thus, different correction models can explain significant discrepancies between different solutions.
As shown in figures 5.22 and 5.23 the results of global network sessions are much less influenced by the high frequency EOP variations than those of single baseline sessions. Thus, the quality of the high-frequency EOP model affects the agreement between the UT1 results of the two types of VLBI observations.

5.5 The impact of the celestial reference frame on UT1 estimates

The celestial reference system officially used by the IERS for the description of earth orientation is the International Celestial Reference System (ICRS) (compare paragraph *Reference Systems* on page 8). It is realized by VLBI estimates of equatorial coordinates of a set of extragalactic compact radio sources, the International Celestial Reference Frame (ICRF).
Within *Intensive* VLBI sessions the realization of the celestial reference system is based on a small subnet of five to ten sources of the ICRF. Due to the changing sidereal epochs of the sessions these subnets vary during a year. Strictly speaking, each *Intensive* session is based on its own realization of the celestial reference system. Slightly incorrect source positions may lead to different axis directions and, thus, may influence the UT1 estimation. As there are always five to ten different sources used within the *Intensive* sessions, the accuracy of the reference system realized results from the position uncertainties of the individually radio sources used.
The propagation of ICRF errors into the *Intensive* UT1 estimates is identical to the interrelations be-

tween nutation offsets and UT1 (compare section 5.2) and, thus, are different for the two baselines.

As pointed out in [McCarthy et. al. 2003] the 212 defining sources of the ICRF are distributed over the sky with a median uncertainty of 0.35 *mas* in right ascension and of 0.40 *mas* in declination. The original formal uncertainties being below 0.1 *mas* were inflated in order to render their values more realistically and to take into account existing systematic influences [Ma 1998].
The CRS is realized within an *Intensive* session by the positions of five to ten different sources. Therefore random errors of

$$\begin{aligned} \sigma_{CRS}(h) &= \frac{1}{\sqrt{10}} \cdot 0.35\,mas \quad \text{to} \quad \frac{1}{\sqrt{5}} \cdot 0.35\,mas \\ &= 0.11\,mas \quad \text{to} \quad 0.16\,mas \end{aligned} \tag{5.31}$$

for the origin of right ascension and of

$$\begin{aligned} \sigma_{CRS}(\delta) &= \frac{1}{\sqrt{10}} \cdot 0.40\,mas \quad \text{to} \quad \frac{1}{\sqrt{5}} \cdot 0.40\,mas \\ &= 0.13\,mas \quad \text{to} \quad 0.18\,mas \end{aligned} \tag{5.32}$$

for the pole can be assumed. The application of the square root law in spite of the existence of correlations is allowed here because the specified mean uncertainties already include a respective inflation accounting for these correlations.

In order to give a reliable assessment of the uncertainty of the axis realizations within *Intensive* sessions and in particular of its impact on the UT1 estimates, a rounded maximum random error of 0.2 *mas* for the axis realization can be assumed. Applying the interrelations derived with respect to the nutation components (section 5.2, figures 5.12 and 5.13 on pages 62f) a maximum UT1 uncertainty of ± 3 μsec for INT1 and of ± 6 μsec for INT2 sessions have to be expected induced by random position errors of the respective subsets of radio sources.

Chapter 6

Conclusions

6.1 Summary and Evaluation

The second *Intensive* series INT2 using the baseline Wettzell - Tsukuba, carried out regularly since April 2003, is first of all a timely complement to the traditional, long-standing Wettzell - Kokee Park series INT1 and makes it possible to monitor UT1 on a daily basis. In addition, for the first time this independent second *Intensive* baseline allows a verification of baseline dependent impacts on the UT1 estimates of short term single baseline sessions. Although the formal errors of both *Intensive* series are of equal order of magnitude, significant baseline dependent elements of uncertainty have been identified. These geometry and time dependent impacts affect the relative as well as the absolute accuracy of each *Intensive* series.

The relative or internal accuracy reflects the scatter and the consistency of the UT1 values of an individual observing series among each other within a certain time-frame. All *Intensive* impact factors varying randomly with time decrease the internal accuracy of the UT1 series. In order to separate these random impact factors from those factors with a constant signature or a long periodic behavior, the internal accuracy stated here is meant to be valid for time segments of about 14 days. Table 6.1 summarizes the *Intensive*-specific sources of random and fast changing errors, assuming realistic basic conditions.

The absolute or external accuracy specifies the agreement and consistency between the two *Intensive* series and with respect to the UT1 values of 24 hour network sessions. All baseline dependent impact factors that are constant or slowly variable with time lead to systematic differences between the results of the two different *Intensive* baselines. For example the standard deviations of station positions and velocities describe the uncertainty of the coordinates but no time variability. Thus, they limit the absolute but not the relative accuracy of each *Intensive* series. In table 6.2 the factors responsible for the external accuracy including the contribution from the internal accuracy are summarized.

Looking at the root sum square of the impacts of predefined parameters in table 6.1, it becomes obvious that the INT2 baseline is almost twice as sensitive to external impact factors as are the INT1 sessions. The total root sum square reflecting the relative accuracy finally is, however, predominantly influenced by the formal errors of the parameter estimation process. These are mainly dependent on the quality of the delay determination within the correlation process of the VLBI observing technique (plus the noise components added to achieve conformity of theoretical and empirical variance of unity), on the functional model used within the parameter estimation and on the geometrical distribution of single observations across the sky. Regarding the formal errors, the INT2 sessions perform significantly better than INT1 and, thus, in total the relative accuracy of INT2 UT1 values is about twice as good as the one of the INT1 series. The main reason for this discrepancy is the considerably better sky distribution of simul-

Internal / Relative Accuracy								
Impact Factor (IF)	**Maximum Propagation Factors**			**Assumption (σ_{IF})**		**UT1 effect [μsec] ($\sigma_{UT1}(\sigma_{IF})$)**		
	INT1	**INT2**	**Unit**	**INT1**	**INT2**	**INT1**	**INT2**	
Polar Motion Assuming standard deviations of polar motion components as given in [IERS Bull. A].								
x_p	-8.7	30.8	$\frac{\mu sec}{mas}$	0.1 mas		0.9	3.1	Section 5.1
y_p	-14.0	0.3	$\frac{\mu sec}{mas}$	0.1 mas		1.4	0	
Nutation Using the WRMS of observed nutation offsets (table 5.6, page 65) with respect to IERS1996 [McCarthy 1996] as measure for the erratic part of nutation uncertainties affecting the internal accuracy. Propagation factors are dependent on the day of the year and their respective maxima are used here.								
$\Delta\psi$	6.7	12.0	$\frac{\mu sec}{mas}$	0.25 mas		1.7	3	Section 5.2
$\Delta\varepsilon$	16.2	30.7	$\frac{\mu sec}{mas}$	0.14 mas		2.3	4.3	
High Frequency EOP correction Applying the WRMS of the differences between jmg96 and hf1102a (table 5.12, page 72).								
						1.6	1.5	Section 5.4
Celestial Reference Frame Applying the standard deviations given in [IERS 2003], adapted using the square root law (equations 5.31 and 5.32, page 76). Propagation factors are equal to those of nutation offsets.								
$h \hat{=} \Delta\psi$	6.7	12.0	$\frac{\mu sec}{mas}$	0.16 mas		1.1	1.9	Section 5.5
$\delta \hat{=} \Delta\epsilon$	16.2	30.7	$\frac{\mu sec}{mas}$	0.18 mas		2.9	5.5	
Root Sum Square (impacts of basic conditions):						**4.8**	**8.6**	
Parameter estimation Assuming a maximum formal error σ_{UT1} valid for 90% of the sessions (cp. page 35).								
						30	10	Section 3.2.2
Root Sum Square (total):						**30.4**	**13.2**	

Table 6.1: Summary of the *Intensive* specific error budget specifying the internal accuracy of both *Intensive* series valid within periods of 14 days (σ_{IF} = assumed uncertainty of the impact factor).

taneously visible radio sources within INT2 sessions due to their shorter baseline length. Caused by the extreme length of the INT1 baseline the visible sector of the sky is very much limited and it is impossible to observe sources in more or less opposed directions. Additionally the much higher number of single observations within the INT2 sessions has a favorable effect on the formal errors.

A very similar situation becomes obvious regarding the absolute accuracy (table 6.2). This is dependent on the relative/internal accuracy and, additionally, on long term and constant impact factors. Uncertainties of these also affect the INT2 accuracy twice as much as that of INT1. Especially the impact of the nutation component in obliquity is remarkable (compare section 5.2.1).
Finally, the initial advantage of the INT2 sessions reflected in their significantly lower level of formal errors is canceled out markedly by their higher sensitivity to the fixed a priori values within the parameter estimation.

Absolute Accuracy								
Impact Factor (IF)	**Maximum Propagation Factors**			**Assumption** (σ_{IF})		**UT1 effect** [μsec] ($\sigma_{UT1}(\sigma_{IF})$)		
	INT1	**INT2**	**Unit**	**INT1**	**INT2**	**INT1**	**INT2**	
Nutation	Assuming the mean bias of observed nutation offsets (table 5.6, page 65) with respect to IERS1996 [McCarthy 1996] as measure for the constant part of nutation uncertainties affecting the absolute UT1 accuracy. Propagation factors are dependent on the day of the year and their respective maxima are used here.							
$\Delta\psi$	6.7	12.0	$\frac{\mu sec}{mas}$	0.33 mas		2.2	4.0	Section 5.2
$\Delta\epsilon$	16.2	30.7	$\frac{\mu sec}{mas}$	0.39 mas		6.3	12.0	
Terrestrial Reference Frame Assuming uncertainties of station positions according to VTRF2005.								
x	0.4	0.5	$\frac{\mu sec}{mm}$	1.22 mm	1.66 mm	0.5	0.8	Section 5.3
y	1.3	1.6	$\frac{\mu sec}{mm}$	0.54 mm	1.51 mm	0.7	2.4	
z	0.1	0.8	$\frac{\mu sec}{mm}$	1.25 mm	2.37 mm	0.1	1.9	
Terrestrial Reference Frame (local)	Variations of station heights due to seasonal effects and changing atmospheric loading. Assumptions are roughly estimated from GPS time series [IGS time series].							
$H_{Tsukuba}$	-	0.6	$\frac{\mu sec}{cm}$	1 cm		-	0.6	Section 5.3
$H_{Wettzell}$	0.3	-0.2	$\frac{\mu sec}{cm}$	0.5 cm		0.2	0.1	
H_{Kokee}	-0.6	-	$\frac{\mu sec}{cm}$	1.5 cm		0.9	-	
Root Sum Square (impacts of basic conditions):						**6.8**	**13.0**	
Internal / Relative Accuracy Compare table 6.1.								
						30.4	13.2	
Root Sum Square (total):						**31.1**	**18.5**	

Table 6.2: Summary of the *Intensive* specific error budget specifying the absolute accuracy of both *Intensive* series.

Recapitulating, it remains to point out that the UT1 estimates of the two single *Intensive* baselines respond to uncertainties of the fixed a priori quantities in a different way and partly dependent on time. These interactions cause inconsistencies between the two observing series and affect their internal as well as their absolute accuracy. As a consequence the real uncertainty of *Intensive* sessions does not satisfy the generally assumed current accuracy level of 20 μsec as documented in e.g. [IVS Working Group 2]. This fact is also reflected in the WRMS differences between the two *Intensive* UT1 series being about 30 μsec (cp. table 4.1, page 42).

6.2 Future Prospects

As documented in [IVS Working Group 2] and in [IVS Working Group 3] the future goal for the next years in terms of *Intensive* UT1 results is at an accuracy level below 10 μsec; even 5 to 7 μsec are considered to be possible. In order to reach this ambitious objective a couple of improvements in terms of model accuracy, observing technique and geometry will be necessary. In the following, a brief overview of the existing room for improvement is given, completely isolated from any economic or organizational limitations. The individual items are shortly beeing discussed in the same order as done in tables 6.1

and 6.2. Finally all aspects are summarized in table 6.4 giving a rough estimate of the reachable floor of UT1 accuracies.

Motion of the terrestrial pole In view of the passably low impact of current pole component uncertainties (table 6.1) on *Intensive* UT1 estimates, only slight UT1 improvements can be expected from perfecting the determination and timeliness of polar motion components e.g. within the IERS. The IVS Working Groups 2 [IVS Working Group 2] and 3 [IVS Working Group 3] suspect an improvement by a factor of 2 to 4 in terms of pole determination accuracy within the next years, mainly realized by improved network geometries, technical developments and refined analysis. If these results will be available with short time delays after the observation and a similar advancement can be realized also in terms of GPS observations and analysis, the standard deviations of a priori pole components available for *Intensive* analysis may be, roughly estimated, reduced to 0.025 *mas*. The associated improvements of UT1 estimates are summarized in table 6.4.

Independent of these improvements in terms of pole information accuracy, a second aspect has to be mentioned in this context. According to the theoretical geometrical interrelations (equations 5.8 and 5.9, page 49), a baseline composed of two telescopes located at equal latitudes would be largely insensitive to pole component uncertainties. Although the empirical tests have shown a divergence between the simplified theory and real behavior, a minimization of the pole impact by using an *Intensive* baseline parallel to the equator may safely be expected.

Nutation Deficiencies in the nutation model are relevant in terms of both relative and absolute accuracy of *Intensive* UT1 series and, thus, the use of a more accurate nutation model would result in a noticeable improvement of the UT1 results. A first and promising action in this direction is the implementation of the new and improved nutation model IAU2000A [IAU 2000] within the software systems used for regular *Intensive* analysis. These days (middle of 2006) the new version of the CALC/Solve [CALC/SOLVE] software including the new nutation model is available and the routine analysis process at the Analysis Centers will be switched over to it in the near future. The improvements in terms of *Intensive* UT1, that have to be expected from the new model are beeing outlined briefly on page 65. In particular the reduction of the offset of $\Delta\epsilon$ (nutation in obliquity) coming along with the new model will have a noticeable improving effect on the *Intensive* results because this component contributes considerably to the total error budget (cp. table 6.2). Its offset with respect to results of VLBI network sessions may be expected to be approximately halved when using the IAU2000 model.

This study revealed that the success of *Intensive* UT1 series highly depends on the nutation information the analysis is based on. In order to reach the optimum in this respect, it should be considered whether nutation information resulting from observations should be used instead of using a geophysical model. One of the future goals of the IVS documented in [IVS Working Group 2] is to provide the nutation components with an accuracy of 25 to 50 μas available within one day after the observation. This improved accuracy and timeliness in conjunction with advanced combination and prediction techniques may allow a considerable reduction of the uncertainties of short term predicted values for nutation components. In the future, nutation offsets from observations or short term predictions may possibly be used for the *Intensive* analysis instead of modeled values. Consequently the constant nutation offsets taken into account in the context of absolute accuracy (table 6.2) would disappear and the erratic part affecting the relative accuracy (table 6.1) would be significantly reduced. The modeling of nutation presumably provides the largest room for improvement in terms of *Intensive* UT1 accuracy.

Ignoring organizational restrictions, it should also be considered whether the observing windows of *Intensive* sessions can be fixed to a constant sidereal time, in order to minimize the time-dependent effect of

nutation mismodelings. In order to find the optimal sidereal time for each of the two *Intensive* baselines, the curves describing the nutation impacts (figures 5.12 and 5.13, page 62) can help. The respective sidereal epochs with minimized nutation influence as summarized in table 6.3 are derived from adding the respective curves for both nutation components and calculating their zero points.

INT1:	2 h 25 min	and	14 h 25 min	GAST
INT2:	10 h 35 min	and	22 h 35 min	GAST

Table 6.3: Fixed sidereal observing epochs of minimized impact of nutation uncertainties on *Intensive* UT1 estimates.

Finally it should be mentioned that, again, two stations situated at equal latitudes would minimize the propagation of nutation uncertainties to UT1 results as well.

High Frequency EOP correction Improvements of the correction models, e.g. by the analysis of newer observing material, may possibly reduce the scatter slightly. With respect to *Intensive* UT1 results the benefit would be relatively small, because its share in the complete error budget is not that large.

Terrestrial Reference Frame Geometrical considerations as well as empirical tests have shown a very low sensitivity of *Intensive* UT1 results to variations in station positions. Both horizontal as well as vertical components do not have a very large impact on the UT1 estimates so that further improvements in terms of the terrestrial reference frame will only slightly improve the *Intensive* results.

Celestial Reference Frame Room for improvement with respect to the celestial reference frame is primarily given if a densification of the source distribution is realized. If more sources equally and densely distributed over the whole hemisphere with precise positions are available, much better schedule geometries and more different sources per session will be possible (see below, paragraph on geometry).
In particular, an increased number of low declination sources, that are essential for the determination of UT1, would have a noticeable beneficial effect on the *Intensive* results. Especially the INT1 sessions observing an extremely long baseline would profit from that, because the inclusion of equatorial sources could be guaranteed for every session. In this respect, more sensitive observing modes using higher data rates are necessary in order to allow the inclusion of weaker radio sources.

Improvements of the source position accuracy by an order of magnitude including further investigations in terms of individual source structures are formulated in [IVS Working Group 2] as a long-term objective in order to satisfy the requirements of future satellite programs. These advancements will, of course, also benefit the *Intensive* results. An increased number of different sources within the observing schedules mentioned before and the accompanied geometrical improvements (see below) due to a denser distribution of cataloged radio sources are expected to be more significant in terms of *Intensive* UT1 results than the beneficial effect of more accurate source positions. Top priority in terms of CRF improvements should therefore be given to a densification.

Formal errors / determinability of unknown parameters In order to improve the formal errors of the estimated parameters different main aspects have to be considered:

- Improvements in terms of observing geometries in order to increase the determinability and separability of unknown parameters,
- Refinements of the physical model describing the local atmosphere in a more realistic manner,

- Enable more observations per session in order to improve redundancy,
- Technical improvements with regard to the observation and recording process of VLBI measurements reducing the noise level of raw observations.

All these endeavors providing a certain room for improvement with respect to *Intensive* UT1 results will briefly be depicted here.

Geometry: In order to improve the observing geometry of an *Intensive* session both, the distribution of observable sources and the location of the telescopes, are relevant.
A significant densification of the observable sources as mentioned above will be very beneficial with respect to the creation of well balanced observing schedules including a sufficient number of equatorial sources in every *Intensive* schedule. Irregular variations in the observing schedules due to a limited amount of possible sources affecting the geometrical constellation can be avoided that way. The usage of a sophisticated scheduling software for the automatic creation of optimized *Intensive* schedules would also contribute to improved schedule geometries. In this context it should also be mentioned that, if fixed sidereal observing epochs are aspired following table 6.3, the number and distribution of simultaneously visible sources should be checked in advance and the epochs should be adapted if necessary. The best estimates resulting from sessions of the past give rise to the assumption that optimized schedules using an expanded number of sources allow improved and uniform formal errors. Comparing the formal errors of the best sessions of each *Intensive* series with the average, an improvement by a factor of 3 for INT1 and of 2 for INT2 may be expected.

In terms of geometry also the baseline length and location has to be considered. From the comparison of typical INT1 and INT2 observing schedules it becomes obvious, that the INT2 baseline, being about 2000 km shorter than INT1, allows significantly better schedules including more equatorial sources, although both baselines are located at similar latitudes. This advantage compensates its slightly reduced sensitivity for daily earth rotation entirely. This gives rise to the assumption that a shorter baseline length than Wettzell - Kokee Park is more suitable and further simulations and theoretical investigations are needed in order to find the optimal lengths. However, the installation and operation of new telescopes is mainly driven by national interests which mostly do not match geometrical optimizations. The positive effect of a shorter baseline length will become less important, if the sky coverage is substantially improved in the future.
In terms of a fictitious equatorial baseline the visibility of low declination sources would be optimal. In that case, an extremely long baseline may be expected to be less problematic as it is now.

Modeling of the local atmosphere: Due to the very low number of observations within an *Intensive* session, the estimation of the atmospheric path delay is currently limited to one constant zenith wet delay per station. This approach is based on the unrealistic assumption that the local atmosphere is evenly stratified within the telescope's visual field. In reality this is not true and scans in different directions pass areas of different refractivity. Thus, the tropospheric path delays of all individual scans cannot be subsumed under one commonly estimated zenith path delay simply projected using a standard mapping function. As the limited observing material does not allow the estimation of atmospheric gradients describing the radial inhomogeneity, it has to be considered if external information may help to overcome this shortcoming. For example, water vapor radiometer (WVR) observations along the line of sight of each VLBI telescope could provide the unknown wet path delay information or, at least, the respective local gradients enabling an improved estimation of the zenith delay within the VLBI analysis. Investigations in the beneficial effect of simultaneous WVR observations for the geodetic VLBI analysis are currently carried out (e.g. [Cho et. al. 2006]).

Another possibility for receiving external information about the atmosphere is provided by GPS observations carried out routinely in the vicinity of the VLBI telescopes. So far, this potential has not been researched thoroughly in the past, but should be revisted as soon as existing biases between VLBI and GPS wet path delay estimates are understood. It may be expected that especially INT1 can benefit from an improved handling of the unknown atmosphere because due to the much longer baseline the possibility of observing enough sources under varying elevation angles is strongly limited and, thus, the estimability of the atmospheric path delay suffers. A justifiable quantification of the possible improvements due to external information about the atmosphere cannot be given here.

More observations per session: A simple increase in the number of observations per session would also reduce the estimated formal errors to some degree. As the improvement expected from additional observations per session is restricted by the geometrical limitation for including independent extra observations, all aspects mentioned above in terms of the observing geometry apply here as well. Actions aiming at enabling more observations per session only make sense, if the available catalog of observable sources is expanded significantly.
For the realization of more observations per session either the session time has to be expanded or the observing workflow has to be sped up. An extension of the session duration significantly beyond one hour causes some new and unwanted side effects in terms of clock stability and timeliness of postprocessing. A speed-up of the observing procedure requires some technical improvements. New small and light telescopes allow quick moves between the individual scans; increased sensitivity by higher data rates would enable shorter scan durations. But, as mentioned before, the beneficial effect of these extensive modifications depends very much on the number and distribution of simultaneously visible sources.
Another possibility of increasing the number of observations is the future usage of so-called Multi-Beam VLBI [Petrachenko et. al. 2002] or VLBI-antenna-clusters [Haase 2006]. Constructions like these will enable simultaneous observations of two or even more different sources at each site. This will not only increase the number of observations but also allow a better detection of the refractive environment.

Technical advancements during the recording procedure: While the delay determination by the VLBI correlators has a noise floor of 8 ps [Ray et. al. 1991] some weak points do exist within the primary recording process. For example the signal propagation path between hydrogen maser atomic clock and formatter which may exceed 100 m is currently suspected to be a possible source of variable delay. Another field of current investigations are potential small observing errors due to polarization impurities that are possibly not constant from scan to scan (Roy, personal communication). Further investigations in terms of observing and recording technique therefore may enable an improved modeling of effects like this and, thus, may improve the accuracy of the delay determination.

The points summarized here outline the extensive room for improvement with respect to the accuracy of *Intensive* UT1 results. The summary in table 6.4 shows a strawman plan for an improved scenario of error contributions and documents the urgent need for advancements especially in terms of observing geometry and nutation modeling. In order to reach the ambitious goal of a UT1 accuracy of 5 to 7 μsec, as considered to be possible by the IVS [IVS Working Group 2], even more improvements than taken into account in table 6.4 will be necessary. In particular the usage of observed or shortly predicted nutation components as mentioned before provides more room for improvement than the usage of the IAU2000A model assumed in table 6.4.

A Vision for the Future of *Intensive* UT1 accuracy							
Impact Factor (IF)	**Maximum Propagation Factors**			**Assumption** (σ_{IF})		**UT1 effect** [μsec] ($\sigma_{UT1}(\sigma_{IF})$)	
	INT1	**INT2**	**Unit**	**INT1**	**INT2**	**INT1**	**INT2**
Polar Motion Rough estimate on the future accuracy of available pole information.							
x_p	-8.7	30.8	$\frac{\mu sec}{mas}$	0.025 mas		0.2	0.8
y_p	-14.0	0.3	$\frac{\mu sec}{mas}$	0.025 mas		0.4	0
Nutation scatter No improvement when using IAU2000A compared to the status quo (table 5.7, page 65).							
$\Delta\psi$	6.7	12.0	$\frac{\mu sec}{mas}$	0.29 mas		1.9	3.5
$\Delta\varepsilon$	16.2	30.7	$\frac{\mu sec}{mas}$	0.13 mas		2.1	4.0
Nutation offset Improving effect due to IAU2000A used instead of IERS1996 (table 5.7, page 65).							
$\Delta\psi$	6.7	12.0	$\frac{\mu sec}{mas}$	0.23 mas		1.5	2.8
$\Delta\varepsilon$	16.2	30.7	$\frac{\mu sec}{mas}$	0.14 mas		2.3	4.3
High Frequency EOP correction Assuming a slight improvement of about 25% when using a new, refined correction model.							
						1.2	1.1
Celestial Reference Frame Assuming 10 different and well distributed sources per session enabled by a significant densification of the source catalog.							
$h\hat{=}\Delta\psi$	6.7	12.0	$\frac{\mu sec}{mas}$	0.11 mas		0.7	1.3
$\delta\hat{=}\Delta\epsilon$	16.2	30.7	$\frac{\mu sec}{mas}$	0.13 mas		2.1	4.0
Terrestrial Reference Frame No significant improvements expected (cp. table 6.2).							
x	0.4	0.5	$\frac{\mu sec}{mm}$	1.22 mm	1.66 mm	0.5	0.8
y	1.3	1.6	$\frac{\mu sec}{mm}$	0.54 mm	1.51 mm	0.7	2.4
z	0.1	0.8	$\frac{\mu sec}{mm}$	1.25 mm	2.37 mm	0.1	1.9
Terrestrial Reference Frame (local) No significant improvements expected (cp. table 6.2).							
$H_{Tsukuba}$	-	0.6	$\frac{\mu sec}{cm}$	1 cm		-	0.6
$H_{Wettzell}$	0.3	-0.2	$\frac{\mu sec}{cm}$	0.5 cm		0.2	0.1
H_{Kokee}	-0.6	-	$\frac{\mu sec}{cm}$	1.5 cm		0.9	-
Root Sum Square (impacts of basic conditions):						**4.9**	**9.2**
Parameter estimation Roughly estimated improving factors of 3 for INT1 and 2 for INT2 derived from ratios of formal errors between best and averaged sessions (cp. table 6.1). Other aspects than geometry are unconsidered, because their beneficial effect cannot be estimated realistically within the scope of this thesis.							
						10	5
Root Sum Square (total):						**11**	**10**

Table 6.4: Error budget of *Intensive* accuracy considering possible improvements. The aspects are listed independently of their prospective of realization and neglecting all financial and organization limitations. All numbers summarized here are conjectural only.

Appendix A

Overview of standard solutions

	Goddard Space Flight Center (GSFC)	**US Naval Observatory** (USNO)	**St. Petersburg University** (SPU)
Software	CALC 9.12 SOLVE 2003.05.15	CALC 9.12 SOLVE 2005.04.11	OCCAM V. 5.0
Adjust. method	Least Square	Least Square	Least Square
Parameterization EOP Atmosph. Clock	 UT1-UTC Zenith wet delay offset per station 2nd order polyn.	 UT1-UTC Zenith wet delay offset per station 2nd order polyn.	 UT1-UTC Zenith wet delay offset per station 1st order polyn.
Tropos. Mapping	Niell Map. Funct.	Niell Map. Funct.	Niell Map. Funct.
Dry Tropos.	Saastamoinen	Saastamoinen	Not specified
Gradients	From weather model	From weather model	No
TRF	GSFC TRF solution gsfc2005a	USNO TRF solution usno_2005c_for_int	ITRF2000
CRF	GSFC CRF solution 2005a_apr.src	USNO CRF solution usno_2005c_for_int.src	ICRF Navy 1997-8
Polar Motion	[IERS Bull. A] aligned to gsf2005e.eops	[IERS Bull. A] aligned to usn2005c.eops	Not specified
Nutation	IERS1996	IERS1996	IAU_2000A
Precession	IERS1996	IERS1996	IAU1976
Hi-Frequ. EOP	hf1102a	hf1102a	IERS Conv. (hfray)
Solid Earth Tides	IERS1996 incl. 3rd order	IERS1996 incl. 3rd order	IERS2000
Ocean Loading	GSFC model with 18 constituents	No	IERS2000
Atmos. Loading	3D-displ. from NCEP Reanalysis model [Petrov et. al. 2004]	No	IERS 1996 Conv. + Explana. Suppl.
Weighting	Stand. deviations of fringe fitting and reweighting to unity of chi square	Stand. deviations of fringe fitting and reweighting to unity of chi square	For elevation $> 15°$: No For elevation $< 15°$: $1/\sin(elev.)$

Table A.1: Analysis features of the *Intensive* solutions as input for the IERS rapid EOP series.

Appendix B

Parameter correlations of the Multi-Intensive Sessions

Sess. No.	Clock vs. Cl.rate	Clock vs. At(Kk)	Clock vs. At(Wz)	Clock vs. UT1	Cl.rate vs. At(Kk)	Cl.rate vs. At(Wz)	Cl.rate vs. UT1	At(Kk) vs. At(Wz)	At(Kk) vs. UT1	At(Wz) vs. UT1
MIN01: Wettzell - Kokee Park										
1	-0.265	-0.913	0.877	0.189	0.100	0.00	0.102	-0.749	-0.165	-0.029
2	-0.243	-0.857	0.635	0.354	-0.025	0.343	-0.116	-0.536	-0.353	-0.176
3	-0.613	-0.840	0.865	0.402	0.272	-0.291	-0.423	-0.738	-0.098	0.272
4	-0.249	-0.840	0.805	0.400	-0.130	0.217	0.00	-0.744	-0.200	0.291
5	0.09	-0.856	0.915	-0.297	-0.391	0.339	-0.234	-0.788	0.466	-0.356
6	-0.165	-0.872	0.825	-0.070	-0.172	0.193	-0.324	-0.730	0.190	-0.320
7	-0.255	-0.853	0.788	0.06	-0.007	0.167	-0.247	-0.612	-0.082	-0.281
8	-0.620	-0.915	0.784	0.481	0.464	-0.187	-0.212	-0.691	-0.414	0.206
9	-0.410	-0.757	0.930	0.870	0.03	-0.164	-0.400	-0.654	-0.469	0.901
10	-0.557	-0.495	0.553	0.01	0.185	0.06	-0.024	0.177	0.638	0.376
11	-0.190	-0.884	0.752	0.247	-0.013	0.263	0.00	-0.578	-0.171	0.208
12	-0.558	-0.783	0.785	0.424	0.158	-0.137	-0.166	-0.567	-0.589	0.290
13	-0.280	-0.877	0.844	0.432	-0.049	-0.021	0.263	-0.682	-0.573	0.419
14	-0.527	-0.599	0.706	0.288	0.06	-0.025	0.07	-0.288	-0.426	0.507
15	-0.534	-0.472	0.752	-0.241	-0.114	-0.155	0.221	-0.144	-0.080	-0.170
16	-0.595	-0.544	0.713	-0.188	0.252	-0.107	-0.234	-0.041	-0.071	-0.372
17	-0.475	-0.565	0.756	-0.045	-0.176	-0.093	0.202	-0.424	-0.396	0.219
18	-0.465	-0.771	0.770	-0.052	0.06	-0.062	-0.010	-0.518	0.09	0.09
19	-0.699	-0.667	0.589	0.132	0.01	0.07	-0.050	-0.716	-0.044	0.196
20	-0.290	-0.647	0.558	-0.114	-0.231	0.147	-0.008	-0.124	0.331	0.307
21	-0.486	-0.793	0.854	0.501	0.06	-0.208	-0.187	-0.602	-0.484	0.533
22	-0.198	-0.820	0.860	0.215	-0.090	0.129	0.05	-0.643	-0.317	0.213
23	-0.185	-0.893	0.887	-0.423	-0.106	0.108	0.164	-0.787	0.386	-0.394
24	-0.404	-0.880	0.750	0.197	0.117	0.05	0.310	-0.656	-0.240	0.182

Table B.1: Parameter correlations resulting from single baseline sessions of the MIN01 project. They exemplify the correlations as they typically occur in INT1 *Intensive* sessions.

Sess. No.	Clock vs. Cl.rate	Clock vs. At(Ts)	Clock vs. At(Wz)	Clock vs. UT1	Cl.rate vs. At(Ts)	Cl.rate vs. At(Wz)	Cl.rate vs. UT1	At(Ts) vs. At(Wz)	At(Ts) vs. UT1	At(Wz) vs. UT1
MIN02: Wettzell - Tsukuba										
3	-0.608	-0.691	0.761	-0.613	0.120	-0.308	0.228	-0.313	0.466	-0.526
4	-0.248	-0.723	0.608	-0.281	-0.200	0.215	-0.243	-0.301	0.326	-0.159
5	-0.654	-0.614	0.493	-0.016	0.204	-0.052	-0.027	0.07	-0.375	-0.301
6	-0.224	-0.733	0.630	-0.403	-0.142	0.267	-0.231	-0.306	0.392	-0.318
7	-0.630	-0.774	0.759	-0.265	0.287	-0.200	0.126	-0.532	0.103	-0.047
8	-0.428	-0.758	0.818	-0.127	0.04	-0.050	0.00	-0.585	0.02	0.05
9	-0.587	-0.721	0.677	-0.315	0.176	-0.090	0.168	-0.389	0.141	-0.054
10	-0.548	-0.568	0.824	-0.301	-0.178	-0.213	0.363	-0.492	-0.135	-0.093
11	-0.381	-0.627	0.612	-0.358	0.01	0.291	-0.205	-0.225	0.265	-0.472
12	-0.629	-0.655	0.659	-0.239	0.191	-0.023	0.204	-0.360	-0.034	-0.059
13	-0.554	-0.504	0.630	-0.283	-0.069	-0.100	0.142	-0.094	-0.091	-0.127
14	-0.352	-0.680	0.767	-0.198	-0.120	0.06	-0.148	-0.459	0.102	-0.118
15	-0.411	-0.580	0.699	-0.316	-0.016	0.118	-0.016	-0.362	-0.140	-0.211
16	-0.451	-0.653	0.727	-0.285	-0.074	0.03	0.179	-0.503	-0.241	-0.185
17	-0.352	-0.680	0.767	-0.198	-0.120	0.06	-0.148	-0.459	0.102	-0.118
18	-0.523	-0.833	0.776	-0.171	0.265	-0.058	-0.078	-0.632	-0.025	-0.103
19	-0.997	-0.185	0.148	0.167	0.126	-0.097	-0.193	-0.164	0.136	0.174
20	-0.607	-0.667	0.669	-0.193	0.236	-0.042	0.102	-0.291	-0.050	-0.027
21	-0.380	-0.589	0.753	-0.332	-0.111	-0.039	-0.205	-0.252	0.00	-0.409
22	-0.518	-0.786	0.763	-0.180	0.105	-0.208	0.00	-0.512	-0.077	-0.184
23	-0.532	-0.573	0.673	-0.073	0.02	-0.029	-0.164	-0.301	-0.236	0.01

Table B.2: Parameter correlations resulting from single baseline sessions of the MIN02 project. They exemplify the correlations as they typically occur in INT2 *Intensive* sessions.

Bibliography

[Astron. Almanac 1984] Supplement to the Astronomical Almanac 1984, *The introduction of the improved IAU system of astronomical constants, time scales and reference frame into the astronomical almanac.* Prepared Jointly by The Nautical Almanac Office, U.S. Naval Observatory and H.M.Nautical Almanac Office, Royal Greenwich Observatory, 1983

[Babcock 1988] Babcock A. K., *Recent improvements in the U.S.N.O. combined solution for earth rotation parameters.* In A. K. Babcock and G. A. Wilkins (eds.), The Earth's Rotation and Reference Frames for Geodesy and Geodynamics, 241-245, 1988

[BIPM 1995] Bureau International des Poids et Mesures (BIPM), *What time is it?*, http://www.bipm.org/en/scientific/tai/time_server.html

[BIPM 1998] Bureau International des Poids et Mesures (BIPM), *The International System of Units (SI).* 7th edition of the brochure, http://www.bipm.fr/en/publications/brochure

[Brockmann 1997] Brockmann E., *Combination of Solutions for Geodetic and Geodynamic Applications for the Global Positioning System (GPS).* Geodätisch-geophysikalische Arbeiten in der Schweiz, Schweizerische Geodätische Kommission, Volume 55, 1997

[CALC/SOLVE] Goddard Space Flight Center, *Mark-5 VLBI Analysis Software Calc/Solve.* User manual and description of the Calc/Solve Software, http://gemini.gsfc.nasa.gov/solve/

[Capitaine et. al. 1986] Capitaine N., B. Guinot, J. Souchay, *A Non-Rotating Origin on the Instantaneous Equator: Definitions. Properties and Use.* Celestial Mechanics 39 (1986), p. 283-307

[Capitaine et. al. 1993] Capitaine N., A.-M. Gontier, *Accurate procedure for deriving UT1 at a submilliarc-second accuracy from Greenwich Sidereal Time or from the stellar angle.* Astronomy and Astrophysics, 275 (1993), p. 645-650

[Capitaine 2000] Capitaine N., *Definition of the Celestial Ephemeris Pole and the Celestial Ephemeris Origin.* Towards Models and Constants for the Sub-Microarcsecond Astrometry, Proceedings of the IAU Colloquium 180, Washington, 27-30 March 2000, pp. 153-163

[Capitaine 2000a] Capitaine N., B. Guinot, D. D. McCarthy, *Definition of the Celestial Ephemeris Origin and of UT1 in the International Celestial Reference Frame.* Astronomy and Astrophysics, February 16, 2000, AA1700E

[Cho et. al. 2006] Cho J.-h., A. Nothnagel, A. Roy, R. Haas, *A generalized scheme to retrieve wet path delays from water vapor radiometer measurements applied to European geodetic VLBI network.* Proceedings of the IVS 2006 General Meeting, 9. - 13. January 2006, Concepcion, Chile, in print

[Clark et. al. 1985] Clark T. A., E. C. Brian, J. L. Davis, G. Elgered, T. A. Herring, H. F. Hinteregger, C. A. Knight, J. I. Levine, G. Lundqvist, C. Ma, E. F. Nesman, R. B. Phillips, A. E. E. Rogers, B. O. Ronnang, J. W. Ryan, B. R. Schupler, D. B. Shaffer, I. I. Shapiro, N. R. Vandenberg, J. C. Webber, A. R. Whitney, *Precision Geodesy Using the Mark-III Very-Long-Baseline Interferometer System.* IEEE Transactions on Geoscience and Remote Sensing, Vol. GE-23, No. 4, July 1985, pp. 438-449

[Davis 1986] Davis J., *Atmospheric propagation effects on radio interferometry.* Scientific Report No. 1, AFGL-TR-86-0243, Air Force Geophysics Laboratory, United States Air Force, Hanscom AFB, MA, April 1986

[Eubanks et. al. 1994] Eubanks M., B. A. Archinal, M. S. Carter, F. J. Josties, D. N. Matsakis, D. D. McCarthy, *Earth Orientation Results from U.S. Naval Observatory VLBI Program.* IERS Technical Note 17, Observatoire de Paris, pp. R65-R79

[Fernandez 2001] Fernandez L. I., D. Gambis, E. F. Arias, *Combination procedure for length-of-day time series according to the noise frequency behaviour.* Journal of Geodesy (2001) 75: 276-282

[Fricke et. al. 1988] Fricke W., H. Schwan, Lederle T., *Fifth Fundamental Catalogue (FK5), Part I. The basic fundamental stars.* Veröffentlichungen Astronomisches Rechen-Institut Heidelberg, No. 32, Karlsruhe, 1988

[Gambis et. al. 2002] Gambis D., T. Johnson, R. Gross, J. Vondrak, *General Combination of EOP Series.* Proceedings of the IERS Workshop on Combination Research and Global Geophysical Fluids, Bavarian Academy of Science, Munich, 18. - 21. November 2002, IERS Technical Note No. 30

[Gambis et. al. 2003] Gambis D., P. Baudouin, C. Bizouard, M. Bougeard, T. Carlucci, N. Essaïfi, G. Francou, D. Jean-Alexis, M. Saïl, *Earth Orientation Center.* IERS Annual Report 2003, pp. 39-48, IERS Central Bureau, Bundesamt für Kartographie und Geodäsie, Frankfurt am Main, 2003, ISBN 3-89888-914-9 http://www.iers.org/documents/publications/ar/2003/ar2003.pdf

[Gipson 1996] Gipson J. M., *Very long baseline interferometry determination of neglected tidal terms in high-frequency Earth orientation variation.* Journal of Geophysical Research, Vol. 101, No. B12, pp. 28,051-28,064

[GSFC] Goddard Space Flight Center, Geodetic VLBI group, http://gemini.gsfc.nasa.gov/solve_save/hf1102a

[Haas et. al. 2004] Haas R., R. Del Cojo López, J. M. Lozano, *Investigations of High-Frequency Earth Rotation Variations from VLBI CONT Observations.* Proceedings of the IVS 2004 General Meeting, 9. - 11. February 2004, Ottawa, Canada, pp. 403 - 407

[Haase 2006] Haase A., *Untersuchungen zur Nutzung von VLBI-Antennen-Clustern.* Unpublished Diploma Thesis at the Geodetic Institute of the University of Bonn, May 2006

[Hefty et. al. 2000] Hefty J., M. Rothacher, T. Springer, R. Weber, G. Beutler, *Analysis of the first year of Earth rotation parameters with a sub-daily resolution gained at the CODE processing center of the IGS.* Journal of Geodesy (2000) 74: 479-487

[IAU 2000] International Astronomical Union (IAU), *Resolution B1.1 Maintenance and Establishment of Reference Frames and Systems.* http://danof.obspm.fr/IAU_resolutions/Resol-UAI.htm, Manchester, 2000, published also in [McCarthy et. al. 2003]

[IERS Bull. A] International Earth Rotation and Reference System Service (IERS), *IERS Bulletin A: Rapid Earth Orientation Data.* http://www.iers.org/iers/products/eop/rapid_eop.html, 2003

[IERS C04] International Earth Rotation and Reference System Service (IERS), *IERS EOP Combined Series EOP_C04.* http://www.iers.org/iers/products/eop/combined04.html

[IERS 2003] International Earth Rotation and Reference System Service (IERS), *IERS Annual Report 2003.* http://www.iers.org/iers/publications/reports/2003

[IGS time series] Jet Propulsion Laboratory, California Institute of Technology, *GPS Time Series.* http://sideshow.jpl.nasa.gov/mbh/series.html

[IVS Analysis Coordinator] Analysis Coordinator of the International VLBI Service for Geodesy and Astrometry, http://vlbi.geod.uni-bonn.de/IVS-AC/index.html

[IVS Working Group 2] Schuh H., P. Charlot, H. Hase, E. Himwich, K. Kingham, C. Klatt, C. Ma, Z. Malkin, A. Niell, A. Nothnagel, W. Schlüter, K. Takashima, N. Vandenberg, *IVS Working Group 2 for Product Specification and Observing Programs, Final Report.* Presented at the 7th Directing Board meeting in Tsukuba, Japan, on February 3, 2002. http://ivscc.gsfc.nasa.gov/about/wg/wg2/index.html

[IVS Working Group 3] Niell A., A. Whitney, B. Petrachenko, W. Schlüter, N. Vandenberg, H. Hase, Y. Koyama, C. Ma, H. Schuh, G. Tuccari, *VLBI2010: Current and Future Requirements for Geodetic VLBI Systems.* Published in IVS 2005 Annual Report, pp. 13-40, http://ivscc.gsfc.nasa.gov/about/wg/wg3/IVS_WG3_report_050916.pdf

[Johnson et. al. 2003] Johnson T., M. S. Carter, A. Myers, W. Wooden, *Rapid Service/Prediction Centre.* IERS Annual Report 2003, pp. 49-58, IERS Central Bureau, Bundesamt für Kartographie und Geodäsie, Frankfurt am Main, 2003 http://www.iers.org/iers/publications/reports/2003/

[Koch 1999] Koch K.-R., *Parameter Estimation and Hypothesis in Linear Models.* Springer-Verlag Berlin Heidelberg, New York, 1999

[Koyama et. al. 2004] Koyama Y., T. Kondo, H. Osaki, M. Hirabaru, K. Takashima, K. Sorai, H. Takaba, K. Fujisawa, D. Lapsley, K. Dudevoir, A. Whitney, *Geodetic VLBI Experiments with the K5 System.* Proceedings of the IVS 2004 General Meeting, 9. - 11. February 2004, Ottawa, Canada, pp. 220 - 224

[Lieske et. al. 1977] Lieske J. H., T. Lederle, W. Fricke, B. Morando, *Expressions for the Precession Quantities based upon the IAU (1976) System of Astronomical Constants.* Astronomy & Astrophysics, Vol. 58, pp. 1-16, 1977

[Ma 1998] Ma C., *The International Celestial Reference Frame as realized by Very Long Baseline Interferometry.* The Astronomical Journal, Vol. 116, pp. 516-546, July 1998

[McCarthy 1996] McCarthy D. D., *IERS Conventions (1996).* IERS Technical Note 21, Observatoire de Paris, http://maia.usno.navy.mil/conventions.html

[McCarthy et. al. 2003] McCarthy D. D., G. Petit, *IERS Conventions (2003).* IERS Technical Note 32, Observatoire de Paris

[MORITZ et. al. 1988] Moritz H., I. I. Mueller, *Earth rotation, Theory and Observation.* The Ungar Publishing Company, New York, 1988

[Mueller 1969] Mueller I., *Spherical and Practical Astronomy as Applied to Geodesy.* Frederick Ungar Publishing Co., New York, 1969

[Munekane et. al. 2004] Munekane H., M. Tobita, K. Takashima, *Groundwater-induced vertical movements observed in Tsukuba, Japan.* Geophysical Research Letters, Vol. 31, L12608, doi: 10.1029/2004GL020158, 2004

[Niell 1996] Niell A., *Global mapping functions for the atmosphere delay at radio wavelengths.* Journal of Geophysical Research, Vol. 101, No. B2, pp. 3227-3246

[Nothnagel 1991] Nothnagel A., *Radiointerferometrische Beobachtungen zur Bestimmung der Polbewegung unter Benutzung langer Nord-Süd-Basislinien.* DGK Reihe C, Heft 368, Verlag des Instituts für Angewandte Geodäsie, Frankfurt am Main, 1991

[Nothnagel et. al. 1994] Nothnagel A., Q. Zhihan, G. D. Nicolson, P. Tomasi, *Earth orientation determination by short duration VLBI observations.* Journal of Geodesy (1994) 68: 1-6

[Nothnagel et. al. 2000] Nothnagel A., G. Engelhardt, H. Hase, R. Kilger, S. Ogi, K. Takashima, V. Thorandt, D. Ullrich, *First Results of the 1999 Tsukuba - Wettzell UT1 Test Series.* Proceedings of the IVS 2000 General Meeting, 21.-24. February 2000, Kötzting, pp. 252-256

[Nothnagel 2005] Nothnagel A., *VTRF2005 - A combined VLBI Terrestrial Reference Frame.* Proceedings of the 17th Working Meeting on European VLBI for Geodesy and Astrometry, Noto, Italy, April 22 and 23, 2005

[Oliveau et. al. 1997] Oliveau S. H., A. P. Freedman, *Accuracy of Earth Orientation Parameter Estimates and Short-Term Predictions Generated by the Kalman Earth Orientation Filter.* In The Telecommunications and Data Acquisition Progress Report 42-129, May 15, 1997, NASA JPL, Pasadena, California

[Petrachenko et. al. 2002] Petrachenko W. T., C. Klatt, V. Ward, *Multi-Beam VLBI.* Proceedings of the IVS 2002 General Meeting, 4.-7. February 2002, Tsukuba, Japan, pp. 162-166

[Petrov et. al. 2004] Petrov L., J.-P. Boy, *Study of the atmospheric pressure loading signal in VLBI observations.* Journal of Geophysical Research, Vol. 109, 10.1029/2003JB002500, No. B03405, 2004

[Ray et. al. 1991] Ray J. R., B. E. Corey, *Current Precision of VLBI Multi-Band Delay Observables.* NOAA Technical Report NOS 137 NGS49, Proceedings of the AGU Chapman Conference on Geodetic VLBI: Monitoring Global Change, American Geophysical Union, Washington D.C., April 22-26, 1991, p. 123-134

[Ray et. al. 1994] Ray J. R., W. E. Carter, D. S. Robertson, *Assessment of the accuracy of IRIS Intensive daily UT1 determination.* Journal of Geophysical Research, Vol. 100, B5, pp. 8193-8200, 1995

[Ray et. al. 1994] Ray J. R., D. J. Steinberg, B. F. Chao, D. E. Cartwright, *Diurnal and Semidiurnal Variations in the Earth's Rotation Rate Induced by Oceanic Tides.* Science, 264, pp. 830-832.

[Richter 1995] Richter B., *Die Parametrisierung der Erdorientierung.* Zeitschrift für Vermessungswesen, 120. Jahrgang, Heft 3, März 1995, p. 109 - 119

[Robertson et. al. 1985] Robertson D. S., W. E. Carter, J. Campbell, H. Schuh, *Daily Earth rotation determinations from IRIS very long baseline interferometry.* Nature, Vol. 316, No. 6027, pp. 424-427, 1 August 1985

[Rothacher 2002] Rothacher M., *Future IERS Products: Implementation of the IAU 2000 Resolutions.* Proceedings of the IERS Workshop on the Implementation of the New IAU Resolutions, IERS Technical Note No. 29, Paris, 18-19 April 2002, pp. 77-84

[Scherneck 1993] Scherneck H.-G., *Ocean tide loading: propagation of errors from the ocean tide into loading coefficients.* manuscripta geodaetica (1993) 18: pp. 59 - 71, Springer-Verlag 1993

[Schödlbauer 1999] Schödlbauer A., *Geodätische Astronomie: Grundlagen und Konzepte.* Berlin, New York: de Gruyter, 1999, ISBN 3-11-015148-0

[Schuh 1987] Schuh H., *Die Radiointerferometrie auf langen Basen zur Bestimmung von Punktverschiebungen und Erdrotationsparametern.* DGK Reihe C, Heft 328, Verlag der Bayrischen Akademie der Wissenschaften, München 1987

[Schuh 1988] Schuh H., *Analysis of UT1 Determinations by VLBI Within Project IRIS.* In A. K. Babcock and G. A. Wilkins (eds.), The Earth's Rotation and Reference Frames for Geodesy and Geodynamics, pp. 171-180. 1988

[Schuh et. al. 2003] Schuh H., R. Dill, H. Greiner-Mai, H. Kutterer, J. Müller, A. Nothnagel, B. Richter, M. Rothacher, U. Schreiber, M. Soffel *Erdrotation und globale dynamische Prozesse.* Mitteilungen des Bundesamtes für Kartographie und Geodäsie, Band 32, Frankfurt am Main, 2003

[Schuh et. al. 2004] Schuh H., J. Böhm, R. Weber, J. Nastula, B. Kolaczek, *High Resolution Earth Rotation Parameters Determined During the CONT02 campaign.* Contribution to the FGS Workshop on Ring Laser Gyroscopes and Earth Rotation, Wettzell, March 24 - 25, 2004

[Tesmer 2004] Tesmer V., *Das stochastische Modell bei der VLBI-Auswertung.* DGK Reihe C, Dissertationen, Heft Nr. 573, München 2004, ISBN 3-76965012-3

[Titov 2000] Titov O., *Influence of Adopted Nutation Model on VLBI NEOS-Intensives Analysis.* Proceedings of the IAU Colloquium 180, Towards Models and Constants for Sub-Microarcsecond Astrometry, 27-30 March 2000, U.S. Naval Observatory, Washington, D. C.

[Thaller 2004] Thaller D., M. Krügel, D. Angermann, M. Rothacher, R. Schmid, V. Tesmer, *Combination Studies Using the CONT02 Campaign.* International VLBI Service for Geodesy and Astrometry 2004 Annual Report, D. Behrend and K. D. Baver (eds.), NASA/TP-2005-212772, pp.13-21

[Vandenberg 1999] Vandenberg N. R., *sked: Interactive / Automatic Scheduling Program.* VLBI Software Documentation, NASA/Goddard Space Flight Center, Space Geodesy Program, August 1999, http://lupus.gsfc.nasa.gov/files_user_manuals/sked/sked.pdf

[Vondrak et. al. 2000] Vondrak J., A. Cepek, *Combined smoothing methods and its use in combining Earth orientation parameters measured by space techniques.* Astronomy and Astrophysics Supplement Series 147, 347-359 (2000)

[Vondrak 2002] Vondrak J., *Background Reasons for the IAU 2000 Resolutions Requiring Actions from the IERS.* Proceedings of the IERS Workshop on the Implementation of the New IAU Resolutions, IERS Technical Note No. 29, Paris, 18-19 April 2002, pp. 1-4

[Vondrak et. al. 2005] Vondrak J., J. Kouba, C. Ron, *Multi-year combination of UT1/lod, based on VLBI and GPS observations.* Proceedings of IERS Combination Workshop (In print), Potsdam, October 2005

[Wahr 1981] Wahr J. M., *Body tides on an elliptical, rotating, elastic and oceanless earth.* Geophysical Journal of the Royal Astronomical Society, Vol. 64, pp. 705-727

[Whitney 2003] Whitney A. R., *Mark 5 Disc-Based Gbps VLBI Data System.* New technologies in VLBI, Proceedings of a symposium of the International VLBI Service for Geodesy and Astrometry held in Gyeong-ju, Korea, 5-8 November 2002. Edited by Y.C. Minh. ASP Conference Series, Vol. 306. San Francisco, CA: Astronomical Society of the Pacific, 2003., p.123

[Whielen et. al. 1999] Wielen R., H. Schwan, C. Dettbarn, H. Lenhardt, H. Jahreiß, R. Jährling, *Sixth Catalogue of Fundamental Stars (FK6); Part I: Basic Fundamental Stars with Direct Solutions.* Veröffentlichungen Astronomisches Rechen-Institut Heidelberg, No. 35, Verlag G. Braun, Karlsruhe, 1999

[Wooden et. al. 2004] Wooden W. H., T. J. Johnson, P. C. Kammeyer, M. S. Carter, A. E. Myers, *Determination and Prediction of UT1 at the IERS Rapid Service/Prediction Center.* Proceedings of the Journées Systèmes de Référence Spatio-Temporels, Observatoire de Paris, 20.-22. September 2004, pp. 260-264

[Yoder et. al. 1981] Yoder C. F., G. J. Williams, M. E. Parke, *Tidal Variations of Earth Rotation.* Journal of Geophysical Research, Vol. 86, No. B2, pp. 881-891, February 10, 1981

[Yoshino et. al. 1986] Yoshino T., S. Hama, T. Shiomo, J. Campbell, H. Cloppenburg, H. Schuh, R. Kilger, *First VLBI experiments between Kashima and Wettzell for monitoring UT1.* Advanced Space Research, Vol. 6, No. 9, pp. 13-16, 1986, Great Britain

[Zhu et. al. 1983] Zhu S.-Y., I. Mueller, *Effects of adopting new precession, nutation and equinox corrections on the terrestrial reference frame.* Bulletin Geodesique (1983) 57: 29-42; 1983

Acknowledgement

Special thanks to my supervisor Axel Nothnagel, to the assessors Heiner Kuhlmann and Harald Schuh, and to
Wolfgang Schlüter, Richard Kilger, Kazuhiro Takashima, Shinobu Kurihara, Nancy Vandenberg, David Gordon, Leonid Petrov, Dan MacMillan, Volkmar Thorandt, Daniela Thaller, Alessandra Roy, Frederik Kunze, Christoph Steinforth, Markus Vennebusch, Philipp Zeimetz, Sarah Böckmann, Thomas Artz,

and to M a r c.